University of Massachusetts Medical School

eScholarship@UMMS

GSBS Dissertations and Theses   Graduate School of Biomedical Sciences

2008-03-20

Myocardial Macrophage Phenotypic Variation and Cytokine-Mediated Induction of HIV-Associated Cardiac Disease: A Dissertation

Jennifer Holmes Yearley
University of Massachusetts Medical School

Let us know how access to this document benefits you.

Follow this and additional works at: https://escholarship.umassmed.edu/gsbs_diss

Part of the Animal Diseases Commons, Cardiovascular Diseases Commons, Immune System Diseases Commons, Pathology Commons, Virus Diseases Commons, and the Viruses Commons

A Dissertation Presented

By

Jennifer Holmes Yearley

Submitted to the Faculty of the

University of Massachusetts Graduate School of Biomedical Sciences, Worcester

in partial fulfillment of the requirements for the degree of

DOCTOR OF PHILOSOPHY

March 20, 2008

MYOCARDIAL MACROPHAGE PHENOTYPIC VARIATION AND CYTOKINE-

MEDIATED INDUCTION OF HIV-ASSOCIATED CARDIAC DISEASE

A Dissertation Presented By

Jennifer Holmes Yearley

The signatures of the Dissertation Defense Committee signifies

completion and approval as to style and content of the Dissertation

_____

Ronald C. Desrosiers, PhD, Thesis Advisor

_____

Keith G. Mansfield, DVM, Member of Committee

_____

Katherine Luzuriaga, MD, Member of Committee

_____

Shan Lu, MD, PhD, Member of Committee

_____

Philip R. Johnson, MD, Member of Committee

The signature of the Chair of the Committee signifies that the written dissertation meets

the requirements of the Dissertation Committee

_____

John Sullivan, MD, Chair of Committee

The signature of the Dean of the Graduate School of Biomedical Sciences signifies

that the student has met all graduation requirements of the school.

_____

Anthony Carruthers, PhD, Dean of the Graduate School of Biomedical Sciences

Interdisciplinary Graduate Program

ACKNOWLEDGMENTS

ABSTRACT

Ventricular dysfunction and dilated cardiomyopathy (DCM) develop among
untreated HIV-infected people at much higher rates than among HIV-negative
individuals, resulting in significant contributions to morbidity and mortality. Mechanisms
underlying development of HIV-associated cardiomyopathy (HIVCM) are as yet poorly
understood. The well-characterized simian immunodeficiency virus (SIV) model of HIV
infection provides a unique context for HIVCM pathogenesis studies in that SIV-infected
rhesus monkeys develop myocardial lesions and contractile dysfunction similar to those
described in HIV-infected people, suggesting a shared disease mechanism.

Lymphocytic myocarditis is a commonly reported finding in AIDS patients at
autopsy and constitutes one of several conditions known to predispose to development of
DCM, irrespective of HIV-infection status. As lymphocytic myocarditis also occurs with
high frequency among SIV-infected rhesus monkeys, a retrospective analysis of rhesus
monkey cardiac tissue collected at necropsy was performed to examine viral and cellular
correlates of lymphocytic inflammation within myocardial tissue. One subpopulation of
macrophages, which has been reported by other groups to be associated with an anti-
inflammatory phenotype, was found to correlate inversely with lymphocytic infiltration
and positively with numbers of virus infected cells, suggesting effects of an anti-
inflammatory cytokine production profile.

In contrast, the detrimental effects of inflammatory cytokines on myocardial
structure and function are well-recognized and HIV infection in general is characterized
by chronic immune activation and inflammatory cytokine dysregulation. To further

investigate a role for myocardial cytokine production in development of HIVCM, a prospective study was conducted in which SIV-infected rhesus monkeys and uninfected controls were treated with recurrent administration of inactivated *Mycobacterium avium* complex bacteria (MAC). SIV-infected, MAC-treated animals rapidly developed significant ventricular systolic dysfunction and chamber dilatation not seen in control groups, suggesting an exaggerated myocardial sensitivity to exogenous antigenic stimulation. Concurrent treatment with the TNFα antagonist etanercept completely abrogated development of these changes, strongly implicating a causative role for TNFα in evolution of the contractile dysfunction and chamber remodeling.

Findings reported from the current studies suggest that characteristics of local myocardial macrophage populations and the myocardial tissue cytokine milieu may play more important roles than lymphocytic infiltration, cardiomyocyte damage, or viral proteins in the pathogenesis of HIVCM.

TABLE OF CONTENTS

LIST OF TABLES

LIST OF FIGURES

LIST OF ABBREVIATIONS

AIDS	acquired immune deficiency syndrome
DCM	dilated cardiomyopathy
DC-SIGN	dendritic cell-specific ICAM-3 grabbing non-integrin
HAART	highly active antiretroviral therapy (combination therapy involving three or more drugs in conjunction)
HIV	human immunodeficiency virus
HIVCM	HIV-associated cardiomyopathy
iNOS	inducible nitric oxide synthase (also known as NOS2)
LVEDD	left ventricular end-diastolic diameter
LVEF	left ventricular ejection fraction
MAC	*Mycobacterium avium* complex
MHC class II	major histocompatibility complex class II
NEPRC	New England Primate Research Center
NYHA	New York Heart Association
SIV	simian immunodeficiency virus
sTNFR2	soluble form of the p75 tumor necrosis factor receptor

PREFACE

The work contained within this thesis is represented in the following publications:

Yearley JH, Pearson C, Carville A, Shannon RP, Mansfield KG. SIV-Associated Myocarditis: Viral and Cellular Correlates of Inflammation Severity. AIDS Res Hum Retroviruses. 2006;22(6):529-540.

Yearley JH, Pearson C, Shannon RP, Mansfield KG. Phenotypic Variation in Myocardial Macrophage Populations Suggests a Role for Macrophage Activation in SIV-Associated Cardiac Disease. AIDS Res Hum Retroviruses. 2007;23(4):515-524.

Yearley JH, Mansfield KG, Carville AL, Sokos GG, Xia D, Pearson CB, Shannon RP. Antigenic Stimulation in the Simian Model of HIV Infection Yields Dilated Cardiomyopathy Through Effects of TNFα. AIDS. 2008;22(5):585-594.

Figure panels 4.1 C and D were contributed by Dr. George Sokos, who was responsible for blinded interpretation and measurements of videotaped echocardiograms from test animals reported in chapter 4. Dr. Sokos' echocardiographic measurements and absolute calculations also constitute a substantial portion of Table 4.1. Plasma viral load data in Figure 4.4 B was derived from assays conducted by Dr. Jeffrey Lifson and Dr. Michael Piatak at the AIDS Vaccine Program, NCI-Frederick.

Additional unrelated studies performed in partial fulfillment of the PhD degree will not be presented in this thesis and are represented in the following publication:

Mansfield KG, Carville A, Wachtman L, Goldin BR, **Yearley J**, Li W, Woods M, Gualtieri L, Shannon R, Wanke C. A diet high in saturated fat and cholesterol accelerates SIV disease progression. J Infect Dis 2007;196(8):1202-1210.

CHAPTER I

GENERAL INTRODUCTION

1.1 Human Immunodeficiency Virus and Cardiac Disease

Currently, an estimated 33.2 million people world-wide are infected with the human immunodeficiency virus (HIV), with 2.5 million new infections and 2.1 million deaths from AIDS in the year 2007 alone [1]. Cardiac abnormalities develop at high frequency in chronically HIV-infected individuals in the absence of antiretroviral therapy, a fact which has been recognized since the early years of the epidemic [2-27]. The spectrum and epidemiology of cardiac disease in HIV infection have been extensively reviewed [28-42], with development of ventricular dysfunction and dilated cardiomyopathy (DCM) being of particular clinical significance and occurring among HIV-infected people at much higher rates than among HIV-negative individuals [28, 30, 37, 38, 43-46]. A high prevalence of cardiac disease has been documented in HIV-infected populations in sub-Saharan Africa as well as in the developed world [30, 43, 47-49], and heart disease appears to be a particularly significant contributor to morbidity and mortality in HIV-infected children, where even mild alterations in left ventricular mass or myocardial contractility are independently and significantly associated with shortened survival [37, 48, 50-57]. While subclinical manifestations of HIV-associated cardiomyopathy (HIVCM) appear to be relatively common, median survival for HIV-infected individuals with DCM is significantly reduced compared to HIV-infected individuals without cardiac dysfunction at similar stages of infection, or HIV-negative individuals with idiopathic DCM [19, 58]. While the advent of highly active anti-retroviral therapy (HAART) has dramatically improved the lives of many HIV-infected people and recent reports suggest that its use may have decreased the frequency of HIV-associated myocardial disease,

roughly 80% of those in need of anti-retroviral drugs globally still do not have access to them [59, 60]. Furthermore, a recent large clinical trial demonstrated significant increases in the incidence of major cardiovascular disease in HIV-infected people who experienced CD4+ count-guided interruptions in antiretroviral therapy as compared to those on continuous therapy, implicating a continued role for HIV infection in development of heart disease which readily reemerges with breaks in therapy [61].

The pathogenesis of cardiomyopathy in HIV infection is poorly understood and likely involves a combination of host, viral, and environmental factors [62-66]. A variety of possible etiologies have been postulated (Table 1.1), with potential mechanisms including tissue damage resulting from lymphocytic myocarditis, an inflammatory process which has been documented at high frequencies in HIV-infected people at later stages of disease progression and which constitutes one of several conditions known to predispose to development of DCM irrespective of HIV-infection status [6, 8, 11, 13, 14, 18, 63] (reviewed in [67-70]). Numerous studies have attempted to draw connections between the lymphocytic myocarditis seen in HIV-infected individuals and development of significant myocardial contractile dysfunction, both with and without concurrent chamber dilatation [5, 6, 8, 11, 12, 20, 27]. Inflammatory infiltrates in HIV-associated myocarditis are consistently documented as comprised predominantly of CD8+ T cells with variable numbers of macrophages [12, 13, 18, 27, 71]. Myocarditis in HIV infection is itself frequently of unknown etiology, with many studies identifying an underlying pathogen in only a minority of cases, though cytomegalovirus, adenovirus, coxsackievirus B3, Epstein-Barr virus, *Toxoplasma gondii, Mycobacterium avium* complex, *Candida* spp.,

Cryptococcus neoformans, Coccidiodes immitis, Histoplasma capsulatum, Aspergillus spp., and *Pneumocystis jiroveci* have all been documented [8, 11, 13, 14, 18, 27, 41, 58, 72-74].

A further important potential contributor to development of HIVCM is proinflammatory cytokine excess resulting from effects of HIV-associated cytokine dysregulation [58, 75, 76]. As discussed below, the myocardium is quite sensitive to proinflammatory cytokine effects, which are uniformly cardiodepressant with chronic exposure, and associated with substantial pathologic remodeling (reviewed in [77] and [78]). As chronic immune activation and cytokine dysregulation are prominent features of HIV-infection [79-83], and local myocardial inflammatory responses have the potential to further augment a proinflammatory cytokine milieu, a role for cytokine-induced myocardial pathology in HIV-infection must be seriously considered [75].

In evaluating whether HIV itself may play a direct role in induction of local myocardial inflammatory responses, contractile dysfunction, or pathologic remodeling, multiple investigators have detected HIV viral genome and/or viral proteins in the hearts of HIV-infected people [13, 27, 71, 84-87]. Numbers of intramyocardial virus-infected cells are consistently very low, however, and in many hearts are undetectable [12, 13, 27, 71, 72, 84, 87]. Investigators using methods with a high degree of morphologic discrimination at the tissue level have in almost all cases found productive HIV infection to be restricted to cells within the myocardial interstitium, most consistent with macrophages and T cells, such that previous longstanding controversy over the potential for HIV to directly infect cardiomyocytes has largely been resolved [13, 71, 87]. In

further support of the inability of HIV-1 to infect cardiomyocytes, experimental attempts
to infect fetal human cardiomyocytes using a wild-type HIV isolate derived from a case
of pediatric AIDS with severe cardiomyopathy proved unsuccessful, though a VSV
pseudotyped HIV-1 based vector demonstrated high efficiency infection of these same
cells [88]. The rarity of HIV genome in myocardial tissue of HIV-infected people
combined with a failure of the presence or absence of HIV-infected cells to correlate with
the presence of inflammatory infiltrates or clinical cardiac disease suggests that direct
infection of cells within the myocardium is unlikely to play a signficant role in the
pathogenesis of HIV-associated cardiac disease, though this has remained controversial
[84, 86].

Further possible contributors to development of HIV-associated cardiac disease
include myocardial effects of viral proteins [89-94], cardiac autoimmunity [95], drug-
related cardiotoxicities [29, 96-100], autonomic dysfunction [101-106], and micronutrient
deficiencies, particularly in the context of wasting or chronic diarrhea [36, 43].

1.2 Cytokines and the Pathogenesis of HIV-associated Cardiomyopathy

Inflammatory cytokine-induced myocardial dysfunction is a well-documented
phenomenon in multiple experimental models, is a significant contributor to
hemodynamic compromise in sepsis, and may play a significant contributory role in
development and progression of heart failure regardless of initiating etiology [77, 78,
107-116]. Roles for inflammatory cytokines in cardiac dysfunction have received
extensive attention in association with their cardiodepressant effects, demonstrated

contributions to myocardial remodeling, and frequent systemic elevations in the context of heart failure [77, 78, 115-125]. The mechanisms by which inflammatory cytokines generate their effects in the myocardium have been studied in some detail. Cytokine-induced products of the sphingomyelinase pathway, nitric oxide generated by inducible nitric oxide synthase (iNOS), and reduced cyclic AMP response to β-adrenergic stimulation all appear to act as mediators of cardiodepressant effects [77, 108, 109, 126-128]. On a molecular level, these effects result from modulation of intracellular calcium transport, antagonism of cyclic AMP-mediated Protein Kinase A effects, alteration of sensitivity of myofilaments to calcium binding, S-nitrosylation of thiol residues on contractile proteins, functional uncoupling of β-adrenergic receptor stimulation from adenylyl cyclase activity, and possibly alteration of β-adrenoreceptor internalization kinetics (reviewed in [77, 108]), [127].

Inflammatory cytokine-induced pathologic remodeling yields chamber dilatation, myocardial hypertrophy, and fibrosis attributable to dysregulation of matrix metalloproteinase (MMP)/tissue inhibitor of metalloproteinase (TIMP) balances, increased expression of TGFβ, alterations in susceptibility to cardiomyocyte apoptosis, and stimulation of hypertrophic and fetal gene expression patterns [125, 128-132]. Experimental work in rodent models demonstrates TNFα to be strongly associated with pathologic remodeling, and pharmacologic antagonism of TNFα in human cardiac transplant recipients significantly decreases allograft hypertrophy and fibrosis, strengthening the implication that TNFα plays an important role in pathologic remodeling *in vivo* in humans, as well as in animal models [129, 130, 133, 134].

Transgenic mice with myocardial expression of TNFα comprise the most thoroughly studied model of inflammatory cytokine excess on the heart. These animals develop severe biventricular dilatation, heart failure, and premature death, with the rapidity of disease development dependent on gene dose [129, 134]. And while inflammatory cytokine excess as a primary effector has well-demonstrated adverse myocardial effects, circulating levels of inflammatory cytokines are also often secondarily elevated in humans with heart failure, a fact which may contribute to heart failure progression (reviewed in [78, 111, 135]). The degree of circulating cytokine elevation in heart failure patients has been demonstrated to correspond to New York Heart Association (NYHA) functional classifications of heart failure severity [117-119, 136, 137], and measures of myocardial systolic function [138]. Supporting a role for elevated circulating inflammatory cytokines in heart failure progression, healthy rats subjected to 15 days of continuous TNFα infusion to generate circulating levels in the range found in humans with end-stage chronic heart failure developed significantly depressed ventricular function and ventricular dilatation with structural remodeling [130].

HIV-infection is intrinsically characterized by chronic immune activation and cytokine dysregulation [79-83, 139]. Exaggerated levels of inflammatory cytokine production by HIV-infected leukocytes or leukocytes derived from HIV-infected persons have been reported by multiple investigators and elevated circulating levels of TNFα and other proinflammatory cytokines have been documented at all stages of HIV infection [140-148]. These elevated levels do not appear to normalize in the face of HAART, and in some reports may rise after initiation of therapy [143, 146, 149, 150].

Numerous features suggest the likelihood of a substantial role for inflammatory cytokines as mediators of HIVCM. The local myocardial tissue environment has been demonstrated to be a rich potential source of inflammatory cytokines, with both cardiomyocytes and locally resident non-myocyte interstitial cell populations competent to produce a variety of inflammatory mediators, and heart tissue capable of generating as much or more TNFα per gram of tissue in response to endotoxin stimulation as liver or spleen [122, 126, 151-155]. Non-myocyte populations comprise up to 70% of the total cellular constituency of the myocardium and consist of a mixed assemblage of cell types, including substantial populations of dendritic cells and macrophages which can serve directly as targets of HIV infection [151, 156-161]. This environment represents a volatile setting in the context of HIV-infection.

1.3 Existing Experimental Support for a Role for Cytokines in HIVCM

Experimental work designed to examine the role of inflammatory cytokines in the pathogenesis of HIVCM has been limited; however, one group has demonstrated significantly increased myocardial TNFα immunostaining signal intensity in HIV-infected individuals with DCM as compared to non-HIV-infected individuals with DCM, suggesting a role for TNFα in the HIV-associated disease process [58]. Several studies in murine models have gone farther, drawing connections between specific HIV proteins expressed in CD4+ cell contexts and development of cardiac disease. Transgenic mice expressing HIV-1 nef protein exclusively in CD4+ cells develop cardiac disease despite the presence of low numbers of HIV-1 transgene-expressing cells in the heart, and the

lack of a significant correlation between cardiac lesion development and levels of expression of the HIV-1 transgene [91]. HIV-1 transgene expression exclusively in CD4+ cells with low numbers of transgene positive cells in the heart mimics the distribution seen with natural HIV-1 infection and implicates an indirect, HIV-protein induced effect on levels of soluble mediators as cause of the myocardial injury. Similarly, cardiac disease has been generated in transgenic mice expressing simian immunodeficiency virus (SIV) nef protein exclusively in CD4+ cells [162].

1.4 A Role for Myocardial Macrophages

Macrophages and dendritic cells constitute cell types widely distributed throughout peripheral tissues including the myocardial interstitium, where they may be found in significant numbers [156, 157, 163-166]. These populations serve as sentinels of the innate immune system, sensitizing the adaptive immune system through antigen presentation, and significantly modulating immune responses through cytokine production [161, 167]. Due to expression of the appropriate receptor and co-receptors, both macrophages and dendritic cells may serve as direct targets of HIV infection, and display a variety of functional abnormalities in HIV-infected individuals, including elevated secretion of inflammatory cytokines, both constitutively and upon stimulation [80, 141, 142, 145, 148, 160, 161, 168]. Furthermore, in rodent models, dendritic cells have been demonstrated to serve as a critical link between cardiotropic viral infections and subsequent autoimmunity against myocardial antigens [169], and macrophages have

been identified as the major effector population in at least one model of myocardial autoimmunity yielding dilated cardiomyopathy, heart failure, and death [170].

As macrophage and dendritic cell populations are well-represented in the interstitial tissues of the myocardium and have been demonstrated to show significant dysregulation of function and inflammatory cytokine production in the context of HIV infection, they have strong potential to contribute to development of HIV-associated myocardial pathology. Increased levels of myocardial macrophage infiltration have been documented in human cases of HIVCM, as well as in a murine model of AIDS with associated cardiomyopathy [71, 171]. HIV-infected perivascular macrophages have been found in some instances to be associated with apoptosis of surrounding cardiomyocytes [94], with significant correlations present between extent of apoptosis and both TNFα expression and expression of the HIV viral protein gp120 [71, 94]. In addition, associations between extent of myocardial macrophage involvement and development of cardiac functional decline have been identified prospectively in a murine model of AIDS [171].

While in many contexts the actions of macrophage and dendritic cell populations contribute to development of inflammatory responses, in other contexts their effects may be tolerogenic or overtly anti-inflammatory, with the differences between these scenarios attributable to differences in the phenotypic subsets of cells involved [167, 172, 173]. Immature dendritic cells have been associated with induction of peripheral tolerance, for instance, and non-classically activated macrophages have been associated with a variety of functional roles, including immunosuppression, tissue repair, and angiogenesis

(reviewed in [167, 172-175]). While phenotypically diverse, some subsets of non-classically activated macrophages are typified by ineffective microbicidal activity and cytokine secretion profiles characteristically dominated by IL-10, TGFβ, and IL-1RA [167, 172-175]. Because of this, characterization of phenotypic subtypes of these cells in tissue has the potential to cast light on how specific subpopulations might serve either injurious or protective roles dependent on the particular properties of the populations involved. In addition to modulation of immune responses through cytokine production, the density, distributional characteristics, and activation phenotype of professional antigen presenting cells within the myocardium could well be expected to play a role in sensitization of the adaptive immune system to both native and exogenous antigens, a function which may be protective, but also has the potential to be detrimental in a tissue with minimal to no regenerative capacity and strictly limited functional reserve.

1.5 The Simian model of HIV-associated Cardiac Disease

Study of the pathogenesis of HIVCM in humans is limited by many factors. Identifying the earliest time points of development of myocardial pathology and placing them within the natural history of HIV infection is generally not possible; complex, variable, and potentially toxic medication regimens are routinely used; substantial variation can exist in environment and lifestyle among patients; and ethical constraints place strict limits on the types of sampling which may be conducted. The simian immunodeficiency viruses (SIV) share a close phylogenetic relationship with HIV-1 and induce a fatal immunodeficiency syndrome in Asian macaques that provides an important

model system for HIV pathogenesis studies [176, 177]. No other model system so closely recapitulates the interplay of virus with the immune system and consequent disease development seen in HIV-infection of humans. In order to study the pathogenesis of end-organ dysfunction resulting from direct or indirect effects of chronic HIV infection, particularly effects that may result from early insults during the period of acute viremia and initial immune containment of the virus, use of an animal model is essential. The SIV model of HIV-infection and AIDS is well-established and provides a strong context for study of HIV cardiomyopathy in that myocardial functional abnormalities and histologic lesions similar to those documented in HIV infection are frequently seen in SIV-infected rhesus monkeys (*Macaca mulatta*), suggesting a shared disease mechanism [178, 179]. The SIV cardiomyopathy model was pioneered at the New England Primate Research Center (NEPRC), where frequent development of DCM among chronically SIV-infected animals was first demonstrated, establishing the utility of the model [178].

1.6 Chronic SIV infection and Simian AIDS are Associated with Dilated Cardiomyopathy

Significant cardiac dysfunction and myocardial pathology have been demonstrated in animals chronically infected with pathogenic strains of SIV [178]. Among fifteen rhesus monkeys infected ≥18 months, six infected with pathogenic strains of SIV and 9 infected with non-pathogenic clones of SIVmac239 containing deletions of the nef gene (SIVmac239Δnef), animals chronically infected with pathogenic strains demonstrated significant decreases in global left ventricular systolic function over time as

indicated by marked decreases in left ventricular ejection fraction (LVEF: 43±7% (pathogenic) versus 61±3% (non-pathogenic)) and evidence of left ventricular dilatation through increases in both left ventricular end-systolic volume indices (ESVI: 16±3 mL/m^2 (pathogenic) versus 9±1 mL/m^2 (non-pathogenic)) and left ventricular end-diastolic volume indices (EDVI: 28±3 mL/m^2 (pathogenic) versus 21±3 mL/m^2 (non-pathogenic)) [178]. In contrast to chronically infected animals, changes were not detected in an acute infection cohort of 16 age-matched young adult rhesus monkeys infected with either pathogenic SIVmac239 or non-pathogenic SIVmac239Δnef [178]. These animals, followed over a 5 week course of infection with weekly M-mode and 2D echocardiography, did not develop significant changes from baseline values, though animals infected with SIVmac239 did experience decreases in CD4+ T cell count consistent with effects of early pathogenic infection [178]. Furthermore, of 24 rhesus monkeys that died of simian AIDS in this study, 9 demonstrated myocarditis, with infiltrates consisting predominantly of CD3+ cells with smaller numbers of CD68+ macrophages. These results, which are consistent with common descriptions of the time course and character of cardiac pathology in HIV-infected people, suggest that the source of myocardial injury in HIV infection is one that either acts gradually over a prolonged period of time, or appears only relatively late in infection.

Further work evaluating possible correlates of ventricular dysfunction in chronically SIV-infected rhesus monkeys has demonstrated induction of myocardial TNFα by immunohistochemistry and Western blot in animals that have histologically demonstrable myocardial inflammatory infiltration [180]. Quantified TNFα levels were found to have a

significant inverse correlation with left ventricular ejection fraction (LVEF), linking the elevation in TNFα to decreased ventricular systolic function in this model [180].

These data were among the first to indicate that the SIV-infection model is associated with substantial myocardial dysfunction in later stages of infection, that this dysfunction appears to be common, and that elevations in myocardial TNFα in the context of SIV-infection may be sufficiently severe as to play a role in depression of ventricular systolic performance. These findings lay the groundwork for use of the SIV-infection model to explore *in vivo* pathogenesis of HIV-associated cardiac dysfunction.

1.7 Rationale and Objectives

In the reported studies, potential viral and non-viral contributors to development of myocardial dysfunction and correlative microscopic pathology in the simian model of HIV infection are investigated using a combination of prospective and retrospective analyses.

As lymphocytic myocarditis is a commonly reported finding both in AIDS patients and chronically SIV-infected rhesus monkeys and constitutes one of several conditions known to predispose to development of DCM irrespective of HIV-infection status [68-70], initial retrospective studies focused centrally on a role for myocardial inflammation in evolution of cardiac pathology in SIV-infected animals, evaluating inflammation frequency, extent, and character, as well as determining viral, cellular, and histomorphologic correlates of these inflammatory infiltrates. Findings in initial work identified subpopulations of myocardial macrophages whose numbers correlated

inversely with lymphocytic infiltration and positively with numbers of virus infected cells, suggesting a role for these populations in modulation of the inflammatory response. The question of a role for myocardial cytokines in development of myocardial functional and structural pathology was then pursued directly in a group of longitudinally evaluated cohorts in an acute infection, augmented immune activation model. Use of a prospective model allowed monitoring of cardiac function by serial echocardiography with concurrent examination of circulating cytokine and chemokine levels, as well as post-mortem assessment of cytokine levels and histomorphologic features of myocardial tissues to determine features correlating most closely with development of contractile dysfunction and chamber dilatation in SIV-infected animals.

Table 1.1 Possible Etiologies and Associations of HIV-Associated Cardiomyopathy[*]

Possible Etiologies:

Drug-related:	Zidovudine, Interferon, Foscarnet, Doxorubicin, IL-2 Amphotericin B, Cocaine
Infectious:	HIV, *Toxoplasma gondii*, Coxsackievirus group B, Epstein Barr Virus, Cytomegalovirus, Adenovirus
Metabolic/Endocrine:	Anemia, Thyroid hormone related, Growth hormone related, Adrenal insufficiency, Hyperinsulinemia
Nutritional Deficiency:	Selenium, B12, Carnitine
Cytokine-mediated:	TNFα, Nitric oxide, TGFβ, Endothelin-1
Autoimmunity:	Anti cardiac myosin, Anti cardiac C protein
Autonomic Dysregulation:	Cardiovascular sympathovagal dysfunction

Associations:

Encephalopathy, Immunodeficiency (CD4 count < 100), Length of immunosuppression, HIV viral load

---

[*]Table modified from [64]

CHAPTER II

SIV-ASSOCIATED MYOCARDITIS: VIRAL AND CELLULAR CORRELATES OF
INFLAMMATION SEVERITY

ABSTRACT

Myocarditis is a common finding in HIV-infected people. Cardiac inflammatory lesions and functional abnormalities similar to those documented in HIV infection are frequently seen in SIV infection of rhesus monkeys, suggesting a shared disease mechanism. A retrospective analysis of cardiac tissue collected at necropsy was performed to assess correlates of myocardial inflammation in SIV-infected rhesus monkeys. Intramyocardial SIV-infected cells were identified in 7 of 21 hearts from SIV-infected animals, with viral protein consistently colocalizing with the macrophage marker HAM 56. Productively infected cells occurred in low numbers, and did not correlate with presence or quantity of inflammation or necrosis. Intramyocardial CMV was identified in 6 of 21 hearts from SIV$^+$ animals, but also did not correlate with presence or quantity of inflammation or necrosis. In contrast, T cell infiltration correlated inversely with DC-SIGN$^+$ cell numbers, which occurred in significantly higher numbers in SIV$^+$ animals with histologically normal myocardium than in SIV$^+$ animals with active or borderline myocarditis or in uninfected controls ($P < 0.001$), suggesting an important immunoregulatory role for this population within the myocardium.

Introduction

Cardiac abnormalities are common in human immunodeficiency virus (HIV) infection, with progression to clinical disease and cardiac death documented in a small but significant proportion of cases [5-7, 17, 20, 27, 34, 41, 53]. Myocarditis is one of the most frequently recognized findings in HIV-infected individuals, with incidence rates as high as 52% reported [6, 8, 11, 13, 72]. While the connection between HIV-associated myocarditis and clinical cardiac disease is still unclear given that the majority of cases are subclinical, there is considerable evidence to suggest the possibility of a contributory role [5, 6, 8, 11, 12, 20, 27]. The etiology of the inflammatory response in this condition is poorly understood. The presence of HIV-infected cells within the myocardium of some HIV-infected individuals has repeatedly been documented [18, 27, 84-86, 94], but the ability of HIV to infect cardiomyocytes remains controversial [13, 63, 71, 88], as is the potential relationship of intramyocardial HIV-infected cells to development of cardiac pathology [12, 13, 72, 84, 86]. Other opportunistic and general cardiotropic pathogens are identified with variable frequency, in most instances accounting for a minority of cases [8, 11-14, 18, 20, 27, 72, 74]. Cardiac autoantibodies have been detected with relatively high frequency in HIV-infected individuals with myocardial disease, suggesting a possible role for autoimmunity [95]. Drug-related cardiotoxicities may also play a role in some cases [34, 99, 100].

Simian immunodeficiency viruses (SIV) are lentiviruses which are genetically closely related to HIV and represent the original sources from which both HIV-1 and HIV-2 derived [176, 177]. SIV infection of Asian macaque species produces a fatal

immunodeficiency syndrome with properties of disease progression very similar to those seen in humans with HIV infection [181-186]. The SIV model of AIDS is well-established, and provides a strong context for study of HIV-associated myocarditis and cardiomyopathy due to the occurrence of cardiac morphologic and functional abnormalities similar to those described in HIV infection [178, 179]. Use of an animal model allows minimization of many confounding factors which accompany study of naturally occurring disease in HIV-infected human populations.

Goals of the present retrospective study included precise quantitation and characterization of inflammatory infiltrates within hearts of SIV-infected rhesus monkeys (*Macaca mulatta*) to allow objective comparison of inflammation severity between cases, and to allow correlations to be drawn between inflammation severity and the presence and number of intramyocardial virus-infected cells, as well as the size and distributional properties of local professional antigen presenting cell populations which could be expected to play a role in sensitization of the adaptive immune system to native or exogenous antigens within the myocardium. Two systems of quantitation were used in order to cross-check results, and to evaluate infiltrates not only in terms of cell numbers, as determined by quantitative image analysis, but also in terms of cell distribution, as determined by a rule-based grading schema.

Materials and Methods

Animals, Case Inclusion Criteria, and Tissues. Paraffin-embedded cardiac tissues from 26 rhesus monkeys (*Macaca mulatta*) were evaluated. Hearts from SIV-infected animals were selected from the pathology archives of the New England Primate Research Center. Hematoxylin and eosin (H&E)-stained sections were assessed to determine the presence or absence of lymphocytic inflammatory infiltrates, with infiltrates being defined as intramyocardial focal clusters comprised of 5 or more cells morphologically consistent with lymphocytes. Fourteen sequential cases with such infiltrates and the first 7 cases without infiltrates were selected for further study. Hearts containing concurrent neutrophilic infiltrates or bacterial colonies were omitted from consideration. Cardiac tissues from 5 healthy, SIV-negative rhesus monkeys with no gross or histologic evidence of cardiac or other significant pathology were used as controls. All SIV-positive animals had been infected with either SIVmac251 or SIVmac239 and had been included in a variety of vaccine and pathogenesis studies. Post-inoculation time to euthanasia and necropsy ranged from 81 to 1502 days. Prior to euthanasia, all animals were housed at the New England Primate Research Center (NEPRC) in accordance with standards of the Association and Accreditation of Laboratory Animal Care and the Harvard Medical School Animal Care and Use Committee. All animals received complete necropsies upon euthanasia.

Immunohistochemistry. Formalin-fixed, paraffin-embedded tissues were sectioned at 5μm for routine, single-label immunohistochemistry following an ABC immunostaining

technique as previously described [187]. Cell populations were characterized using antibodies specific for CD3 (rabbit polyclonal, A 0452, DakoCytomation, Carpinteria, CA), CD4 (clone 1F6, VP-C318, Vector Laboratories, Burlingame, CA), CD8 (clone 1A5, VP-C325, Vector), CD68 (clone KP1, M 0814, DakoCytomation), DC-SIGN (polyclonal, gift of R. Doms, University of Pennsylvania, Philadelphia, PA, and clone 120612, DZX02, R & D Systems, Minneapolis, MN), HAM 56 (clone HAM56, M0632, DakoCytomation), cleaved caspase 3 (polyclonal, Cell Signaling Technology, Beverly, MA), and Ki67 (clone MIB-1, M 7240, DakoCytomation). Intramyocardial virus was evaluated using antibodies against SIV nef protein (clone KK75, donor Dr. K. Kent and Ms C. Arnold, obtained from the NIBSC Centralised Facility for AIDS Reagents supported by EU Programme EVA contract (BMH4 97/2515) and the UK Medical Research Council), rhesus cytomegalovirus IE1 protein (polyclonal, provided by Dr. Peter Barry, UC Davis), and adenovirus (clone 20/11, MAB8052, Chemicon International, Temecula, CA). Formalin-fixed, paraffin-embedded (FFPE) splenic tissue from a rhesus monkey experimentally infected with SIV at the NEPRC served as positive control for immunohistochemical analysis of hearts for SIV nef protein. Formalin-fixed, paraffin-embedded jejunal tissue from an SIV infected rhesus monkey which developed severe adenoviral enteritis prior to euthanasia at the NEPRC served as positive control for adenoviral antigen. Formalin-fixed, paraffin-embedded tissue from the urinary bladder of an experimentally immunosuppressed cynomolgus monkey which spontaneously developed disseminated cytomegalovirus infection in an organ transplantation study at the NEPRC served as positive control for rhesus cytomegalovirus IE1 protein. Sections

were deparaffinized in xylene and rehydrated through graded ethanols, followed by

blocking of endogenous peroxidase by incubation in 3% H_2O_2 in phosphate buffered

saline. Antigen retrieval in most cases consisted of microwaving in citrate buffer

(Vector). Antigen retrieval for CD4 consisted of microwaving in EDTA buffer (Lab

Vision, Fremont, CA), for adenovirus consisted of 5 minutes digestion with proteinase K

(DakoCytomation), for CD8 consisted of 20 minutes pressure cooker treatment in Trilogy

solution (Cell Marque, Hot Springs, AK), and for the DC-SIGN monoclonal consisted of

microwaving in Tris HCl buffer (Lab Vision). Sections were incubated with primary

antibody followed by an avidin-biotin block (Vector) to block endogenous biotin, and

sequential incubation with biotinylated secondary antibody and horseradish peroxidase-

conjugated avidin (ABC Standard or ABC Elite, Vector), or the EnVision polymer

system (DakoCytomation) applied according to manufacturer's instructions. Antigen-

antibody complex formation was detected by use of 3,3'diaminobenzidine (DAB)

chromogen (DakoCytomation) and tissues were counterstained with Mayer's

hematoxylin. Irrelevant primary antibodies were used in place of the test antibody as

negative controls in all immunohistochemical studies.

Grouping and Scoring. Hearts from the 21 SIV[+] cases were grouped into 3 cohorts of 7

animals each based on application of the Dallas criteria to H&E stained sections from

paraffin blocks containing left ventricular tissue [188]. Hearts assigned to the active

myocarditis group had lymphocytic inflammatory infiltrates directly associated with

regions of cardiomyocyte degeneration or necrosis, hearts assigned to the borderline

myocarditis group had lymphocytic infiltrates without associated cardiomyocyte degeneration or necrosis, and hearts assigned to the SIV normal group lacked inflammatory infiltrates and had no other histologic evidence of myocardial pathology. For each SIV-infected and control animal, sections of left ventricle were scored for necrosis on 2 non-serial H&E stained sections, and for immunohistochemical CD3 and CD68 signal according to specified distributional and quantitative parameters (Table 1). In brief, for each animal a single section of left ventricular tissue was scored for focal T cell infiltration, perivascular T cell infiltration, diffuse T cell infiltration, infiltrate-associated macrophage involvement, and myofiber degeneration/necrosis, as defined. CD3 and CD68 scoring was limited to intramyocardial signal. Two composite scores were derived from the individual components: a total T cell infiltration score, generated as the sum of the 3 individual CD3 distributional scores, and a cumulative inflammation score, generated as the sum of the total T cell infiltration score, the necrosis score, and the infiltrate-associated macrophage score. Cytomegalovirus (CMV) involvement as detected by immunohistochemistry was scored semi-quantitatively on a 0-3 scale, with 0 representing no positive signal, and 3 representing frequent signal.

Quantitative Image Analysis. For each SIV-infected and control animal, sections immunohistochemically labeled for SIV nef protein, CD3, CD68, and DC-SIGN as described were individually examined by use of an Olympus Vanox-S AHBS microscope interfaced with a Leica personal computer equipped with Leica QWin image analysis software (Leica Imaging Systems Ltd., Cambridge, England), via a DEI 750 charge-

coupled device camera (Optronics, Goleta, CA). In brief, for a single section of left

ventricular tissue from each animal, images of 20-30 random fields were captured at 200x

magnification. The total number of DAB stained cells per field was quantitated based on

the number of flagged foci of discrete signal occupying a minimum number of

contiguous pixels. The number of positive cells per mm^2 was calculated based on the

known area of each field and total number of positive cells in the overall examined area.

In Situ Hybridization. In situ hybridization for SIV RNA in cardiac tissue was

performed as previously described [189]. Briefly, tissue sections were deparaffinized and

rehydrated in xylene and graded ethanols. Endogenous alkaline phosphatase activity was

blocked in 5 mM levamisole (Sigma Chemical Co., St. Louis, MO). Sections were

hydrolyzed in 0.2N HCl (Sigma), digested with proteinase K (Roche Diagnostics Corp.,

Indianapolis, IN), acetylated in acetic anhydride (Sigma), and hybridized overnight at

50°C with digoxigenin-labeled antisense riboprobe that spans the entire genome of the

SIVsmmPGm5.3 molecular clone of SIVsmmFGb (Lofstrand Laboratories, Gaithersburg,

MD). Bound probe was detected by immunohistochemistry using alkaline phosphatase-

conjugated sheep anti-digoxigenin F(ab) fragments (Roche) and the chromogen nitro blue

tetrazolium/5-bromo-4-chloro-3-indolyl-phosphate (NBT/BCIP, Roche). Sections were

counterstained with nuclear fast red (Vector). Splenic tissue from an SIV-positive rhesus

monkey hybridized with antisense riboprobe served as positive control. Splenic tissue

from an SIV-negative rhesus monkey hybridized with antisense riboprobe and from an

SIV-positive rhesus monkey hybridized with sense riboprobe served as negative controls.

Confocal Microscopy. Double-label immunofluorescence confocal microscopy was performed on paraffin sections. Briefly, sections were routinely deparaffinized, rehydrated, subjected to antigen retrieval as described for single-label immunohistochemistry, washed in 1x phosphate-buffered saline in doubly distilled water with 0.2% fish skin gelatin (PBS-FSG), and blocked with 10% normal goat serum diluted in PBS-FSG. Monoclonal primary antibodies (specific for SIV nef, HAM 56, DC-SIGN) were incubated on sections overnight. Polyclonal primary antibodies (specific for CD3) were incubated on sections for 30 minutes. Anti-mouse IgG1 Alexa 488 and anti-mouse IgG2a Alexa 568, anti-mouse IgM Alexa 568, or anti-rabbit IgG Alexa 568 secondary antibodies (Molecular Probes, Inc., Eugene, OR) were incubated for 30 minutes on sections as appropriate for the species and isotype of primary antibody. To-Pro3 (Molecular Probes) was incubated on sections for 5 minutes then washed with PBS. Confocal microscopy was performed using a Leica TCS SP laser scanning microscope equipped with 3 lasers (Leica Microsystems, Exton, PA). Thirty-two individual optical slices were collected at 512 x 512 pixel resolution. The fluorescence of individual fluorochromes was captured separately in a sequential mode, after optimization to reduce bleed-through between channels (photomultiplier tubes) using Leica software. Adobe Photoshop Elements 3.0 (Adobe Photosystems, San Jose, CA) was used to assign correct colors to 3 channels collected: Alexa 488 (green), Alexa 568 (red), and To-Pro3 (blue). Colocalization of antigens was demonstrated by the addition of colors.

Serology. Banked sera from 50 rhesus monkeys of various ages and from various housing circumstances at the New England Primate Research Center were evaluated for the presence of anti-coxsackieviral IgG to assess the prevalence of coxsackievirus exposure in the Center's rhesus population. A commercial ELISA kit with broad coxsackievirus serotype specificity and manufacturer-provided control sera was used according to manufacturer's instructions (Serion ELISA, QED Biosciences, San Diego, CA).

Statistical Analysis. Linear regression analysis and statistical comparisons between groups were performed with commercially available software (SigmaStat 3.1, Systat Software, Inc., Richmond, CA). Groups were compared using the *t* test or Mann-Whitney Rank Sum Test, as appropriate. Fisher's exact test was used to evaluate categorical data between groups. Probability values of $P < 0.05$ were interpreted as significant. Statistical analysis of quantitative image analysis data was performed on pooled individual data points collected for each animal within the evaluated groups.

Results

Correlation between grading schema-derived composite scores and image analysis-based T cell quantification

There were no significant differences in age, sex, viral inoculum, or number of days post-infection among the groups. AIDS-defining lesions, including disseminated opportunistic infections, giant cell disease, and SIV encephalitis, were present in a majority of animals in all SIV-infected groups at necropsy. Prevalence of AIDS diagnosis did not differ significantly between groups, being found in 4 of 7 cases with active myocarditis, 6 of 7 cases with borderline myocarditis, and 5 of 7 cases with histologically normal myocardium. Mononuclear inflammatory infiltrates within the myocardium (Figure 2.1, A) were quantified using both quantitative image analysis and a rule-based grading schema (Table 2.1). Lymphocytic infiltrates detected with CD3 immunohistochemistry were scored according to focal (Figure 2.1, B), perivascular (Figure 2.1, C), and diffuse (Figure 2.1, D) distributions. Summation of individual, grading schema-derived distributional T cell scores yielded a composite total T cell infiltration score for each heart. A significant correlation (P < 0.001) existed between composite T cell infiltration scores and values for the number of $CD3^+$ cells/mm^2 generated by quantitative image analysis (Figure 2.2, A). Infiltrate-associated macrophage involvement and cardiomyocyte degeneration and necrosis (Figure 2.1, E-F) were separately scored and combined with the T cell infiltration score to yield a cumulative inflammation score which significantly correlated with the T cell infiltration score itself (P < 0.001) and with image analysis values for $CD3^+$ cells/mm^2 (P = 0.003, R = 0.566) (Figure 2.2, B). The

pattern of significant correlations for individual grading schema derived T cell

distribution scores was identical to that identified for image analysis derived quantitation

of CD3$^+$ cells, and each individual distribution score correlated significantly with image

analysis derived T cell quantitation itself (P < 0.025). Individual T cell distributional

scores also correlated significantly with each other (P ≤ 0.005) with the exception of the

focal and diffuse scores (P = 0.09). In linear regression analyses examining the

relationship between T cell infiltration and other examined parameters, the significance

or non-significance of correlations patterned identically regardless of which T cell

quantitation method was used for all parameters except one. The highly significant

correlation of composite T cell infiltration scores with image analysis derived values for

the number of CD3$^+$ cells per unit area indicates that grading schema derived scoring may

confidently be used as an alternate method for quantitation of inflammatory infiltrates in

contexts where image analysis is not readily available.

Quantitation and characterization of inflammatory infiltrates by group

The amount of T cell infiltration, infiltrate-associated macrophage involvement, and

cumulative inflammation as defined under the grading schema was determined for each

group and compared between groups. Statistically significant elevations in T cell

infiltration score (P < 0.05), infiltrate-associated macrophage score (P < 0.02), and

cumulative inflammation score (P ≤ 0.03) were present in hearts with active or borderline

myocarditis relative to SIV normal hearts and uninfected controls (Figure 2.3).

Differences in these parameters between hearts with active myocarditis and those with

borderline myocarditis were not significant, nor were differences in values between SIV

normal hearts and uninfected controls. Infiltrate-associated macrophage scores between

the active and borderline myocarditis groups approached but did not achieve statistical

significance ($P = 0.064$). Values for T cell infiltration score, $CD3^+$ cells/mm^2, cumulative

inflammation score, and infiltrate-associated macrophage score did not differ

significantly between animals with and without AIDS-defining lesions (all $P > 0.10$).

Immunohistochemical analysis for CD8 and CD4 antigens was performed to

further characterize the identified $CD3^+$ cell populations. A strong predominance of $CD8^+$

cells was noted in almost all cases (Figure 2.4, A), though 2 hearts had roughly equal

numbers of $CD4^+$ and $CD8^+$ round cells within inflammatory foci, without an obvious

correspondence between the $CD4^+$ population and the $CD68^+$ population evaluated from

a separate section of the same tissue. CD4 signal in general was rare and, when present,

occurred predominantly in loose distribution in the subendocardial space in a pattern also

identified for CD68 (not shown). A minority of hearts, however, had large numbers of

$CD4^+$ cells with a spindloid morphology distributed throughout the myocardial

interstitium (Figure 2.4, B). Hearts with high levels of interstitial spindloid $CD4^+$ cells

were unique in also having especially high numbers of interstitial DC-SIGN$^+$ cells.

Relation of cardiomyocyte necrosis to macrophage and T cell involvement

Cardiomyocyte degeneration and necrosis were variably present among SIV$^+$ animals

with lymphocytic infiltrates and served as the defining criterion for inclusion in the active

myocarditis group. Areas of necrosis were characteristically small and localized to a

single cardiomyocyte or directly adjacent cardiomyocytes (Figure 2.1, F). Three of 7

hearts from the active myocarditis group also contained patchy regions of replacement

fibrosis consistent with a process of chronic injury, a finding which was not present in

hearts from any of the other 3 groups. A statistically significant correlation existed

between the necrosis score and both the infiltrate-associated macrophage score ($P <$

0.001, $R = 0.666$) and the cumulative inflammation score ($P = 0.007$, $R = 0.517$). No

significant correlation was detected between necrosis score and either measure of T cell

quantitation (T cell infiltration score $P = 0.479$, $R = 0.145$; $CD3^+$ cells/mm^2 $P = 0.433$, R

$= 0.161$).

The possibility of cardiomyocyte apoptosis as a significant contributor to

myocardial pathology was investigated through immunohistochemical evaluation of the

presence, frequency, and distribution of cleaved caspase 3. Cleaved caspase 3 signal was

strong in sections of rhesus duodenum and tonsil used as positive controls, but very rare

in hearts of all groups. Occasional cells morphologically consistent with leukocytes

displayed strong positive signal within inflammatory foci or within the myocardial

interstitium (not shown), but no positive signal in cells morphologically consistent with

cardiomyocytes was identified.

Intramyocardial SIV-infected cells and inflammation

Intramyocardial SIV-infected cells were detected in 7 of the 21 hearts from SIV-infected

animals by in situ hybridization using probes spanning the entire SIV genome. Infected

cells were found in 3 of 7 hearts with active myocarditis, 1 of 7 hearts with borderline

myocarditis, and 3 of 7 hearts from the SIV normal group. SIV nef

immunohistochemistry had a lower sensitivity than in situ hybridization, detecting only 5

of 7 cases containing infected cells. Infected cells occurred with an interstitial distribution

and had a compact, discrete, frequently spindloid morphology (Figure 2.4, C). Double-

label immunofluorescence confocal microscopy demonstrated consistent colocalization

of SIV nef protein with HAM 56, indicating productive infection of macrophages (Figure

2.4, D). A lack of colocalization of CD3 and SIV nef protein signal indicated a lack of

productive infection of intramyocardial T cells (not shown). With one exception,

numbers of infected cells in hearts where SIV antigen was detected were extremely low,

ranging from <1 to 4 cells/mm^2 by quantitative image analysis. A single heart within the

SIV normal group contained substantially higher quantities of infected cells at 36

cells/mm^2, though with morphologic and distributional properties similar to those

identified in other hearts. The quantity of SIV-infected cells per unit area was

significantly higher among hearts from the SIV normal group than among hearts from

either the active or borderline myocarditis groups ($P < 0.04$). No correlation was

identified between the number of SIV-infected cells/mm^2 and T cell infiltration score ($P

= 0.646$, $R = 0.106$), CD3$^+$ cells/mm^2 ($P = 0.742$, $R = 0.0821$), cumulative inflammation

score ($P = 0.382$, $R = 0.201$), necrosis score ($P = 0.535$, $R = 0.144$), infiltrate-associated

macrophage score ($P = 0.188$, $R = 0.299$), or diffuse macrophage infiltration within the

myocardial interstitium (CD68$^+$ cells/mm^2) as quantified by image analysis ($P = 0.858$, R

$= 0.0417$).

Frequency of potentially contributory cardiotropic infections

To evaluate the extent to which other opportunistic or general cardiotropic infections might contribute to induction of the myocardial inflammatory response in the hearts under study, specific screening was conducted for coxsackievirus, adenovirus, and cytomegalovirus, along with reviews of non-serial H&E stained sections for histologic evidence of opportunistic agents. Coxsackieviral IgG serology performed using manufacturer-provided controls was conducted on sera from 50 rhesus monkeys of various ages and housing circumstances at the New England Primate Research Center. Negative results were found in all cases, indicating that coxsackievirus infection is unlikely to play an important role among monkeys within the facility. Immunohistochemical screening for adenoviral antigen yielded strong, frequent signal on positive control tissues, but in all hearts revealed no positive signal. Strong nuclear signal for rhesus cytomegalovirus IE1 protein was detected in cardiomyocytes of 6 of 21 SIV$^+$ animals by immunohistochemistry, with staining pattern and intensity matching that of positive control tissues. Cardiomyocyte CMV signal was identified in 2 hearts with active myocarditis and 4 hearts with borderline myocarditis, but not in any SIV normal or control hearts. Evidence of infection was not found in any cells other than cardiomyocytes. In all cases, infected cells occurred in low numbers and were not directly associated with inflammation or necrosis. The difference in CMV scores between hearts with active or borderline myocarditis as compared to SIV normal and uninfected

control hearts approached but did not reach statistical significance (P = 0.066). Of 10

animals with myocardial CMV-infected or SIV-infected cells, 3 contained both. Of these,

2 were in the active myocarditis group, 1 was in the borderline myocarditis group.

Cumulative inflammation scores for these 3 animals included 1 above the mean for all

SIV$^+$ animals as a group, 1 equal to the mean, and 1 below the mean. All of these hearts

had very low numbers of myocardial SIV-infected cells. No correlation was detected

between CMV score and T cell infiltration score (P = 0.853, R = 0.038), CD3$^+$ cells/mm^2

(P = 0.640, R =0.00963), cumulative inflammation score (P = 0.520, R = 0.132), necrosis

(P = 0.493, R = 0.141), DC-SIGN$^+$ cells/mm^2 (P = 0.226, R = 0.246), SIV$^+$ cells/mm^2 (P

= 0.643, R = 0.107), or CD68$^+$ cells/mm^2 (P = 0.826, R = 0.0453).

Multiple reviews of H&E stained sections by 2 individuals (JHY, KGM) revealed

no histologic evidence of other protozoal, fungal, bacterial, or viral infections.

DC-SIGN$^+$ cells and T cell infiltration

Distribution of DC-SIGN was evaluated as a dendritic cell marker which also labels some

macrophage populations in both humans and macaques.[190-193] Tissue sections of left

ventricle were immunohistochemically labeled for DC-SIGN with signal subsequently

quantified by image analysis. DC-SIGN$^+$ cells were identified in 23 of 26 hearts

examined. DC-SIGN$^+$ cells occurred exclusively in the interstitium and perivascular

connective tissue and were never found within inflammatory foci (Figure 2.4, E). The

number of DC-SIGN$^+$ cells was highly variable among samples, ranging from 0-77

cells/mm^2, and while variation in DC-SIGN$^+$ cell numbers was found in all groups,

numbers of intramyocardial DC-SIGN^{+} cells were significantly increased in hearts of the

SIV normal group relative to all other groups (P < 0.001) (Figure 2.5, A). DC-SIGN[+]

cells were also significantly increased in hearts from the active myocarditis group relative

to the control group (P = 0.006); however, differences between DC-SIGN[+] cell numbers

in the active and borderline myocarditis groups, and between the borderline myocarditis

and control groups were not significant (P = 0.113, and P = 0.220, respectively). The

possibility of intramyocardial proliferation of the DC-SIGN[+] population being

responsible for the dramatically higher levels of expression noted in some hearts was

evaluated by assaying for the proliferating cell marker Ki67. Ki67 signal was detected

among leukocytes within focal aggregates, but was not identified in more widely

dispersed interstitial and perivascular cells consistent with the DC-SIGN[+] populations

identified.

Hearts with high levels of T cell infiltration as quantitated by either method

uniformly had low numbers of myocardial DC-SIGN^{+} cells, and among hearts from SIV-

infected animals there was a statistically significant inverse correlation between the

number of DC-SIGN^{+} cells/mm^2 and the T cell infiltration score (P = 0.027) (Figure 2.5,

B). A statistically significant direct correlation also was identified between the number

of SIV-infected cells/mm^2 and the number of DC-SIGN^{+} cells/mm^2 (P = 0.038, R =

0.456); however, the significance of this latter correlation depended critically on

inclusion of the single SIV normal sample with very high numbers of myocardial SIV-

infected cells/mm^2. Double-label immunofluorescence confocal microscopy

demonstrated consistent absence of colocalization of DC-SIGN signal and SIV nef

protein within individual cells, indicating a lack of productive SIV infection in DC-SIGN$^+$ cells (Figure 2.4, F).

Distinctness of DC-SIGN$^+$ and CD68$^+$ cell populations

Distribution of CD68$^+$ cells was evaluated to quantify macrophages, both within inflammatory foci and more diffusely throughout the myocardial interstitium. Quantity of CD68 signal was compared to image analysis derived quantification of DC-SIGN labeled sections of the same tissue in order to assess overall numbers and distribution of antigen presenting cells. CD68 immunohistochemistry revealed a population of cells with distribution and spindloid morphology similar to that identified for DC-SIGN, though CD68$^+$ cells were also noted occurring within inflammatory foci (Figure 2.1, E). Myocardial CD68$^+$ cell numbers were significantly increased in the active myocarditis group relative to uninfected controls (P = 0.034), and were significantly increased in the SIV normal group relative to the borderline myocarditis and uninfected control groups (P = 0.007 and P = 0.002, respectively). However, the frequency of CD68$^+$ cells was lower than the frequency of DC-SIGN$^+$ cells in sections of the same tissue, with DC-SIGN$^+$ cell numbers being significantly higher in the SIV normal group (P < 0.001) (Figure 2.5, A, C). Linear regression analysis of the relationship of CD68$^+$ cell frequency to DC-SIGN$^+$ cell frequency demonstrated a statistically significant, but highly outlier dependent, correlation between the two (P = 0.020).

Discussion

Quantification of infiltrates by image analysis and application of a rule-based grading schema provided two methods for objectively enumerating the extent and type of inflammation present in examined hearts, with the rule-based grading schema also allowing assessment of distributional patterns of infiltrates and derivation of composite scores incorporating multiple pathological features. The highly significant correlation of grading schema derived composite T cell infiltration scores with image analysis derived values for $CD3^+$ cells/mm^2 ($P < 0.001$) suggests that the inflammation grading schema may be used with confidence for quantitation of infiltrates in circumstances where computer-based image analysis is either not practical or not possible, such as in most clinical and diagnostic contexts. Interestingly, significant correlations from each of the individual distributional T cell scores did not differ from those of the image analysis derived quantitation of $CD3^+$ cells per unit area, suggesting that the different distributional patterns identified within the tissues were not associated with different pathogenetic mechanisms or consequences, despite the fact that different hearts sometimes had pronounced differences in the distributional patterns of T cells present.

The fact that cardiomyocyte necrosis scores lacked significant correlation with T cell infiltration, and that the active and borderline myocarditis groups consistently patterned together with regards to both the histologic characteristics of infiltrates and significant correlations with other examined parameters, suggests that these two groups represent slightly different manifestations of a single disease process. The fact that often only a small proportion of the infiltrates in hearts of the active myocarditis group were

directly associated with cardiomyocyte degeneration or necrosis further supports the existence of a continuum between these two groups, though the underlying cause of the cardiomyocyte injury and why it occurs in some cases and not others remains obscure.

The potential role of macrophages in pathogenesis of cardiac disease in HIV infection has been raised as a point of interest in work by other groups [71]. In the present study, overall CD68$^+$ cell numbers as quantitated throughout the myocardium by image analysis were not significantly different between hearts with active myocarditis and those which were histologically normal (Figure 2.5, C). CD68$^+$ cell accumulation was most focally prominent in inflammatory cell infiltrates from hearts classified as having active myocarditis (Figure 2.3, B), but the fact that infiltrate-associated macrophage scores also correlated significantly with necrosis suggests the probability of a secondary clean-up response of macrophages to the presence of necrotic tissue in the context of active myocarditis as a possible explanation for this finding.

Productively SIV-infected cells were identified in 33% of the hearts from SIV$^+$ animals; however, numbers of infected cells were generally very low. Productively infected cells were morphologically inconsistent with cardiomyocytes and consistently demonstrated colocalization of SIV nef protein with the macrophage marker HAM 56 when examined by double-label immunofluorescence confocal microscopy, arguing against direct SIV infection of cardiomyocytes as a mechanism of myocyte injury. The fact that the highest numbers of productively SIV-infected cells were found in hearts with histologically normal myocardium strongly argues against cardiomyocyte injury or secondary inflammatory reaction in response to the presence of SIV-infected leukocytes

within the myocardium. The finding of cardiomyocyte cytomegalovirus infection at relatively high frequency among the hearts with myocarditis, as has also been reported in several HIV-based studies [13, 18, 74], was suggestive of a possible role for CMV in the pathogenesis of this condition. Despite this, the lack of a significant correlation with either presence or quantity of inflammatory response, the fact that CMV-infected cells were never directly associated with regions of inflammation or necrosis, and the fact that most hearts with myocarditis did not contain evidence of CMV indicates that CMV infection is not sufficient to account for the full spectrum of cases examined. Furthermore, these facts taken together indicate that any role played by CMV would need to be indirect, possibly through induction of an autoimmune response, as has been documented in murine models of CMV infection [194-196].

DC-SIGN$^+$ cell numbers were dramatically increased in the SIV normal group compared to all other groups and showed an inverse correlation with quantity of T cell infiltration, suggesting an important immunoregulatory role for this population within the myocardium. The distribution of DC-SIGN$^+$ cells diffusely throughout the interstitium and in perivascular locations suggests a surveillance function, and it may be that increased levels of surveillance by this cell population result in more rapid recognition and clearance of potential pathogens, thereby protecting against development of myocarditis. Conversely, the presence of significantly increased levels of local antigen presenting cells within the myocardium may increase the likelihood of inappropriate sensitization to native myocardial antigens under some circumstances, leading to increased likelihood of autoimmune responses. The exact identity of the DC-SIGN$^+$

population is not clear; however, the consistent lack of productive infection by SIV and the distinctness of this population from the CD68^{+} population based on quantitative inconsistencies between the two suggests that they are not macrophages and may well represent an immature dendritic cell population. Regardless of their exact identity, the nature of the correlations observed in these cohorts suggests that the recruitment of DC-SIGN^{+} cells to the myocardium under conditions of SIV infection may play an important role in whether lymphocytic myocarditis develops in a given individual or not.

Table 2.1. Myocardial inflammation grading criteria

_____

Focal* T cell infiltration:

0 = no focus ≥5 CD3$^+$ cells

1 = 1-3 foci of ≥5<10 CD3$^+$ cells

2 = 4-6 foci of ≥5<10 CD3$^+$ cells, OR 1-3 foci of ≥10<20 CD3$^+$ cells

3 = >6 foci of ≥5<10 CD3$^+$ cells, OR >3 foci of ≥10<20 CD3$^+$ cells, OR 1 or more foci of ≥20

   CD3$^+$ cells

Perivascular[†] T cell infiltration:

0 = No 40x field containing ≥5 CD3$^+$ cells associated with a single vessel

1 = 1-2 40x fields each containing ≥5<10 CD3$^+$ cells associated with a single vessel

2 = ≥5<10 CD3$^+$ cells associated with each of 3-5 vessels, OR 1 40x field containing ≥10<20

   CD3$^+$ cells associated with a single vessel

3 = ≥5<10 CD3$^+$ cells associated with each of >5 vessels, OR ≥10<20 CD3+ cells associated

   with each of ≥2 vessels, OR 1 40x field containing ≥20 CD3$^+$ cells associated with a single vessel

Diffuse[‡] T cell infiltration:

0 = no 40x field with ≥8 CD3$^+$ cells

1 = 1-2 40x fields with ≥8<14 CD3$^+$ cells

2 = 3-6 40x fields with ≥8<14 CD3$^+$ cells, OR 1-2 40x fields with ≥14<20 CD3$^+$ cells

3 = >6 40x fields with ≥8<14 CD3$^+$ cells, OR 3 or more 40x fields with ≥14<20 CD3$^+$ cells,

   OR 1 or more 40x fields with ≥20 CD3$^+$ cells

Infiltrate-associated[§] macrophages:

0 = No CD68^{+} cells associated with any infiltrate

1 = 1-5 CD68^{+} cells are present within a single infiltrate

2 = 1-5 CD68^{+} cells are present within each of 2 or more infiltrates, OR >5 CD68^{+} cells are present

within a single infiltrate

3 = >5 CD68^{+} cells are present within each of 2 or more infiltrates

Myofiber degeneration/necrosis:

0 = none

0.5 = 1 or more small foci cumulatively less than ¼ the size of a 40x field.

1 = 1 or more small foci cumulatively less than ½ the size of a 40x field

2 = 1 or more foci cumulatively greater than ½ the size of a 40x field but less than

the size of a full 40x field

3 = 1 of more foci cumulatively greater the size of a full 40x field

---

*Focal T cell infiltrate: All CD3^{+} cells scored within a focus must be separated by no greater than 3 lymphocyte diameters from another CD3^{+} cell within the focus. CD3^{+} cells within perivascular connective tissue are excluded from focal scoring.

[†]Perivascular T cell infiltrate: All CD3^{+} cells scored as perivascular infiltrates must occur directly within perivascular connective tissue which does not overlap with any previously scored field. Infiltrates associated with multiple vessels (scores of 2 and above) may be in the same or different 40x fields.

[‡]Diffuse T cell infiltrate: All CD3^{+} cells scored as diffuse infiltrates must be separated by greater than 3 lymphocyte diameters from any focal or perivascular CD3^{+} infiltrate.

[§]Infiltrate-associated macrophages: CD68^{+} cells scored as infiltrate-associated macrophages must be directly associated with a focal, diffuse, or perivascular lymphocytic infiltrate, as defined.

Figure 2.1 Myocardial infiltrates in SIV-associated myocarditis illustrating basic patterns evaluated under the grading schema. **A:** Interstitial mononuclear infiltrate with lymphocyte predominance and cardiomyocyte disruption (H&E) **B:** Predominantly focal aggregate of T cells (CD3 immunohistochemistry with Mayer's hematoxylin) **C:** Perivascular T cell infiltration (CD3 immunohistochemistry with Mayer's hematoxylin) **D:** Diffuse infiltration of T cells without focus formation (CD3 immunohistochemistry with Mayer's hematoxylin) **E:** Infiltrate-associated macrophage involvement (CD68 immunohistochemistry with Mayer's hematoxylin) **F:** Cardiomyocyte necrosis with associated inflammatory infiltrate (H&E)

Figure 2.1
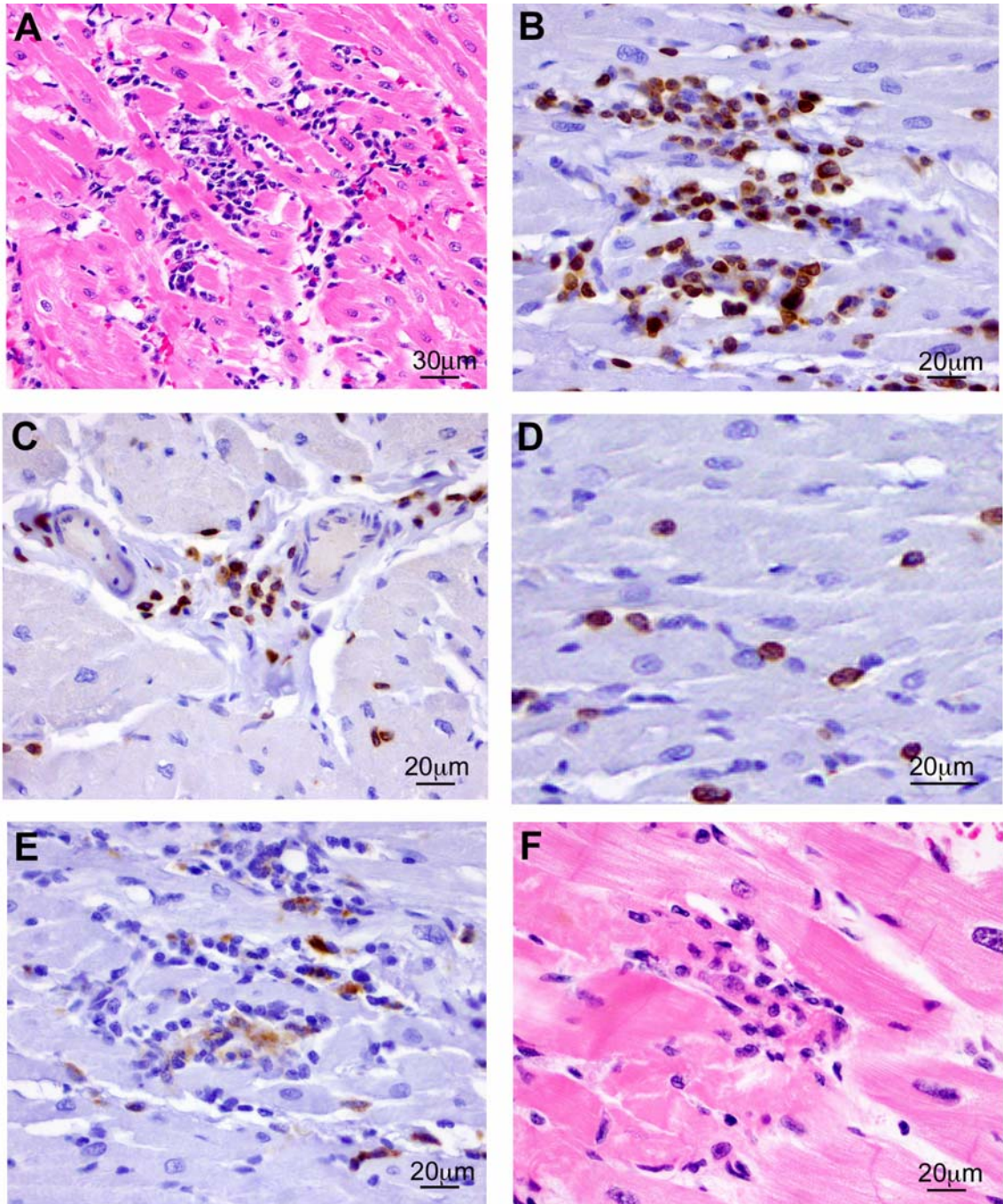
Figure 2.2 Linear regressions illustrating correlations between grading schema derived T cell infiltration scores and image analysis based T cell quantitation, (**A**), and between grading schema derived T cell infiltration and cumulative inflammation scores, (**B**). **A:** A statistically significant correlation was present between the numbers of CD3$^+$ cells/mm^2 as determined by image analysis and the grading schema derived composite T cell infiltration score, which incorporated individual scores for 3 different T cell distributional patterns (P < 0.001). **B:** A statistically significant correlation was present between the image analysis derived quantitation of CD3$^+$ cells/mm^2 and the grading schema derived cumulative inflammation score, which incorporated the T cell infiltration score, the infiltrate-associated macrophage score, and the necrosis score (P = 0.003).

Figure 2.2
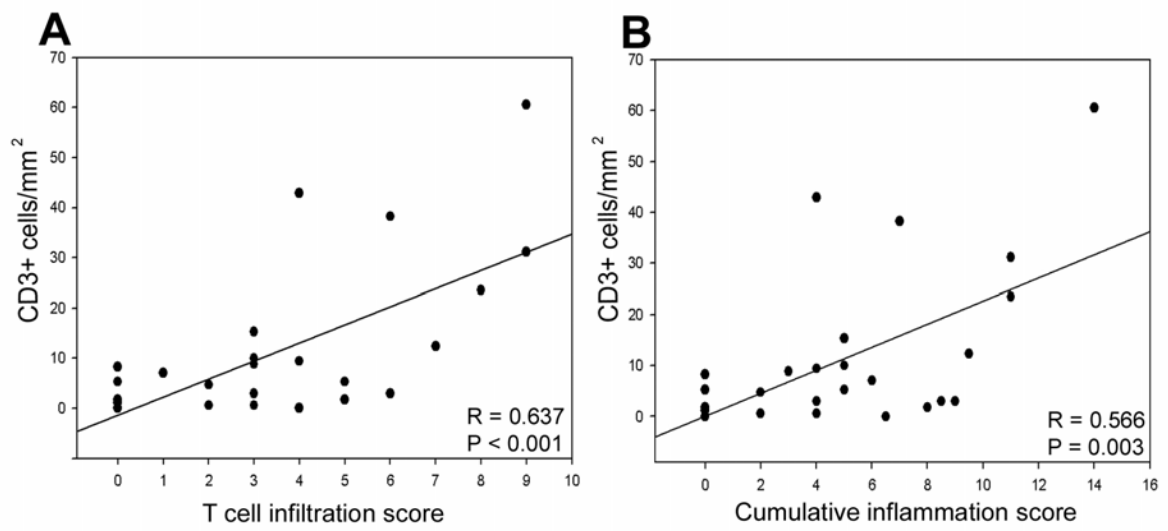
Figure 2.3 Distribution of T cell infiltration scores, infiltrate-associated macrophage scores, and cumulative inflammation scores across groups. **A:** T cell infiltration scores within the active and borderline myocarditis groups were significantly higher than within the SIV normal and control groups ($P < 0.05$). The difference in T cell infiltration scores between the active and borderline myocarditis groups and between the SIV normal and uninfected control groups was not significant. **B:** Infiltrate-associated macrophage scores within the active and borderline myocarditis groups were significantly higher than within the SIV normal or control groups ($P < 0.02$). The difference in infiltrate-associated macrophage scores between the active and borderline myocarditis groups and between the SIV normal and uninfected control groups was not significant. **C:** Cumulative inflammation scores within the active and borderline myocarditis groups were significantly higher than within the SIV normal and uninfected control groups ($P \leq 0.03$). The difference in cumulative inflammation scores between the active and borderline myocarditis groups and between the SIV normal and uninfected control groups was not significant. Boxes represent the 25th to 75th percentile of scores within each group. Central lines within boxes represent median values. Boxes without central lines have median values either equal to the box maximum (**B**: borderline group), or the box minimum (**A**: control group; **B**: active and control groups; **C**: control group). Active = active myocarditis group, borderline = borderline myocarditis group, SIV norm = SIV normal group, control = uninfected control group.

Figure 2.3

Figure 2.4 Immunophenotypic characterization and viral localization. **A:** Cells comprising cellular aggregates within the myocardium consisted predominantly of CD8$^+$ lymphocytes. (CD8 immunohistochemistry with Mayer's hematoxylin) **B:** An extensive interstitial spindloid CD4$^+$ cell population was present in a small subset of SIV$^+$ animals. This same subset of animals also had extremely high numbers of interstitial DC-SIGN$^+$ cells. (CD4 immunohistochemistry with Mayer's hematoxylin) **C:** Cells productively infected by SIV were characterized by compact, often spindloid morphology and interstitial distribution. (SIV nef immunohistochemistry with Mayer's hematoxylin) **D:** Double-label immunofluorescence confocal microscopy for HAM 56 and SIV nef protein showed prominent cytoplasmic colocalization of nef protein signal with HAM 56 as indicated by addition of colors in the merged image (800x magnification). **E:** DC-SIGN$^+$ cells had prominent spindloid morphology with a consistently interstitial and perivascular distribution. DC-SIGN$^+$ cells were never identified within inflammatory foci. (DC-SIGN immunohistochemistry with Mayer's hematoxylin) **F.** Double-label immunofluorescence confocal microscopy for DC-SIGN and SIV nef protein demonstrated a consistent lack of signal colocalization, indicating a lack of productive SIV infection in DC-SIGN$^+$ cells (800x magnification).

Figure 2.4
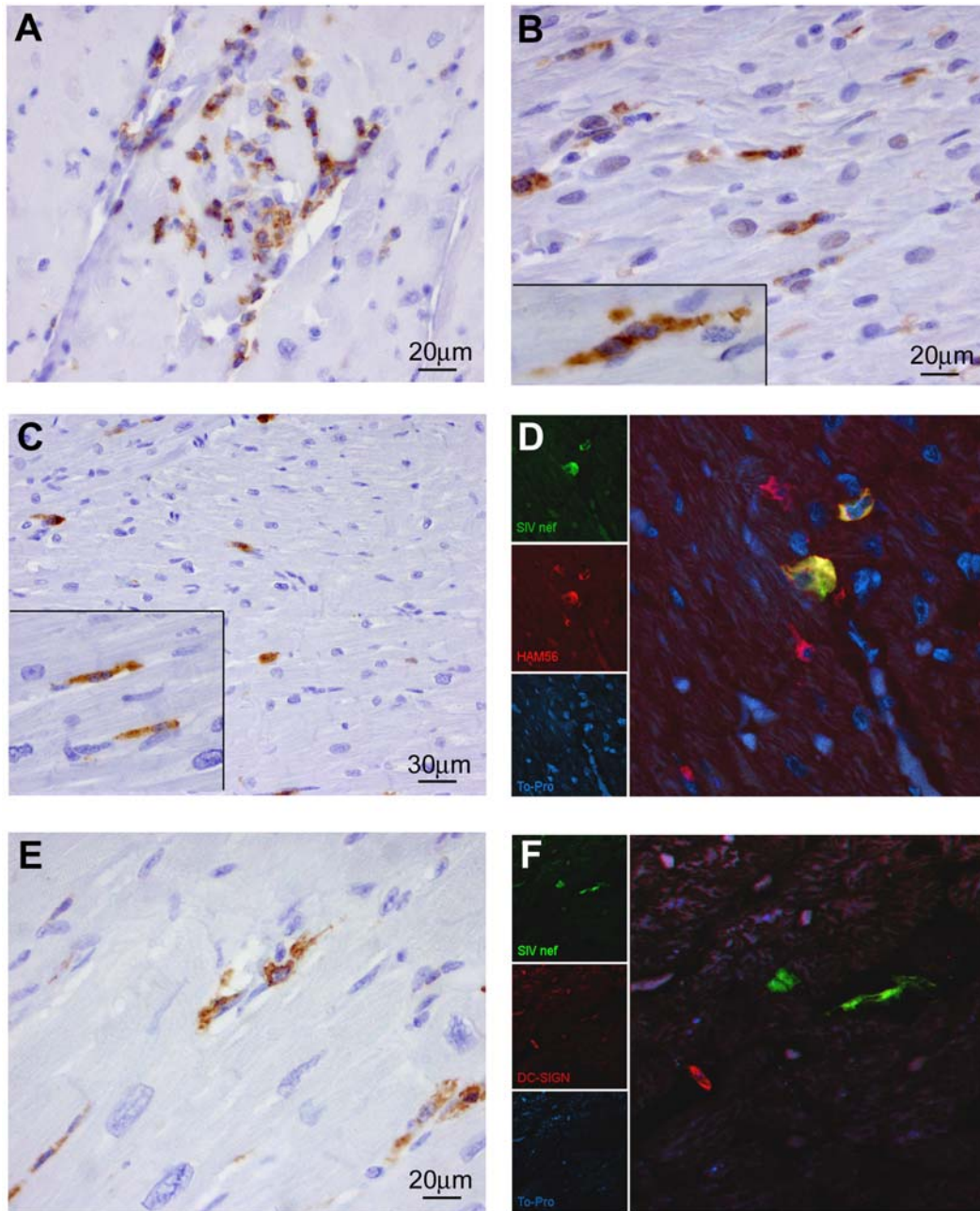
Figure 2.5 Image analysis based quantitation of DC-SIGN⁺ and CD68⁺ cells. **A:** DC-SIGN⁺ cell numbers per unit area as measured by quantitative image analysis were significantly higher in the SIV normal group than in the active and borderline myocarditis groups or the uninfected control group (P < 0.001). **B:** The grading schema derived T cell infiltration score was inversely correlated with the number of DC-SIGN⁺ cells/mm^2 (P = 0.027). **C:** CD68⁺ cell numbers per unit area as measured by quantitative image analysis were significantly higher in the SIV normal group than in the borderline myocarditis group or the uninfected control group (P = 0.007 and P = 0.002, respectively), and were higher in the active myocarditis group than in the uninfected control group (P = 0.034). Differences in CD68⁺ cell numbers between the active and borderline myocarditis groups and between the active myocarditis and SIV normal groups were not significant. **A, C:** The number of DC-SIGN⁺ and CD68⁺ cells per unit area differed significantly within the SIV normal group (P < 0.001). Boxes in (**A**) and (**C**) represent the 25th to 75th percentile of scores within each group. Central lines within boxes represent median values. Boxes without obvious central lines have median values visually indistinguishable from the box minimum (**A, C:** control group) or the box maximum (**C:** borderline group). Active = active myocarditis group, borderline = borderline myocarditis group, SIV norm = SIV normal group, control = uninfected control group.
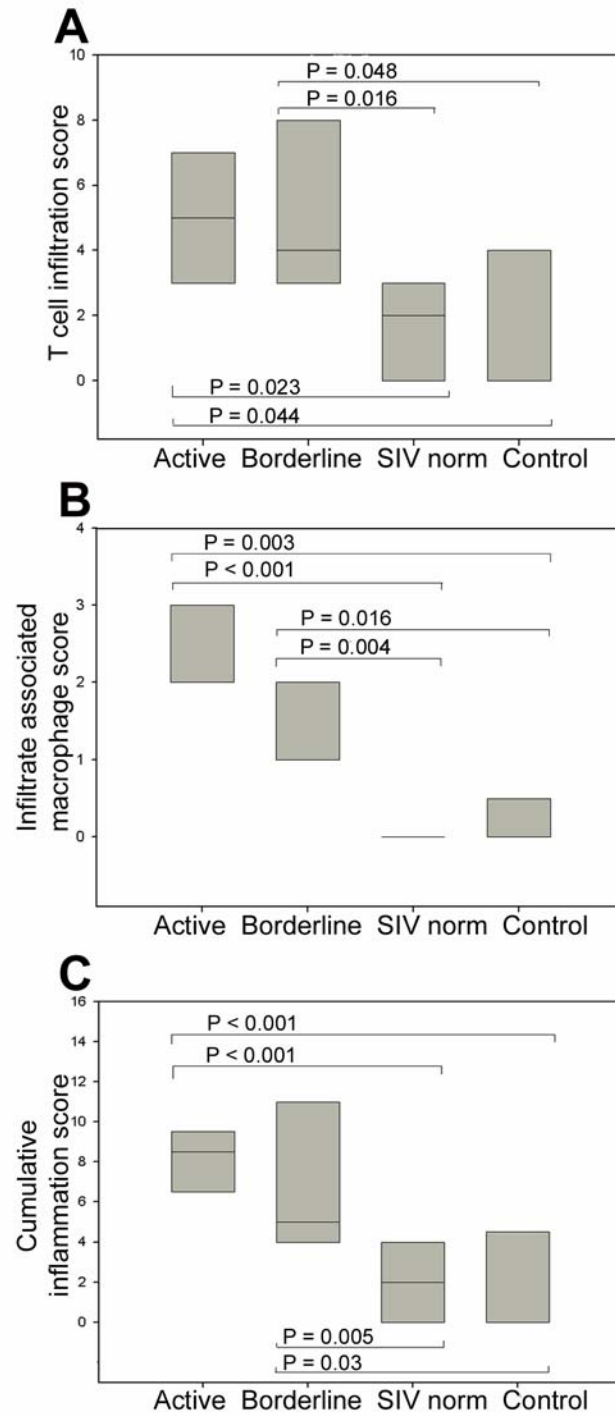
Figure 2.5
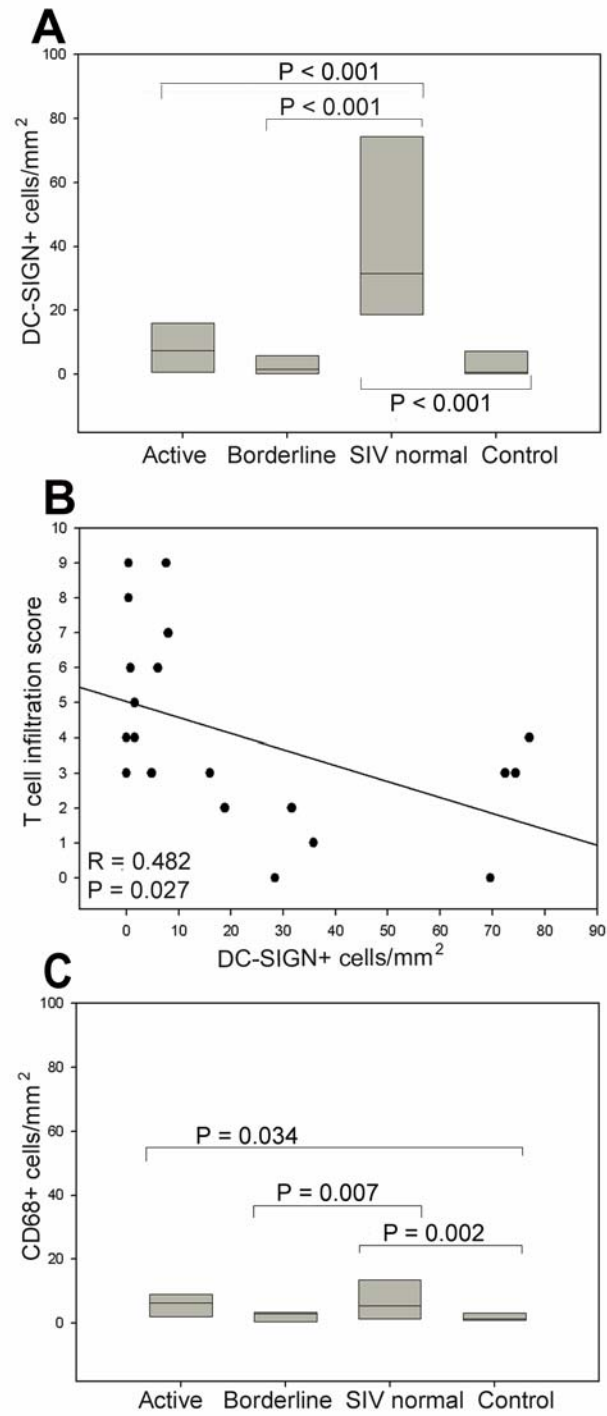
CHAPTER III

PHENOTYPIC VARIATION IN MYOCARDIAL MACROPHAGE POPULATIONS
SUGGESTS A ROLE FOR MACROPHAGE ACTIVATION IN SIV-ASSOCIATED
CARDIAC DISEASE

ABSTRACT

Cardiac abnormalities are common in HIV-infected individuals, and have been especially well-documented as contributors to mortality in HIV-infected children. Underlying pathogenetic mechanisms responsible for myocardial disease in HIV-infection remain imperfectly understood. SIV-infected rhesus monkeys develop a similar spectrum of cardiac lesions to those seen in HIV-infected people, providing an important model for pathogenesis studies. Retrospective analysis of cardiac tissue collected at necropsy from SIV-infected rhesus monkeys was performed to evaluate myocardial macrophage and dendritic cell populations as a function of previously quantitated lymphocytic inflammatory infiltrates and cardiomyocyte degeneration or necrosis. Variations in the size and phenotype of macrophage and dendritic cell populations were examined as possible contributors to the pathogenesis of SIV-associated inflammatory lesions. Macrophages labeling immunohistochemically for CD163 differed substantially from macrophages labeling for HAM56 in overall number, distribution across groups, involvement in inflammatory clusters, correlation with the DC-SIGN$^+$ subpopulation of macrophages , and correlation with numbers of SIV-infected cells. CD163$^+$ macrophages occurred in significantly higher numbers in uninflamed hearts from SIV-infected animals than in hearts from SIV-infected animals with myocarditis or uninfected controls (P< 0.01). Numbers of CD163$^+$ cells correlated positively with numbers of SIV-infected cells (P < 0.05) suggesting that the CD163$^+$ population was associated with decreased inflammatory infiltration and reduced control of virus within the heart. As CD163 has been associated with non-classical macrophage activation and an anti-inflammatory

phenotype, these results suggest that a balance between classical and non-classical

activation may affect levels of inflammatory infiltration and of myocardial virus burden.

Introduction

Currently, an estimated 38.6 million people world-wide are HIV-infected [60]. Cardiac abnormalities, including myocarditis and dilated cardiomyopathy, are common in HIV-infected individuals, and have been especially well-documented as contributors to mortality in HIV-infected children [28, 54]. Underlying pathogenetic mechanisms responsible for myocardial disease in HIV-infection remain imperfectly understood. HIV-associated myocarditis has been a focus of interest given its high rate of occurrence, and the possibility that it may represent an etiologic precursor to cardiomyopathy [28, 63]. While recent reports suggest that use of highly active anti-retroviral therapy (HAART) may have decreased the frequency of HIV-associated myocardial disease, roughly 80% of those in need of anti-retroviral drugs globally still do not have access to them [59, 60].

Macrophages and dendritic cells constitute cell types which are widely distributed throughout peripheral tissues, serving as sentinels of the immune system and able to significantly modulate immune responses through cytokine production. While in some contexts the actions of these populations may result in the development of inflammatory responses, in other contexts their effects may be tolerogenic or overtly anti-inflammatory, with the differences between these scenarios attributable to differences in the phenotypic subsets of cells involved [167, 172, 173]. Immature dendritic cells have been associated with induction of peripheral tolerance, for instance, and non-classically activated macrophages have been associated with anti-inflammatory cytokine production profiles [172, 173]. As different subsets of macrophages and dendritic cells are capable of mediating profoundly different effects in tissue and previous work has demonstrated a

significant inverse correlation between numbers of myocardial DC-SIGN^{+} cells and local T cell infiltration in hearts from SIV-infected animals [158], it was hypothesized that phenotypic variations in antigen presenting cell populations within the myocardium could significantly affect induction of local inflammatory responses.

The simian immunodeficiency viruses (SIV) share a close phylogenetic relationship with HIV-1 and induce a fatal immunodeficiency syndrome in Asian macaques that provides an important model system for the study of HIV pathogenesis [176, 181], Cardiac lesions and dysfunction in SIV-infection of rhesus monkeys (*Macaca mulatta*) closely match those described in HIV infection, suggesting a shared disease mechanism [158, 178]. Cardiomyopathy has been frequently documented among chronically SIV-infected rhesus monkeys, and while randomly distributed myocardial lymphocytic inflammatory infiltrates are frequently identified throughout the four chambers in these populations at necropsy, the inflammatory lesions tend to be mild with minimal associated necrosis [158, 178]. This suggests that factors other than direct myocardial damage by infiltrating inflammatory populations may be responsible for the development of cardiac dysfunction and raises the possibility that secreted soluble mediators may play a role in development of clinically significant cardiac pathology among HIV/SIV-infected individuals. Macrophages and dendritic cells are important producers of inflammatory cytokines and chemokines, many of which have been demonstrated to have potent adverse effects on the heart [77, 113, 125, 134]. This is a point of particular relevance in HIV/SIV infection, a context intrinsically characterized by chronic immune activation and cytokine dysregulation [79, 81]. In the current study,

macrophage and dendritic cell populations are examined in archival myocardial tissue from SIV-infected and uninfected rhesus monkeys in which lymphocytic infiltration, viral involvement, and limited investigations into macrophage population sizes and phenotype have been previously reported [158]. Goals of the current study were to build on previous findings by characterizing the size, distribution, and phenotype of myocardial macrophage and dendritic cell populations, and to investigate a possible role for classical vs non-classical macrophage activation in SIV-associated myocardial inflammation.

Materials and Methods

Tissue Groups. Formalin-fixed paraffin-embedded (FFPE) cardiac tissues from 26 rhesus monkeys (*Macaca mulatta*) from the pathology archives of the New England Primate Research Center were assessed in the present study. As previously described, twenty-one hearts were from SIV-infected animals, 5 were from healthy SIV-negative animals, and all had been previously characterized for myocardial inflammation, cardiomyocyte necrosis, and myocardial viral involvement [158]. Case groupings have been previously described and were based on the presence or absence of lymphocytic infiltrates and cardiomyocyte degeneration or necrosis, in accordance with the Dallas criteria [158, 188]. In brief, H&E stained sections of left ventricle from SIV-positive animals were determined to have active myocarditis (lymphocytic infiltrates in direct association with cardiomyocyte degeneration or necrosis, referred to as the active group), borderline myocarditis (lymphocytic infiltrates with no associated cardiomyocyte degeneration or necrosis, referred to as the borderline group), or to be histologically unremarkable (referred to as the SIV normal group), with each group containing 7 hearts. Hearts from uninfected control animals (control group) contained no histologic lesions. A majority of animals in all SIV-infected groups had AIDS-defining conditions at necropsy. Detailed criteria used in case selection, characteristics of the animals used, and grouping of cases have been described previously [158]. No significant effects of gender, strain of viral inoculum, or number of days post infection were noted with respect to any features examined.

Immunohistochemistry. Immunohistochemistry was performed on FFPE following an ABC immunostaining technique as previously described [187]. Tissues were assessed using antibodies specific for CD163 (clone 10D6, Lab Vision, Fremont CA), HAM 56 (clone HAM56, DakoCytomation, Carpinteria CA), CD83 (clone 1H4b, Vector Laboratories, Burlingame CA), fascin (clone 55K-2, DakoCytomation), HLA-DP, DQ, DR (clone CR3/43, Dakocytomation), and HLA-DR (clone LN-3, Novocastra, Newcastle upon Tyne, United Kingdom). Sections were deparaffinized and rehydrated, followed by incubation in 3% H_2O_2 in phosphate buffered saline (PBS). Antigen retrieval consisted of microwaving in sodium citrate buffer (Vector) or Tris HCl buffer (Lab Vision). Sections were incubated with primary antibody followed by an avidin-biotin block (Vector), and sequential incubation with biotinylated secondary antibody and horseradish peroxidase-conjugated avidin (ABC Standard or ABC Elite, Vector). Antigen-antibody complex formation was detected by use of 3,3'diaminobenzidine (DAB) chromogen (DakoCytomation). Irrelevant, isotype-matched primary antibodies were used in place of the test antibody as negative controls in all immunohistochemical studies.

Image Analysis and Scoring. Sections immunohistochemically labeled for CD163, HAM56, and CD83 were examined with an Olympus Vanox-S AHBS microscope interfaced with a Leica personal computer equipped with Leica QWin image analysis software (Leica Imaging Systems Ltd., Cambridge England), via a DEI 750 charge-coupled device camera (Optronics, Goleta, CA) [197]. In brief, for a single section of left ventricular tissue from each animal, images of 20-30 random fields of myocardium were

captured at 200x magnification. The total number of DAB stained cells per field was quantitated based on the number of flagged foci of discrete signal occupying a minimum number of contiguous pixels. The number of positive cells per mm^2 was calculated based on the known area of each field and total number of positive cells in the overall examined area.

Sections immunohistochemically labeled for HLA-DP, DQ, DR (hereafter referred to as "MHC class II") and fascin were scored semiquantitatively on a 0-3 scale, with scores being applied blinded to group categorization of the samples. Separate scores were assigned for endothelial signal and for non-endothelial signal such that endothelial signal scores took into account only signal lining the myocardial intersitium in a pattern morphologically consistent with endothelium and non-endothelial signal scores took into account only clustered aggregations of signal not histomorphologically consistent with endothelium. In scoring, 0 represented no positive signal; 1 represented infrequent to rare signal; 2 represented moderate signal; and 3 represented extensive signal. Methods used for quantitation of necrosis through application of a rule-based grading schema have been previously described [158]. In brief, two non-serial H&E stained sections of left ventricle from each animal were scored on a 0-3 scale based on the cumulative area of necrosis in the two examined sections. Non-zero necrosis scores occurred exclusively in the active myocarditis group in keeping with the Dallas criteria-based definition of active vs borderline myocarditis.

Confocal Microscopy. Confocal microscopy was performed on FFPE sections using primary antibodies specific for CD163, HAM56, and HLA-DR, as described for single-label immunohistochemistry, as well as anti-DC-SIGN (clone DCN46, BD Pharmingen, San Diego CA), anti-CD3 (rabbit polyclonal, DakoCytomation), anti-SIV nef (clone KK75, donor Dr. K. Kent and Ms C. Arnold, obtained from the NIBSC Centralized Facility for AIDS Reagents supported by EU Programme EVA contract (BMH4 97/2515) and the UK Medical Research Council), and anti-HIV-1 p24/SIV p27 (clone 183-H12-5C, obtained through the NIH AIDS Research and Reference Reagent Program, Division of AIDS, NIAID, NIH: from Dr. Bruce Chesebro and Kathy Wehrly) [198-200]. Briefly, sections were deparaffinized, rehydrated, and subjected to antigen retrieval as for immunohistochemistry, washed in 1x PBS in ultrafiltered water with 0.2% fish skin gelatin (Sigma Aldrich, St. Louis MO) and 0.1% Triton X-100 (Sigma) (PBS-FSG-Triton) and blocked with 10% normal goat serum diluted in PBS-FSG-Triton. Monoclonal primary antibodies were incubated on sections overnight. Polyclonal primary antibody was incubated on sections for 30 minutes. Irrelevant, isotype-matched primary antibodies or rabbit immunoglobulin fraction from healthy non-immunized rabbits (DakoCytomation) were used as irrelevant negative controls for each primary test antibody. Fluorochrome conjugated secondary antibodies (Molecular Probes, Eugene OR) were incubated on sections for 30 minutes. To-Pro3 (Molecular Probes) was incubated on sections for 5 minutes. Confocal microscopy was performed using a Leica TCS SP laser scanning microscope equipped with 3 lasers (Leica Microsystems, Exton PA). Colocalization of antigens was demonstrated by the addition of colors. Single- and

double-color positive controls were run in addition to irrelevant negative controls with each confocal experiment.

As only 5 out of 21 hearts from SIV-infected animal had infected cells evident in the myocardium by nef immunohistochemistry and 3 of these 5 had infected cells occurring only in extremely low numbers, double-label experiments involving the antibodies SIV nef and SIV p27 were conducted using tissue from the 3 cases in which the largest number of SIV-infected cells had been documented by quantitative image analysis in previous work [158]. All specifically-labeled cells in all examined tissue sections were evaluated to ensure consistency of double-labeling patterns.

Statistical Analysis. Significance of differences between groups was determined using Kruskall-Wallis One Way ANOVA on Ranks with post-hoc pairwise comparison by Dunn's test. Significance of distinctions between single paired evaluation categories was determined using the t-test or Mann-Whitney Rank Sum test as appropriate. Linear regressions were conducted to determine significance of correlations between CD163$^+$, HAM56$^+$, and CD83$^+$ population sizes as well as endothelial and non-endothelial signal scores for MHC Class II and fascin (quantitation and scoring described above). Population quantitations and signal scores determined were further analyzed by linear regression with previously determined core parameters reflecting lymphocyte infiltration (CD3$^+$ cells/mm^2), numbers of virally infected cells (SIV nef$^+$ cells/mm^2), preliminary macrophage markers (DC-SIGN$^+$ cells/mm^2, CD68$^+$ cells/mm^2), and necrosis scores.[158] (SigmaStat 3.1, Systat Software, Richmond CA). Probability values of P <

0.05 were interpreted as significant. Statistical analysis of quantitative image analysis data was performed on pooled individual data points for each animal within evaluated groups.

Results

Macrophage phenotype and population size varies significantly across groups

Macrophages were enumerated and characterized using quantitative image analysis of sections immunohistochemically labeled for the macrophage-specific antigens CD163 and HAM56. CD163 is a receptor which mediates endocytosis of hemoglobin-haptoglobin complexes and has been associated with anti-inflammatory effects proceeding via multiple mechanisms [201, 202]. HAM56 is an as yet uncharacterized antigen which labels a large subset of cells of the monocyte-macrophage lineage and is frequently used to define tissue macrophage populations [203, 204]. Numbers of cells positive for each antigen were compared across the four groups: SIV active myocarditis, SIV borderline myocarditis, SIV normal, and uninfected controls. The number of CD163^{+} cells/mm^2 varied dramatically across groups, with the highest numbers of positive cells found in the hearts of SIV^{+} animals with histologically normal myocardium (P < 0.01), (Figure 3.1, A). Cells labeled for CD163 by immunohistochemistry occurred predominantly as individuated cells within the myocardial interstitium and perivascular tissue (Figure 3.2, A). While significantly higher numbers of CD163^{+} cells were found in the active group than the borderline and control groups (P < 0.01), the median number of CD163^{+} cells/mm^2 in the active group (2.4 cells/mm^2) was 40 times lower than that of the SIV normal group (96.4 cells/mm^2), and maximal values in the active group (67 cells/mm^2) were less than half those of the SIV normal group (142 cells/mm^2), (Figure 3.1, A). Numbers of CD163^{+} cells were disproportionately increased in the active myocarditis group relative to the borderline group, but median values for numbers of

CD163$^+$ cells/ mm^2 between the active and borderline groups were essentially identical

(2.4 positive cells/mm^2 vs 3.2 positive cells/mm^2, respectively). The significant

difference between these two groups arose due to high CD163$^+$ cell numbers in a

minority of active myocarditis hearts that had especially low levels of T cell infiltration

based on image analysis for CD3$^+$ cells, suggesting a strong propensity for higher

numbers of CD163$^+$ cells to be associated with lower levels of lymphocytic infiltration,

irrespective of the presence or absence of necrosis.

Numbers of myocardial HAM56$^+$ cells/mm^2 showed less variability across groups

than numbers of CD163$^+$ cells, but were significantly higher in the active group than in

any other group ($P < 0.05$) (Figure 3.1, B). Similar to CD163$^+$ cells, HAM56$^+$ cells

occurred widely distributed within the myocardial interstitium and perivascular tissue

(Figure 3.2, B-C). Numbers of myocardial CD163$^+$ cells/mm^2 differed significantly from

numbers of HAM56$^+$ cell/mm^2 in evaluated hearts overall ($P < 0.001$), with significant

differences in expression frequency of the two markers in the active myocarditis group (P

< 0.01), the borderline myocarditis group ($P < 0.01$), and the uninfected control group (P

< 0.01).

Differences in distribution and correlations of CD163$^+$ and HAM56$^+$ cells

Numbers of SIV infected cells cells/mm^2 as previously determined by quantitation of

cells labeling positive for SIV nef protein [158], correlated significantly with numbers of

CD163$^+$ cells/mm^2 ($P < 0.05$, $R = 0.465$), but not with numbers of HAM56$^+$ cells/mm^2 (P

$= 0.833$, $R = 0.049$). Neither CD163$^+$ cell numbers nor HAM56$^+$ cell numbers showed

significant correlations with previously quantitated numbers of CD3$^+$ cells/mm^2 or necrosis scores. Therefore, CD163$^+$ macrophage populations demonstrated a significant relationship with numbers of virally infected cells which HAM56$^+$ macrophage populations lacked, but neither population had a detectable correlation with the extent of myocardial inflammation or necrosis.

Numbers of cells positive for CD163 correlated significantly with numbers of cells positive for all other examined macrophage markers including cells positive for HAM56 ($P < 0.01$, $R = 0.512$), and cells positive for the previously quantitated markers DC-SIGN ($P < 0.001$, $R = 0.715$) and CD68 ($P < 0.05$, $R = 0.489$). Numbers of CD163$^+$ cells correlated particularly strongly with numbers of DC-SIGN$^+$ cells, a population which has been previously demonstrated to have a significant inverse correlation with myocardial T cell infiltration in hearts from SIV-infected animals [158]. Numbers of HAM56$^+$ cells also demonstrated a significant correlation with numbers of DC-SIGN$^+$ cells, but the correlation was much weaker than that shown by CD163$^+$ cells ($P = 0.041$, $R = 0.403$). Numbers of HAM56$^+$ cells did not correlate significantly with numbers of CD68$^+$ cells ($P = 0.07$, $R = 0.362$).

While both CD163$^+$ and HAM56$^+$ macrophages occurred predominantly in a dispersed distribution within the myocardial interstitium and perivascular connective tissue (Figure 3.2, B), marked differences were noted in the involvement of the two populations in focal aggregates of inflammatory cells. HAM56 signal within clusters of inflammatory cells was frequently extensive and strong, with only sparse CD163 signal in serial sections of the same clusters (Figure 3.2, D-E). The different levels of

involvement of these populations in such cellular aggregates suggests that HAM56$^+$ cells may play a role distinct from CD163$^+$ cells in the myocardial inflammatory response in SIV-infection.

All myocardial SIV-infected cells and all myocardial DC-SIGN$^+$ cells are CD163$^+$

Double-label confocal microscopy showed the significant correlations between CD163$^+$ population size and numbers of SIV-infected cells, DC-SIGN$^+$ cells, and HAM56$^+$ cells to be due at least in part to co-expression of the evaluated markers. Double-labeling for SIV nef antigen and CD163 showed SIV nef signal occurring exclusively in CD163$^+$ cells, though these cells constituted a minority of the total CD163$^+$ population (Figure 3.3, A). Double-labeling studies for SIV p27 antigen and CD163 yielded findings identical to those determined for nef and CD163, confirming the restriction of SIV infection to CD163$^+$ cells (results not shown). Double-labeling studies for CD163 and DC-SIGN demonstrated DC-SIGN signal also to be consistently localized to CD163$^+$ cells, though CD163$^+$/DC-SIGN$^-$ cells were common (Figure 3.3, B). Double-labeling for CD163 and HAM56 demonstrated moderate numbers of cells positive for both markers in some hearts (Figure 3.3, C). CD163$^+$/HAM56$^+$ phenotypes, CD163$^+$/HAM56$^-$ and CD163$^-$/HAM56$^+$ phenotypes were all identified; however, with distributional frequency varying markedly across individual cases.

Endothelial MHC class II expression correlates inversely with DC-SIGN$^+$ cell numbers

MHC class II expression was evaluated as a marker for macrophage and dendritic cell activation. Strong MHC class II expression was present diffusely in many inflammatory clusters (Figure 3.4, A). Expression scores differed significantly across groups ($P < 0.01$), with higher scores in the active group than among uninfected controls ($P < 0.05$). Double-labeling studies examining distribution of HLA-DR and CD3 antigens resolved the MHC class II signal onto a set of discretely labeled cells, interspersed among T cells (Figure 3.4, B).

MHC class II expression scores correlated significantly with previously determined numbers of myocardial CD3$^+$ cells ($P < 0.05$) and scores for necrosis ($P < 0.001$, $R = 0.654$), and by confocal microscopy showed a pattern of distribution in inflammatory clusters similar to that noted for HAM56 by immunohistochemistry (Figure 3.4, B and Figure 3.2, E).

Strong MHC class II labeling of microvascular endothelium in hearts from uninfected control animals was also present. Expression was variably reduced in hearts from SIV-infected animals, with hearts from animals of the active group in most cases having levels of signal indistinguishable from controls (Figure 3.4, C), but a majority of hearts in the SIV normal group having profound reduction or elimination of endothelial MHC class II signal. Differences in endothelial MHC class II scores between groups were significant ($P < 0.05$), and there was a significant inverse correlation between endothelial MHC class II scores and DC-SIGN$^+$ cell numbers ($P < 0.01$, $R = -0.517$), suggesting a role for this population in homeostasis of MHC class II expression by cardiac endothelium (Figure 3.5).

Distribution and correlations of the dendritic cell markers CD83 and fascin

Myocardial dendritic cell populations were evaluated using the antigens CD83 and fascin. Signal for CD83, an adhesion molecule of the immunoglobulin superfamily and highly specific marker for mature and activated dendritic cells [205, 206], and non-endothelial signal for fascin, a 55kD actin bundling protein expressed at high levels in mature dendritic cells [207], were identified almost exclusively in hearts from the two myocarditis groups. CD83^{+} cells occurred in very low numbers, both individuated in the myocardial interstitium and in small aggregates within clusters of inflammatory cells (Figure 3.6, A). CD83^{+} cell numbers correlated strongly with levels of T cell infiltration (P < 0.001, R = 0.923), (Figure 3.6, B).

Distribution of fascin signal differed from that of CD83, with signal occurring in both endothelial and inflammatory-cluster-associated non-endothelial patterns which were separately scored. The non-endothelial signal pattern was found exclusively within clusters of inflammatory cells and occurred predominantly in the active myocarditis group (Figure 3.6, C). Non-endothelial fascin scores differed significantly across groups (P < 0.05), with scores being significantly higher in the active group than in the SIV normal group (P < 0.05). Non-endothelial fascin scores did not correlate significantly with numbers of myocardial CD3^{+} T cells (P = 0.679), but did correlate strongly with necrosis scores (P < 0.001, R = 0.635). Neither non-endothelial fascin scores nor CD83^{+} cell numbers correlated significantly with any of the evaluated macrophage markers, or with numbers of SIV infected cells. Endothelial fascin scores unlike inflammatory-

cluster-associated fascin scores did not differ significantly across groups. However, like

the inflammatory-cluster-associated scores, endothelial fascin scores showed a significant

positive correlation with necrosis scores ($P < 0.05$, $R = 0.467$) and did not demonstrate

any other significant correlations.

Discussion

In hearts examined in the current study, CD163^{+} macrophages, which have been associated with an anti-inflammatory phenotype, occurred in significantly higher numbers in uninflamed hearts from SIV-infected animals than in hearts from SIV-infected animals with myocarditis or uninfected controls. In addition, numbers of CD163^{+} cells showed a significant positive correlation with cell-associated myocardial virus burden. CD163^{+} macrophages have been associated with decreased lymphocyte activation, with inhibition of lymphocyte proliferation through release of soluble CD163 cleaved from the membrane, and with anti-inflammatory cytokine production profiles [173-175, 202, 208-214]. Given this, our findings suggest that soluble mediators generated by the CD163^{+} population may have served to minimize lymphocytic infiltration, but possibly at the cost of increased tolerance of local viral infection.

While overall numbers of CD163^{+} cells in examined hearts did not correlate significantly with levels of T cell involvement, the DC-SIGN^{+} subpopulation of CD163+ cells has previously been shown to correlate inversely with T cell infiltration, suggesting distinct functional roles for particular macrophage phenotypes within the myocardium [158]. Further supporting a unique role for this subpopulation was the finding of a significant inverse correlation between numbers of DC-SIGN^{+} cells and quantity of endothelial MHC class II signal, suggesting that secreted mediators produced by this population may modulate endothelial MHC class II expression.

HAM56[+] macrophages, in contrast, appeared in the highest numbers in hearts of animals with active myocarditis and occurred in disproportionately high numbers in the

inflammatory foci found exclusively in hearts of the two myocarditis groups. Hearts from the two myocarditis groups have been shown in previous work to contain significantly lower numbers of SIV-infected cells relative to hearts of the SIV normal group [158], suggesting that the inflammatory response present in the hearts of the myocarditis groups plays a role in containing local myocardial virus. However, many proinflammatory mediators, the secretion of which is characteristic of classically activated macrophages, have been shown in model systems to have significant adverse effects on the myocardium even in the absence of cardiomyocyte necrosis or apoptosis [77]. High levels of inflammatory cytokines have been demonstrated to be capable of inducing cardiomyopathy and heart failure in experimental models [134].These findings suggest that macrophages of the HAM56$^+$/CD163$^-$ phenotype while associated with better control of local virus as part of a classical inflammatory response, may generate soluble mediators that could be associated with independent pathologic sequelae through direct effects on cardiomyocyte contractile function and/or hypertrophic gene expression patterns and through chemokine secretion attracting inflammatory cell populations into the tissue. The fact that numbers of HAM56$^+$ cells showed no significant correlation with measures of T cell infiltration or necrosis suggests that overall HAM56$^+$ cell numbers within the myocardium are likely to be determined by features other than simple responsiveness to inflammatory stimuli, though such responsiveness may be superimposed on effects of other factors determining steady state levels of resident macrophages within myocardial tissue.

SIV-infected cells within examined hearts were found to be uniformly CD163$^+$, a finding consistent with a recent report demonstrating uniform expression of CD163 by SIV-infected cells in the brain, but contrasting with another report which found consistent downregulation of CD163 in HIV-infected macrophages *in vitro* [215, 216]. While productive SIV infection of DC-SIGN$^+$ cell populations has been documented by other investigators in macaque intestinal tissue, previous work in cardiac tissue from this cohort has demonstrated that SIV-infected cells are consistently HAM56$^+$ and DC-SIGN$^-$, strongly suggesting that it is the CD163$^+$/HAM56$^+$ double-positive subpopulation which demonstrates productive SIV-infection, and that this population is distinct from the CD163$^+$/DC-SIGN$^+$ population [158, 217].

In contrast to patterns identified for macrophage populations, distributional and correlative patterns of the activated dendritic cell markers CD83 and fascin suggest that they predominantly constituted reactive subsets responding to inflammation and necrosis present in hearts with myocarditis.

In conclusion, the striking differences in frequency of specific macrophage phenotypes among groups, their different levels of involvement directly within inflammatory lesions, and the prominent manifestation of a population which has been associated with an anti-inflammatory character in hearts lacking inflammation and with higher levels of myocardial virus, strongly suggests a role for macrophage phenotypic differences in susceptibility or protection from SIV-associated myocarditis, and raises the question whether myocardial macrophage populations may not also play an important

role in the development of cardiomyopathy through cytokine-mediated effects on the

local tissue milieu.

Figure 3.1 Image analysis-based quantitation of CD163$^+$ and HAM56$^+$ cells by group. **A:** The number of CD163$^+$ cells per unit area as measured by quantitative image analysis was significantly higher in the SIV normal and active myocarditis groups than in the borderline myocarditis or uninfected control groups ($P < 0.01$). Numbers of CD163$^+$ cells per unit area were significantly higher in the SIV normal group than in the active myocarditis group ($P < 0.01$). The median number of CD163$^+$ cells/mm^2 in the SIV normal group (96 cells/mm^2, central bar in box) was 40 times higher than the median number of CD163$^+$ cells/mm^2 in the active myocarditis group (2.4 cells/mm^2, indicated by arrow). **B:** The number of HAM56$^+$ cells per unit area was significantly higher in the active myocarditis group than in the borderline myocarditis group ($P < 0.01$), the SIV normal group ($P < 0.05$), or the uninfected controls group ($P < 0.01$). The number of HAM56$^+$ cells per unit area in the SIV normal group was higher than in the uninfected control group ($P < 0.01$). Differences in numbers of HAM56$^+$ cells per unit area between the borderline myocarditis and uninfected control groups were not significant. Boxes represent the 25th to 75th percentile of values within each group. Central lines within boxes represent median values. Boxes without evident central lines have median values visually indistinguishable from the box minimum (**A:** active myocarditis and control groups).

Figure 3.1
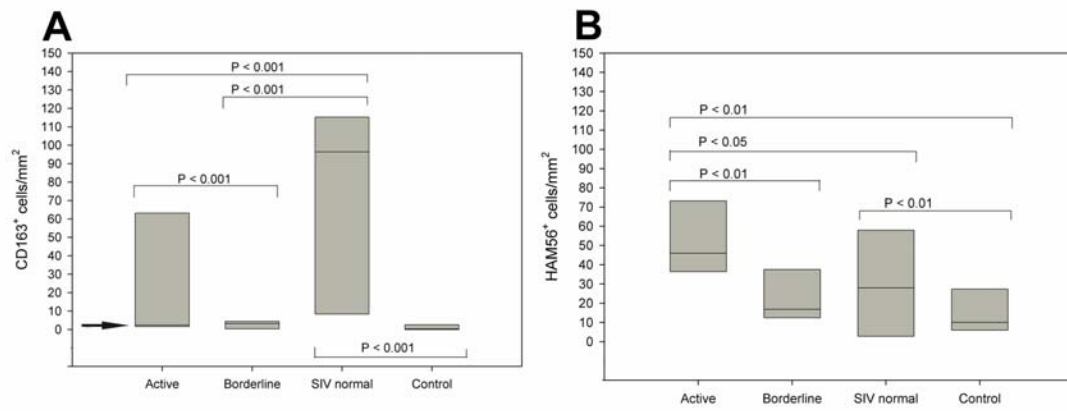
Figure 3.2 Immunophenotype, distribution, and morphology of macrophages within inflamed and uninflamed myocardium. **A:** CD163 cells had spindloid to occasionally stellate or rounded morphology and occurred predominantly as individuated cells within the myocardial interstitium and perivascular tissue. The frequency of positive cells varied across individual hearts from rare to profuse, with the highest numbers of positive cells occurring among hearts in the SIV normal group, in which histologic evidence of inflammation was absent. (CD163 immunohistochemistry with Mayer's hematoxylin.) **B:** HAM56$^+$ cells occurred widely distributed within the myocardial interstitium and perivascular connective tissue. The highest numbers of positive cells were found among hearts in the SIV-positive, active myocarditis group. (HAM56 immunohistochemistry with Mayer's hematoxylin.) **C:** Morphology of HAM56+ cells ranged from elongate and spindled to compact and stellate. (HAM56 immunohistochemistry with Mayer's hematoxylin.) **D:** CD163 signal was identified within myocardial clusters of inflammatory cells, but signal was often sparse and occurred in dramatically lower numbers than HAM56 signal present in serial sections of the same cluster, (compare to **(E)**). (CD163 immunohistochemistry with Mayer's hematoxylin.) **E:** HAM56 signal within myocardial clusters of inflammatory cells was frequently extensive and strong, indicating the presence of a substantial macrophage population within such clusters (HAM56 immunohistochemistry with Mayer's hematoxylin.)

Figure 3.2
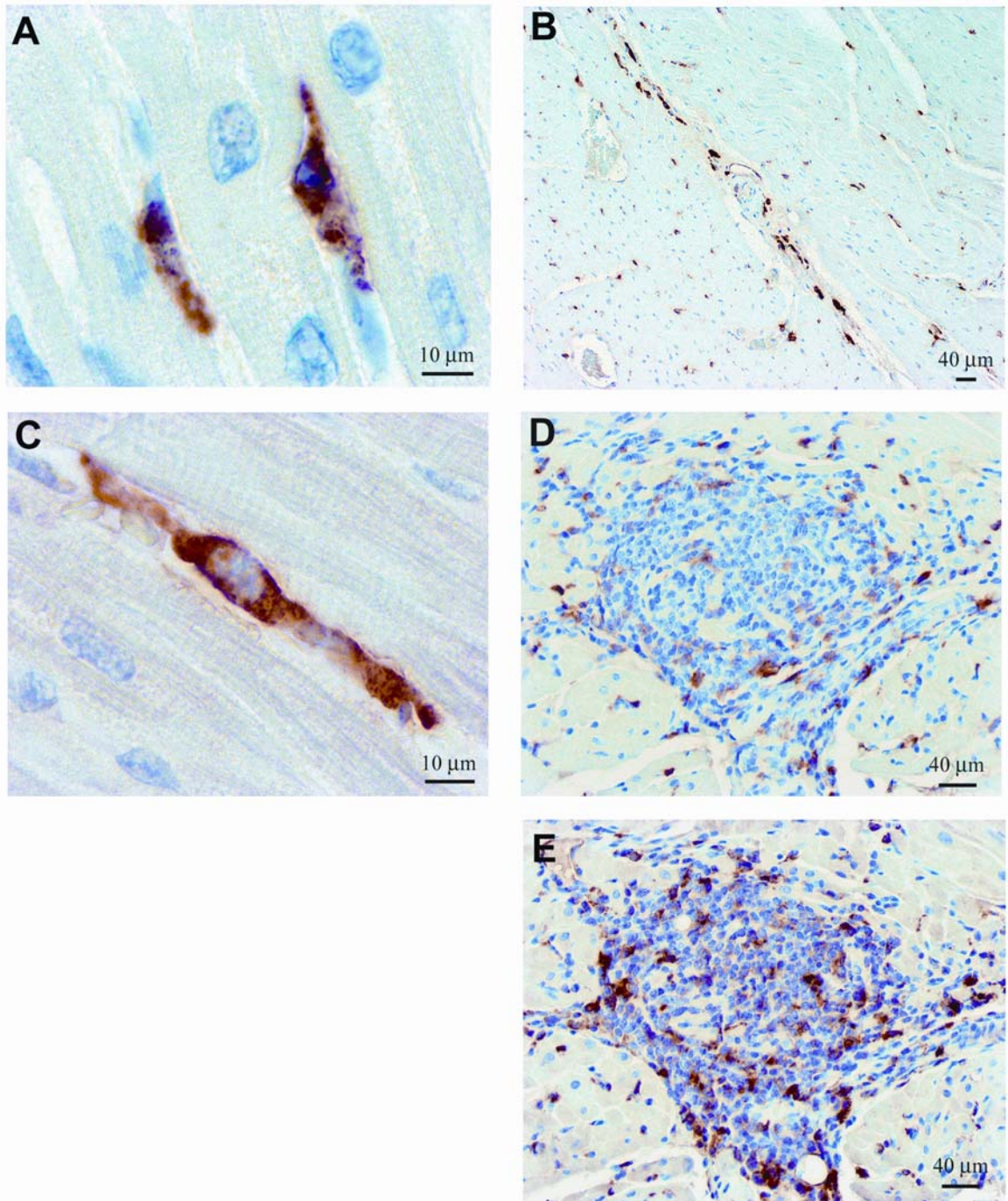
Figure 3.3

DC-SIGN$^+$ cells and SIV-infected cells represent subsets of the CD163$^+$ macrophage population. **A:** Double-label immunofluorescence confocal microscopy for CD163 and SIV nef protein showed productive infection of a subset of CD163$^+$ cells. Nef$^+$/CD163$^-$ cells were not identified.(CD163 and SIV nef immunofluorescence.) **B:** Double-label immunofluorescence confocal microscopy for CD163 and DC-SIGN showed delicate membranous colocalization of signal in a subset of spindloid interstitial cells. (CD163 and DC-SIGN immunofluorescence.) **C:** Double-label immunofluorescence confocal microscopy for CD163 and HAM56 showed many cells positive for both CD163 and HAM56 signal. Signal varied from multifocal, noncolocalizing as shown, to diffusely colocalized (CD163 and HAM56 immunofluorescence).

Figure 3.3
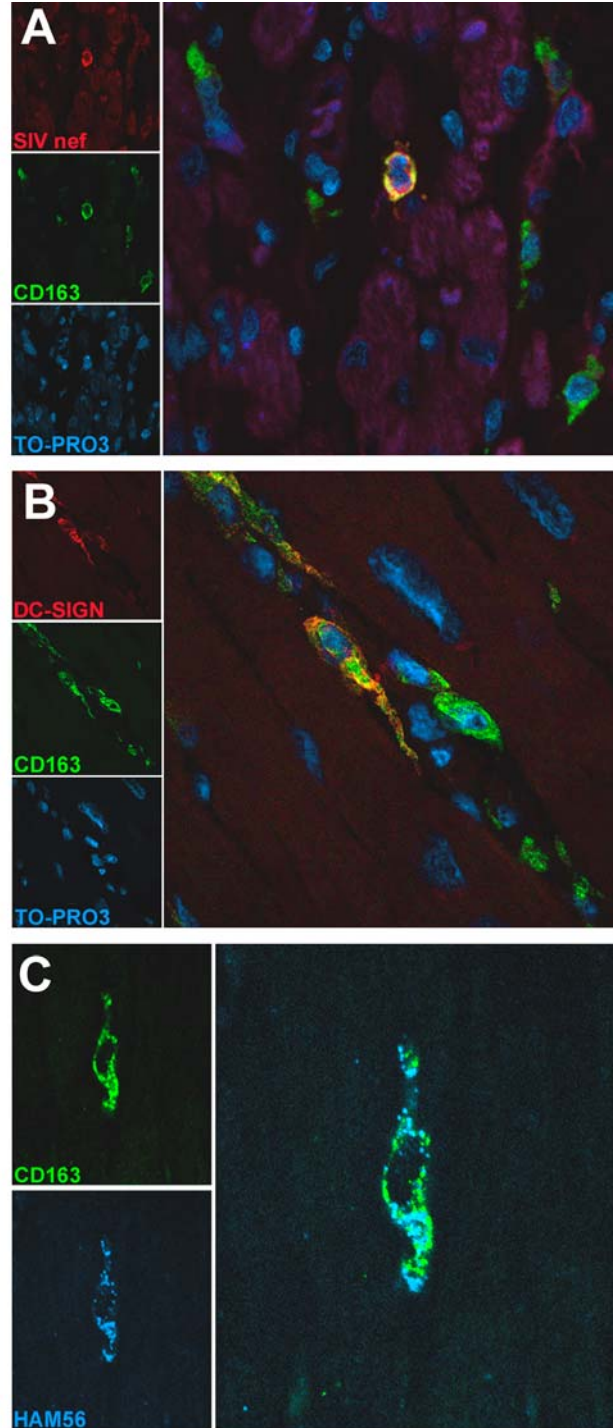
Figure 3.4 Intramyocardial MHC class II expression **A:** Profuse MHC class II signal within clusters of inflammatory cells was often strong enough to significantly obscure nuclei of cells within the cluster. (HLA-DP, DQ, DR immunohistochemistry with Mayer's hematoxylin.) **B:** Double-label immunofluorescence confocal microscopy consistently demonstrated failure of colocalization of MHC class II signal with CD3, instead labeling a separate population of often very numerous interspersed, discrete, CD3⁻ round cells. (HLA-DR and CD3 immunofluorescence, 400x magnification.). Dispersed punctate to linear regions of intense 3-way colocalization not associated with the central inflammatory cell cluster are a product of erythrocyte autofluorescence in the myocardial microvasculature. **C:** MHC class II expression by cardiac microvascular endothelium in uninfected controls was profuse and strong. Expression was variably reduced in hearts from SIV-infected animals. Hearts from the active myocarditis group most closely resembled those of uninfected controls while dramatic reduction or elimination of signal was often found in hearts from the SIV normal group. (HLA-DP, DQ, DR immunohistochemistry with Mayer's hematoxylin.)

Figure 3.4
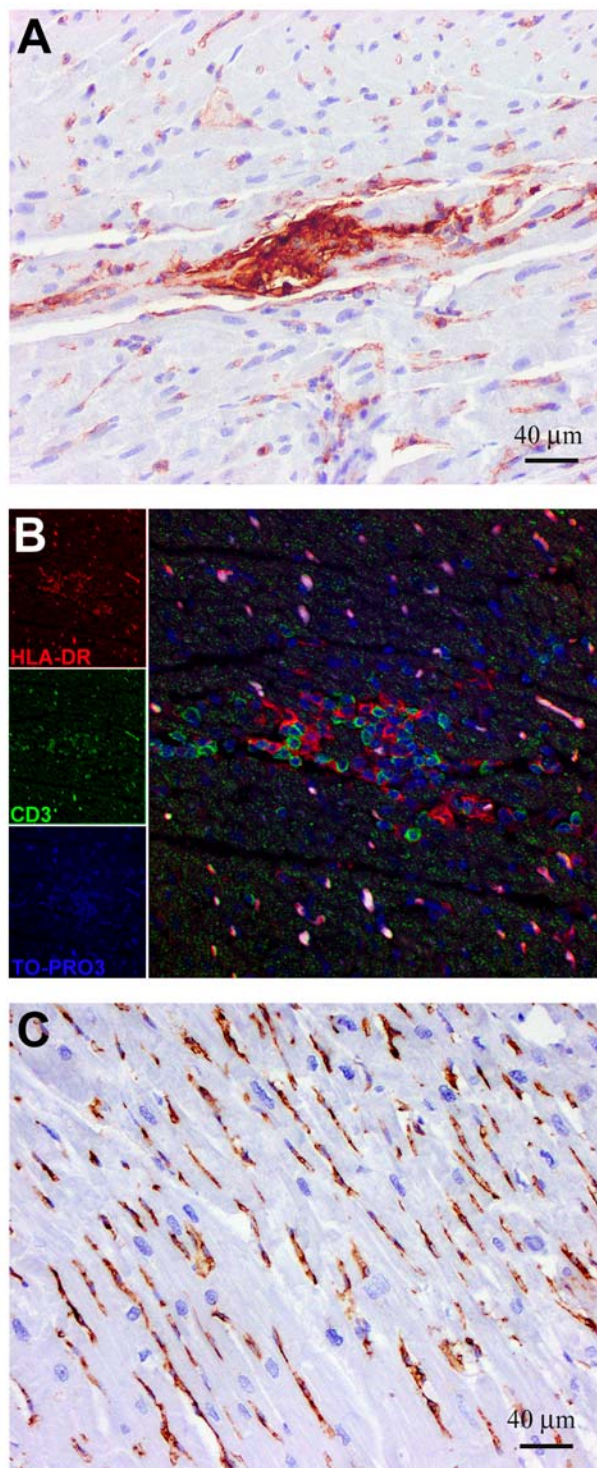
Figure 3.5 A statistically significant inverse correlation was present between endothelial

MHC class II scores and numbers of DC-SIGN$^+$ cells/mm^2 (P < 0.01, R = -0.517).

Figure 3.5
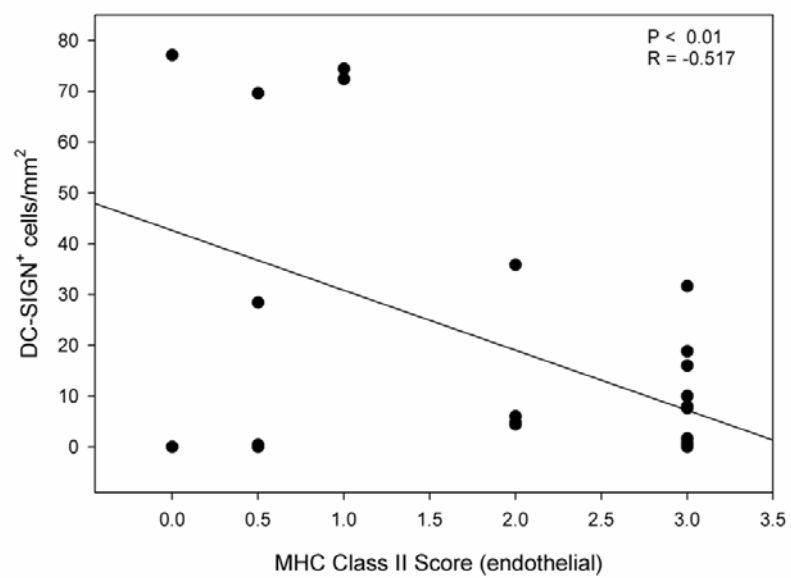
Figure 3.6 Morphology and distributional patterns of cells labeled with the dendritic cell

markers CD83 and fascin and correlation of myocardial CD83^{+} cell numbers with T cell

infiltration. **A:** CD83^{+} cells occurred in low numbers, being found both individuated in

the myocardial interstitium and rarely in small aggregates within clusters of inflammatory

cells, as shown. (CD83 immunohistochemistry with Mayer's hematoxylin.) **B:** A highly

significant correlation was present between the number of myocardial CD83^{+} cells/mm^2

and the number of myocardial CD3^{+} cells/mm^2, (P < 0.001). **C:** Strong fascin signal was

found within clusters of inflammatory cells, with signal typically arborizing through

interstitial spaces between individual cells within the cluster. (fascin

immunohistochemistry with Mayer's hematoxylin.)

Figure 3.6

A

B

C

$P < 0.001$
$R = 0.923$

$CD3^+$ cells/mm^2

$CD83^+$ cells/mm^2

25 µm

40 µm
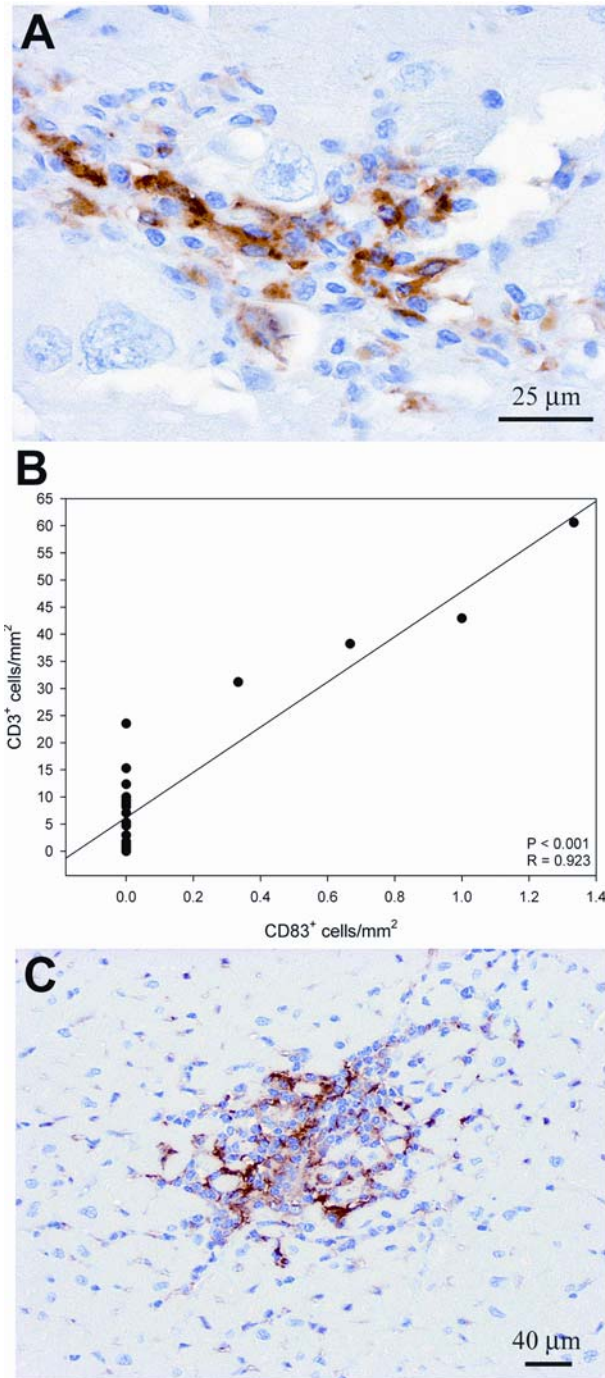
CHAPTER IV

ANTIGENIC STIMULATION IN THE SIMIAN MODEL OF HIV INFECTION
YIELDS DILATED CARDIOMYOPATHY THROUGH EFFECTS OF TNFα

ABSTRACT

Objective: To investigate a role for endogenous myocardial cytokine production in development of HIV-associated cardiomyopathy.

Design: Cardiomyopathy is a late-stage sequela of HIV infection. While pathogenesis of this condition in HIV infection is poorly defined, inflammatory cytokines are recognized for their detrimental effects on myocardial structure and function. HIV infection is characterized by chronic immune activation and inflammatory cytokine dysregulation. As the myocardium itself is a rich potential source of inflammatory cytokines, HIV-mediated cytokine dysregulation may be an important contributor to development of HIV cardiomyopathy. An antigenic stimulation protocol conducted in the SIV model of HIV infection was used to study effects of endogenous cytokine production on myocardial structure and function.

Methods: Twenty-six rhesus monkeys were assigned to treatment groups for a 35 day study. Animals were SIV-infected; SIV-infected and treated with killed *Mycobacterium avium* complex bacteria (MAC); SIV-infected, MAC-treated, and given the TNFα antagonist etanercept; or uninfected and MAC-treated. All animals were given weekly echocardiograms. Hearts were collected for further evaluation at euthanasia.

Results: SIV-infected, MAC-treated animals developed significant systolic dysfunction (left ventricular ejection fraction (LVEF) decline of 19±2 %) and ventricular chamber dilatation (left ventricular end-diastolic diameter (LVEDD) increase of 26±6 %) not seen

in other groups. Concurrent treatment with etanercept prevented development of these changes, implicating a causative role for myocardial TNFα.

Conclusions: SIV-infected animals develop exaggerated myocardial pathology on stimulation with the ubiquitous environmental agent MAC. These responses are TNFα-dependent and may play a significant role in development of cardiomyopathy in HIV infection.

Introduction

Ventricular dysfunction and dilated cardiomyopathy are well-documented sequelae of late-stage HIV infection [28, 37, 38, 53]. Factors influencing development of myocardial pathology in HIV infection are at present poorly defined. Hypothesized mechanisms have included cytokine-induced effects, tissue damage resulting from myocarditis, drug-induced cardiotoxicities, and effects of viral proteins [63, 76, 87, 89, 91, 99, 100]. While current evidence suggests that highly active anti-retroviral therapy (HAART) has reduced the incidence of clinically significant cardiac disease among HIV-infected people, such treatment is available to only a minority of those in need [59, 60]. In addition, HIV infection provides a defined venue for exploring the role of chronic immune activation and host inflammatory response in development and progression of myocardial injury, features which have relevance beyond the context of HIV-infection itself.

The myocardial tissue environment is a rich potential source of inflammatory cytokines, with both cardiomyocytes and local non-cardiomyocyte cell populations competent to produce a variety of inflammatory mediators, and heart tissue capable of generating as much or more TNFα per gram of tissue in response to endotoxin stimulation as liver or spleen [126, 151, 152, 155]. Non-myocyte populations comprise up to 70% of the total cellular constituency of the myocardium and consist of a mixed assemblage of cell types, including substantial populations of dendritic cells and macrophages [151, 156-159]. This represents a volatile setting in the context of HIV

infection, which is intrinsically characterized by chronic immune activation and inflammatory cytokine dysregulation [79, 81]. Inflammatory cytokine-induced myocardial dysfunction is a well-documented phenomenon in multiple experimental models, is a significant contributor to hemodynamic compromise in sepsis, and may play a contributory role in development and progression of heart failure regardless of initiating etiology [77, 78, 113, 129, 130, 134]. Mechanisms of cytokine-induced contractile dysfunction are complex and multifactorial [77].

Study of the pathogenesis of HIV-associated cardiomyopathy (HIVCM) in humans is limited by many factors. Identifying the earliest time points of development of myocardial pathology and placing them within the natural history of HIV infection is generally not possible; complex, variable, and potentially toxic medication regimens are routinely used; and there may be substantial variation in environment and lifestyle among patients. The SIV model of HIV infection is well-established, has been extensively characterized, and provides a strong context for study of HIVCM in that dilated cardiomyopathy and histologic myocardial lesions similar to those documented in HIV infection are frequently seen in chronically SIV-infected rhesus monkeys, implying a shared pathogenesis [158, 178].

In the present study, an acute SIV infection model employing recurrent antigenic stimulation with whole, heat-killed *Mycobacterium avium* complex (MAC) bacteria was used to evaluate patterns of early SIV-associated myocardial injury. Pathogenesis studies focused on early time points post-infection allow evaluation of changes while viral loads are high, sufficient immune competence is retained to prevent opportunistic infections,

and effects of viral replication or viral determinants can be examined without complication by effects of differential disease progression. MAC bacteria are environmentally ubiquitous and disseminated MAC infections are among the most common opportunistic infections encountered in AIDS patients [218-220]. The MAC stimulation protocol applied represents an experimentally-induced augmentation of normal environmental antigenic stimulation, using an organism with a high degree of clinical relevance to late-stage HIV and SIV infection.

Materials and Methods

Animals and Study Design. Twenty-six male rhesus macaques (*Macaca mulatta*) aged 2 to 4 years were housed at the New England Primate Research Center (NEPRC) in a biolevel 3 animal-containment facility in accordance with standards of the Association for Assessment and Accreditation of Laboratory Animal Care and Harvard Medical School's Animal Care and Use Committee. Prior to initiation of experimental protocols, all animals tested negative for infection with simian retrovirus type D, SIV, simian T-lymphotropic virus-1, and herpes B virus. Animals were divided into 4 cohorts for study over a 35 day period. Eighteen animals were subjected to infection with uncloned, pathogenic SIVmac251 (25ng p27 antigen in 1mL sterile phosphate buffered saline (PBS), IV) at day 0. Of these, 12 animals received 4 doses of heat-killed *Mycobacterium avium* complex bacteria (MAC, 10^7 CFU-equivalents in 1mL sterile PBS per administration, IV) with the first dose given at day 7, then repeated on days 12, 14, and 21. Of the 12 SIV-infected, MAC-treated animals, 4 were treated with the TNFα antagonist etanercept (Enbrel™, Amgen, Thousand Oaks, CA) at 0.4mg/kg, IM every other day for the duration of the study. A control group of 8 SIV-uninfected animals was administered MAC treatments as described on the same schedule as the SIV-infected, MAC-treated animals. Blood drawn from all animals before virus inoculation at day 0, and weekly thereafter was evaluated for circulating cytokine and chemokine levels, peripheral T cell subset composition, and plasma viral load evaluation as appropriate. Echocardiograms were performed weekly, including prior to SIV inoculation on day 0, and prior to MAC treatments on days 7, 14, and 21. All echocardiographic studies were

conducted under ketamine sedation (10-15 mg/kg, IM). All SIV-infected animals and 4 of the 8 uninfected, MAC-treated animals were euthanized at the end of the study (30 mg/kg pentobarbital sodium, IV, followed by 2 mEq/kg potassium chloride, IV). Complete gross and microscopic post-mortem examinations were performed on all euthanized animals. Hearts were removed with myocardial tissue snap frozen and collected into formalin within 15 minutes of confirmation of death.

***Mycobacterium avium* Complex (MAC) Inocula.** The MAC isolate used (no. 88415) was derived from a case of spontaneous disseminated mycobacterial disease in a rhesus monkey with simian AIDS, and retains the ability to generate disseminated infections in SIV-infected animals when not inactivated.[221] Frozen stocks of the isolate were grown out in Middlebrook 7H9 broth at 37° C and 5% CO_2 for 8 days, titered, diluted to 10^7 CFU/mL in PBS, and killed by immersion in boiling water for 2 minutes. One mL of the heat-treated preparation was administered intravenously per animal per MAC treatment. The inoculum used produced no systemic signs of illness in treated animals as determined by clinical veterinary staff.

Echocardiography. M-mode and 2D echocardiograms were performed using a Hewlett Packard Image Point HX ultrasound machine and 5MHz transducer. Standard parasternal long and short axis views as well as standard two and four chamber apical views were obtained and recorded on VHS tape for later analysis using ImageView DCR (Nova Microsonics, Mahwah, NJ) and modified American Society of Echocardiography

volumetric analysis and regional and global wall motion scores. Heart rate was recorded using lead II of standard ECG. Analyses were conducted blinded to animal group allocations.

ELISAs. Commercial ELISA kits for soluble TNF receptors 1 and 2 (sTNFR1 and sTNFR2), monocyte chemoattractant protein-1 (MCP-1), and interleukin-18 (IL-18) (R&D Systems, Minneapolis, MN) were used on batched samples of previously frozen plasma according to manufacturers' instructions. Evaluation of sTNFR2 levels in animals treated with etanercept was not possible due to cross-reactivity of the assay with etanercept itself.

Western Blot. Membrane fractions prepared using differential centrifugation of homogenates of snap frozen myocardial apex and semitendinosus muscle collected at necropsy were subjected to electrophoretic separation by SDS-PAGE, and electrotransferred onto PVDF membrane (Immobilon-P^{SQ}, Millipore, Bedford, MA). Nonspecific protein binding was blocked and membranes were probed with primary antibody (anti-TNFα, AB-210-NA and clone 28410, R&D; anti-iNOS, clone 54, BD Biosciences, San Jose, CA). Blots were washed and incubated with secondary antibody conjugated to horseradish peroxidase (A5420, Sigma Aldrich, Milwaukee, WI; sc-2005, Santa Cruz Biotechnology, Santa Cruz, CA). Immunoreactive proteins were detected by chemiluminescence (PerkinElmer, Boston, MA) and exposed to X-ray film (Hyperfilm ECL, Amersham Pharmacia Biotech, Piscataway, NJ). Densitometric analysis of bands

was carried out using a Personal Densitometer SI and Image QuanNT Software (Molecular Dynamics, Sunnyvale, CA).

Progression of SIV infection. Plasma viral loads were determined by quantitative reverse transcription PCR, as described previously [222]. T cell subsets and total lymphocyte counts were monitored weekly throughout the study period.

Histologic Examination and Immunohistochemistry. Left and right ventricular free wall, interventricular septum, left and right atria, and aortic outflow tract were histologically examined for each animal. Immunostaining was performed as previously described, using an avidin-biotin complex method with diaminobenzidine (DAB, DakoCyomation, Carpineteria, CA) as chromogen [158]. Tissues were evaluated using antibodies specific for CD3 (A0452, DakoCytomation), cleaved caspase 3 (9661L, Cell Signaling Technology, Beverly, MA), SIV nef (clone KK75, donor Dr. K. Kent and Ms C. Arnold, from NIBSC Centre for AIDS Reagents supported by EU Programme EVA contract (QLKZ-CT-1999-00609) and the UK Medical Research Council), HIVp24/SIV p27 (clone 183-H12-5C, obtained through NIH AIDS Research and Reference Reagent Program, Division of AIDS, NIAID, NIH: from Dr. Bruce Chesebro and Kathy Wehrly), rhesus cytomegalovirus IE1 protein (polyclonal, provided by Dr. Peter Barry, UC Davis), and adenovirus (clone 20/11, Chemicon International, Temecula, CA) [198].

Tissue Scoring. Myocardial tissue was scored in a blinded fashion for lymphocytic infiltration using a grading schema applied to sections immunohistochemically labeled for CD3, as previously described [158].

Statistical Analysis. Significance of differences between groups was determined using One Way ANOVA and Kruskall-Wallis ANOVA on Ranks as appropriate, with post-hoc pairwise comparison by Holm-Sidak or Dunn's method, respectively. Linear regressions were conducted to determine significance of correlations. All analyses were conducted with commercially available software (SigmaStat 3.1, Systat Software, Richmond CA). Probability values of $P < 0.05$ were interpreted as significant.

Results

Mycobacterial Antigenic Stimulation Yields Biventricular Dilatation and Myocardial Dysfunction in SIV-infected Rhesus Monkeys which is Preventable by TNFα Blockade

Significant biventricular chamber dilatation developed among SIV-infected, MAC-treated animals (SIV+MAC group) by day 35 as evidenced by increased right and left ventricular end-diastolic and end-systolic diameters relative to baseline ($P < 0.001$) (Table 4.1). Chamber diameters of MAC-treated, uninfected controls (MAC group) also showed significant changes relative to baseline ($P < 0.05$), but these were mild and consistent with dilatation only in the right ventricle (Table 4.1). Significant changes in chamber diameter were absent in SIV-infected animals not treated with MAC (SIV group) (Table 4.1).

Significant decreases in systolic function developed in SIV+MAC animals over the course of the study period as identified through declines in right and left ventricular fractional shortening and in left ventricular ejection fraction relative to baseline values ($P < 0.05$ right ventricular change; $P < 0.001$ left ventricular changes) (Table 4.1; Fig. 4.1 C, D). Such changes were absent in animals of the SIV group, and changes in the MAC group while significant, were mild and limited to declines in left ventricular fractional shortening ($P < 0.05$) (Table 4.1). In keeping with the structural and functional changes which occurred in members of the SIV+MAC group, a mild but statistically significant ($P < 0.05$) increase in heart rate also developed in these animals which did not occur in other groups (Table 4.1). Strikingly, treatment of SIV-infected, MAC-treated animals with the

TNFα antagonist etanercept was completely protective against development of both chamber dilatation and systolic dysfunction (Table 4.1).

Different kinetics characterized the observed alterations in ventricular chamber size and onset of systolic dysfunction (Fig. 4.1, A-B). Indicators of ventricular chamber size, such as left-ventricular end-diastolic diameter (LVEDD), showed an abrupt increase in the SIV+MAC group at the final examined time point (Fig. 4.1, A), while indicators of systolic dysfunction developed gradually, becoming prominent from day 21 onward (Fig. 4.1, B).

Significant differences in percent change LVEDD from baseline were present among the test groups over the study period ($P < 0.001$ overall, $P < 0.01$ at day 35) (Fig. 4.1, A). Percent change in LVEDD relative to baseline at day 35 differed significantly between the SIV+MAC group and the uninfected MAC group ($P < 0.001$) (Fig. 4.1, E). Significant differences in percent change LVEF from baseline were also present among test groups ($P < 0.001$ overall, $P < 0.001$ at day 28) (Fig. 4.1, B). Percent change in LVEF relative to baseline at day 28 differed significantly between the SIV+MAC group and each of the other three groups ($P < 0.001$ between SIV+MAC and the SIV-infected, MAC-treated, etanercept-treated group, $P < 0.001$ between SIV+MAC and the SIV group, and $P < 0.05$ between SIV+MAC and the MAC group). Percent change in LVEF for the MAC group at day 28 also differed significantly from percent change LVEF for the SIV-infected, MAC-treated, etanercept-treated group ($P < 0.05$), a product of the combined mild decrease in LVEF for the MAC group and the mild increase in LVEF for the etanercept-treated group.

Mycobacterial Antigenic Stimulation Significantly Increases Myocardial TNFα Levels in SIV-Infected Animals, an Effect Prevented by Etanercept Treatment

Levels of myocardial TNFα as evaluated by densitometric analysis of western blots were significantly higher in hearts from animals of the SIV+MAC group than in hearts from animals of the SIV group (P < 0.05) (Fig. 4.2, A). Levels of TNFα were also significantly higher in cardiac muscle than in skeletal muscle for animals of the SIV+MAC group (P < 0.05), suggesting a tissue-specific effect of the mycobacterial antigenic stimulation rather than a generalized systemic increase in TNFα production (Fig. 4.2, B). In contrast, levels of myocardial TNFα in SIV-infected, MAC-treated, etanercept-treated animals remained low, approximating those in skeletal muscle (Fig. 4.2, B).

Plasma sTNFR2 and IL-18 Levels at Day 14 Correlate Significantly with Changes in Left Ventricular Chamber Diameter while Baseline Levels of IL-18 Correlate with Development of Systolic Dysfunction

In SIV-infected groups, plasma levels of both sTNFR2 and IL-18 became significantly elevated (P < 0.001) relative to baseline by day 14, corresponding with the occurrence of peak viremia (Fig. 4.3 A, B). Percent change in LVEDD at day 35 correlated significantly with sTNFR2 levels at every time point from day 14 forward (day 14: P = 0.005, R = 0.578; day 21: P = 0.006, R = 0.567; day 28: P = 0.028, R = 0.479; day 35: P = 0. 018, R = 0.499) such that higher levels of sTNFR2 were associated with greater left ventricular

chamber enlargement at the final measured time point (Fig. 4.3, C). Elevations in plasma IL-18 at day 14 also correlated significantly with increased LVEDD at day 35 ($P < 0.05$, $R = 0.407$) such that higher levels were associated with greater left ventricular chamber enlargement at the final measured time point (Fig. 4.3, D). In contrast, baseline IL-18 levels correlated negatively with development of systolic dysfunction as measured by percent change in LVEF at day 35 ($P < 0.05$, $R = 0.445$), such that higher levels of IL-18 at day 0 were associated with greater preservation of systolic function at the terminal time point (Fig. 4.3, E).

Neither plasma sTNFR1 nor plasma MCP-1 showed significant correlations with echocardiographic parameters at any time point.

Inducible Nitric Oxide Synthase (iNOS) Levels, Lymphocytic Infiltration, Plasma Viral Load, Myocardial SIV-infected Cell Burden, and Peripheral CD4 T Cell Counts Show No Significant Correlations with Measures of Ventricular Chamber Diameter or Systolic Function

The cardiodepressant effects of nitric oxide serve as one of the central effector mechanisms by which inflammatory cytokines impact cardiac function [77]. Myocardial iNOS levels were higher in all SIV-infected groups relative to the uninfected MAC control group, and this difference was statistically significant between the MAC group and the SIV+MAC group ($P < 0.05$); however, myocardial iNOS levels did not differ significantly among SIV-infected groups (Fig. 4.4, A) and there were no significant

correlations between iNOS levels and any examined measure of either ventricular chamber diameter or systolic function.

Histologically, mild inflammatory infiltrates were present in multiple hearts, though cardiomyocyte necrosis was not a prominent feature in any. Quantitation of lymphocytic infiltrates based on rule-based scoring of CD3-labeled tissue sections [158] demonstrated no significant differences between groups (P > 0.1) and no significant correlations with any measure of systolic function or ventricular chamber diameter.

Myocardial infected cell burden, assessed by quantitation of positive signal in sections immunohistochemically labeled for SIV nef and SIV p27 gag proteins, demonstrated infected cells within hearts of 6 of the 18 SIV-infected animals. In each case, SIV-infected cells were rare (1-3 per animal), were exclusively interstitial in location, and were morphologically consistent with lymphocytes or macrophages (Fig. 4.4, C). All hearts were negative for adenovirus and cytomegalovirus by immunohistochemistry. Numbers of myocardial SIV-infected cells did not correlate significantly with any measure of systolic dysfunction or ventricular dilatation.

Plasma viral load in SIV-infected groups also did not correlate significantly with any measure of ventricular chamber diameter or systolic function. Viral loads within the SIV-infected, MAC-treated, etanercept-treated group, which developed no structural or functional pathology, were significantly higher (P < 0.05) than in the SIV+MAC group, which developed significant adverse structural and functional changes (Fig. 4.4, B).

CD4 T cell counts differed significantly among groups overall (P < 0.001), as all three SIV-infected groups developed significant decreases relative to the uninfected

MAC group over the course of the study (P < 0.01). Counts among the SIV-infected groups did not significantly differ however, and there were no significant correlations between CD4 T cell counts and any evaluated echocardiographic parameter (Fig. 4.4, D).

Immunohistochemical staining of tissue sections for cleaved caspase 3 as an early indicator of apoptosis revealed infrequent staining within inflammatory cell clusters, and strong appropriate staining on positive control sections of ileum, but no staining of cardiomyocytes in any section and no correlations with any echocardiographic parameter.

Discussion

In the presented model, recurrent antigenic stimulation with heat-killed, opportunistic mycobacteria yielded significant myocardial contractile dysfunction and ventricular chamber dilatation in SIV-infected animals during acute infection which was not seen with SIV-infection alone and was mild to absent in uninfected animals treated with the same stimulation protocol. While the rapidity of induction of cardiac dysfunction in this model differs from that seen in natural disease, the findings suggest a fundamental hyperresponsivity of hearts from SIV-infected animals to antigenic stimulation. The cardiac changes induced by antigenic stimulation in this acute SIV-infection model reached magnitudes similar to those previously identified in studies of dilated cardiomyopathy in chronic SIV infection [178], while excluding many potential confounders which complicate interpretation in late stage infection. Concurrent etanercept treatment protected SIV-infected, MAC-treated animals from development of pathologic myocardial changes, suggesting a critical role for TNFα in induction of these changes. While it is not possible to control for variation in host immune response using small numbers of test subjects, these findings suggest that endogenous production of TNFα upon antigenic stimulation in the context of SIV infection is sufficient to induce significant cardiac dysfunction and implies exaggerated myocardial production of and/or responsiveness to TNFα by SIV-infected animals. In addition, the striking difference in myocardial TNFα levels between SIV-infected, MAC-treated animals which received etanercept and those which did not implies an important role for TNFα autoinduction in generation of the observed elevations in SIV-infected, MAC-treated animals [223]. This

finding suggests that even mild hyperresponsivity in the initial TNFα response might be rapidly enhanced through positive feedback loops.

As further evidence of the importance of activation of the TNF system in evolution of the observed changes, plasma sTNFR2 levels from day 14 onward correlated significantly with extent of LVEDD change at day 35, predicting chamber dilatation with high sensitivity. IL-18 levels at day 14 also correlated positively with extent of LVEDD change, but as plasma IL-18 and sTNFR2 values correlated closely with one another, (day 14: $P < 0.001$) the relationship between IL-18 and LVEDD may have simply reflected a connection between myocardial remodeling and the overall systemic inflammatory response. Nevertheless, the finding that higher levels of both sTNFR2 and IL-18 at day 14 correlated with increased percent change LVEDD at day 35 suggests that the degree of activation of the inflammatory response around the period of peak viremia, during which viral replication is largely uncontrolled and early components of the innate immune response are activated, may directly contribute to the extent of subsequent structural change. This suggests that immune activation, well recognized as a major contributor to progression of SIV and HIV infection [139], may also play an important role in myocardial end organ damage. In contrast, while elevated levels of IL-18 have been associated with myocardial contractile dysfunction [113, 115, 116], lower levels of IL-18 at baseline were associated with more severe declines in LVEF at later time points, suggesting that pre-infection innate immune activation state may also play an important role in divergent post-infection myocardial effects.

In the present model of HIVCM pathogenesis, no evidence was found for a role played by plasma viral load, myocardial infected cell burden, peripheral CD4 T cell count, myocardial lymphocytic infiltration, cardiomyocyte apoptosis, or cardiomyocyte necrosis. While iNOS has been implicated in the impairment of myocardial function in inflammatory contexts [77], myocardial iNOS levels did not differ significantly among SIV-infected groups in this model. Likewise, while HIV gp120 protein has been demonstrated to be negatively inotropic *in vitro*[89] and high viral loads might therefore be expected to be associated with alterations of contractile function, no correlations were identified between plasma viral load and any examined measure of ventricular chamber diameter or systolic function.

Prominent myocardial pathology developed over the 35 day study period in SIV-infected, MAC-treated animals, but not in uninfected MAC-treated controls or animals which were SIV-infected alone. Treatment with the TNFα blocking agent etanercept proved fully protective from development of myocardial pathology, indicating that abnormal TNFα responses to the administered mycobacterial stimulus played a critical role in development of the observed changes. These findings suggest that aberrant inflammatory cytokine responsiveness to antigenic stimulation in the context of SIV or HIV infection may play an important role in the pathogenesis of cardiomyopathy. As myocardium-specific abnormalities in the cytokine response to antigenic stimulation appear central to the cardiac changes documented, defining the mechanism by which this occurs will be critical to understanding their ultimate causation.

Table 4.1. Cardiac Functional and Structural Parameters

	SIV+MAC		SIV		Etanercept		MAC	
	Day 0	Change(%)	Day 0	Change(%)	Day 0	Change(%)	Day 0	Change(%)
LVEDD[*] (cm)	1.8±0.06	26±6[‡]	1.9±0.04	1±3	1.6±0.04	4±6	1.9±0.06	-5±2[§]
LVESD[*] (cm)	1.1±0.07	41±6[‡]	1.1±0.08	6±7	1.0±0.08	4±9	1.1±0.05	3±4
LVEF[†] (%)	75±1	-17±4[‡]	76±4	-1±4	74±3	5±7	79±2	-7±4
LVFS (%)	37±2	-20±5[‡]	40±4	0±10	34±4	23±28	42±1	-11±5[§]
RVEDD[†] (cm)	1.6±0.1	21±4[‡]	1.0±0.04	-6±6	1.1±0.05	4±9	1.5±0.09	7±3[§]
RVESD[†] (cm)	1.0±0.05	45±10[‡]	0.7±0.03	-10±7	0.7±0.06	19±12	1.0±0.05	14±6[§]
RVFS (%)	37±2	-30±11[§]	29±3	17±15	36±5	-16±17	29±2	-11±6
HR (bpm)	143±4	11±5[§]	147±12	-12±12	145±16	13±17	168±7	-2±6

SIV+MAC: SIV-infected animals treated with recurrent doses of heat-killed *M. avium* complex (MAC); SIV: SIV-infected animals not subjected to MAC treatments; Etanercept: SIV-infected, MAC-treated, etanercept-treated animals; MAC: uninfected, MAC-treated controls

Day 0: Baseline value; Change(%): Percent change from baseline at day 35; All values given as mean ± standard error.

LVEDD indicates left ventricular end-diastolic diameter; LVESD, left ventricular end-systolic diameter; LVEF, left ventricular ejection fraction; LVFS, left ventricular fractional shortening; RVEDD, right ventricular end-diastolic diameter; RVESD, right ventricular end-systolic diameter; RVFS, right ventricular fractional shortening; HR, heart rate; bpm, beats per minute

Difference between groups is significant: [*]$P < 0.001$, [†]$P < 0.05$.

Percent change from baseline to day 35 is significant: [‡]$P < 0.001$, [§]$P < 0.05$

Figure 4.1 Echocardiographic changes among study groups. (A) Animals in the SIV+MAC group developed abrupt, significant increases in left ventricular end-diastolic diameter (LVEDD) at the final examined time point which were absent in other treatment groups. Differences between groups were statistically significant (P < 0.001). (B) Animals in the SIV+MAC group developed progressive decreases in left ventricular ejection fraction (LVEF) which were minimal to absent in other treatment groups. Differences between groups were statistically significant (P < 0.001). (C) M-mode image from rhesus monkey with normal left ventricular function (LVEF, 80%). (D) M-mode image from rhesus monkey with markedly decreased left ventricular function (LVEF, 45%). (E) Percent change in LVEDD at day 35 differed significantly across groups (P < 0.01). Percent increase in LVEDD for the SIV+MAC group differed significantly (*) from baseline (P < 0.001) and from percent change LVEDD at day 35 for the uninfected MAC group (P < 0.001). (F) Percent change in LVEF at day 28 differed significantly across groups (P < 0.001). Percent decrease in LVEF at day 28 for the SIV+MAC group differed significantly (*) from baseline (P < 0.001), as well as from percent change LVEF in the SIV group (P < 0.001), the etanercept-treated group (P < 0.001), and for the MAC group (P < 0.05). Percent change LVEF for the MAC group at day 28 differed significantly (**) from percent change LVEF for the etanercept-treated group (P < 0.05). SIV+MAC: SIV-infected, *M. avium* complex (MAC)-treated group; SIV: SIV-infected animals not subjected to MAC treatments; SIV+MAC+Enbrel and Enbrel: SIV-infected, MAC-treated, etanercept-treated animals; MAC: uninfected, MAC-treated controls.

Figure 4.1

Figure 4.2 Local TNFα levels in myocardial and skeletal muscle tissue. (A)

Myocardial TNFα levels were significantly higher in hearts from the SIV+MAC group

(*) than in hearts from the SIV group ($P < 0.05$). (B) TNFα levels in cardiac muscle of

animals from the SIV+MAC group (SIV+MAC H) were significantly higher (*) than in

skeletal muscle from either the SIV+MAC group (SIV+MAC SM) ($P < 0.05$) or the SIV-

infected, MAC-treated, etanercept-treated group (Enbrel SM) ($P < 0.05$). TNFα levels in

cardiac muscle of the SIV-infected, MAC-treated, etanercept-treated group (Enbrel H)

did not differ significantly from levels in skeletal muscle derived from either group. All

measurements conducted by densitometric analysis of western blots of myocardial and

skeletal muscle tissue homogenates. (C) TNFα levels in cardiac muscle of animals from

the SIV+MAC group (SIV+MAC H) exceeds that in skeletal muscle of the SIV+MAC

group (SIV+MAC SM), cardiac muscle of the etanercept-treated group (Enbrel H), and

skeletal muscle of the etanercept-treated group (Enbrel SM). SIV+MAC: SIV-infected,

M. avium complex (MAC)-treated group; SIV: SIV-infected animals not subjected to

MAC treatments; SIV+MAC H: heart muscle from SIV+MAC group; SIV+MAC SM:

skeletal muscle from SIV+MAC group; Enbrel H: heart muscle from SIV-infected,

MAC-treated, etanercept-treated animals; Enbrel SM: skeletal muscle from SIV-infected,

MAC-treated, etanercept-treated animals.

Figure 4.2
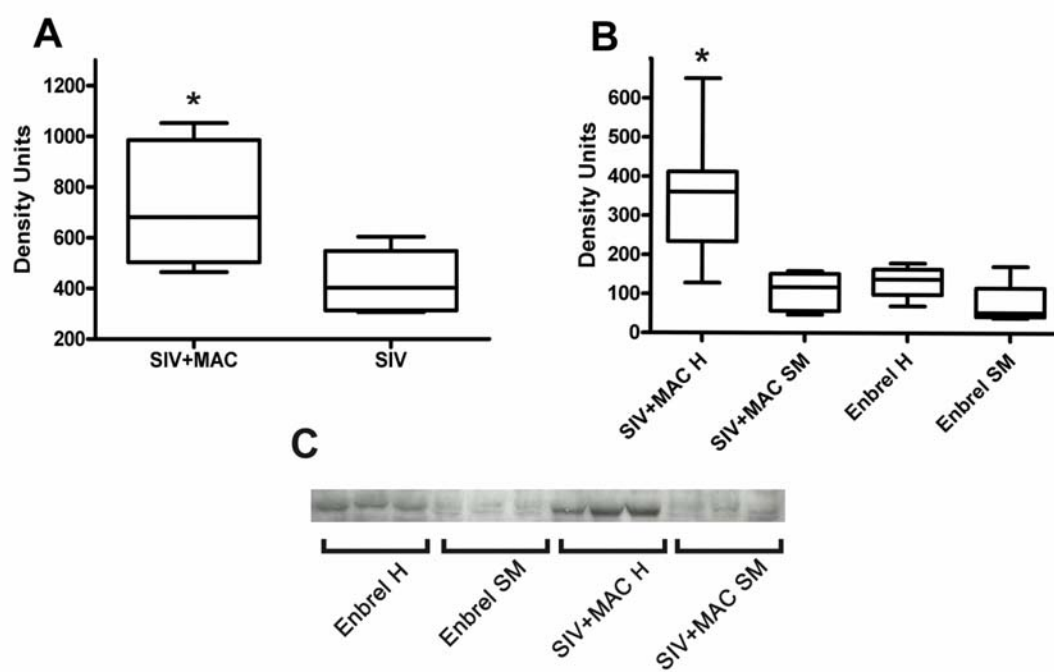
Figure 4.3 Plasma sTNFR2 and IL-18 levels correlate significantly with changes in ventricular chamber size and systolic function. (A) Plasma sTNFR2 levels rose significantly from baseline (P < 0.001) in SIV-infected animals by day 14, corresponding to the period of peak viremia, and remained elevated thereafter. Data from etanercept-treated animals are not included due to cross-reactivity of etanercept itself (a fusion protein comprised of the extracellular ligand-binding portion of sTNFR2 bound to the Fc portion of human IgG1) with antibodies specific for sTNFR2 in the assay. (B) Plasma IL-18 levels rose sharply in SIV-infected animals by day 14, reaching levels significantly above baseline (P < 0.001), then dropped rapidly back toward pre-infection levels. (C) Plasma levels of sTNFR2 at day 14 correlated significantly with percent change in LVEDD at day 35 (P < 0.01, R = 0.578) such that higher plasma sTNFR2 levels were associated with greater chamber enlargement at the final time point. (D) Plasma levels of IL-18 at day 14 also correlated significantly with percent change in LVEDD at day 35 (P < 0.05, R = 0.407), with higher plasma IL-18 being associated with greater chamber enlargement at the final time point. (E) Plasma IL-18 levels at day 0 correlated significantly with percent change in LVEF at day 35 (P < 0.05, R = 0.445), such that higher baseline IL-18 levels were associated with greater preservation of ejection fraction at the terminal time point. SIV+MAC: SIV-infected, *M. avium* complex (MAC)-treated group; SIV: SIV-infected animals not subjected to MAC treatments; SIV+MAC+Enbrel: SIV-infected, MAC-treated, etanercept-treated animals; MAC: uninfected, MAC-treated controls.
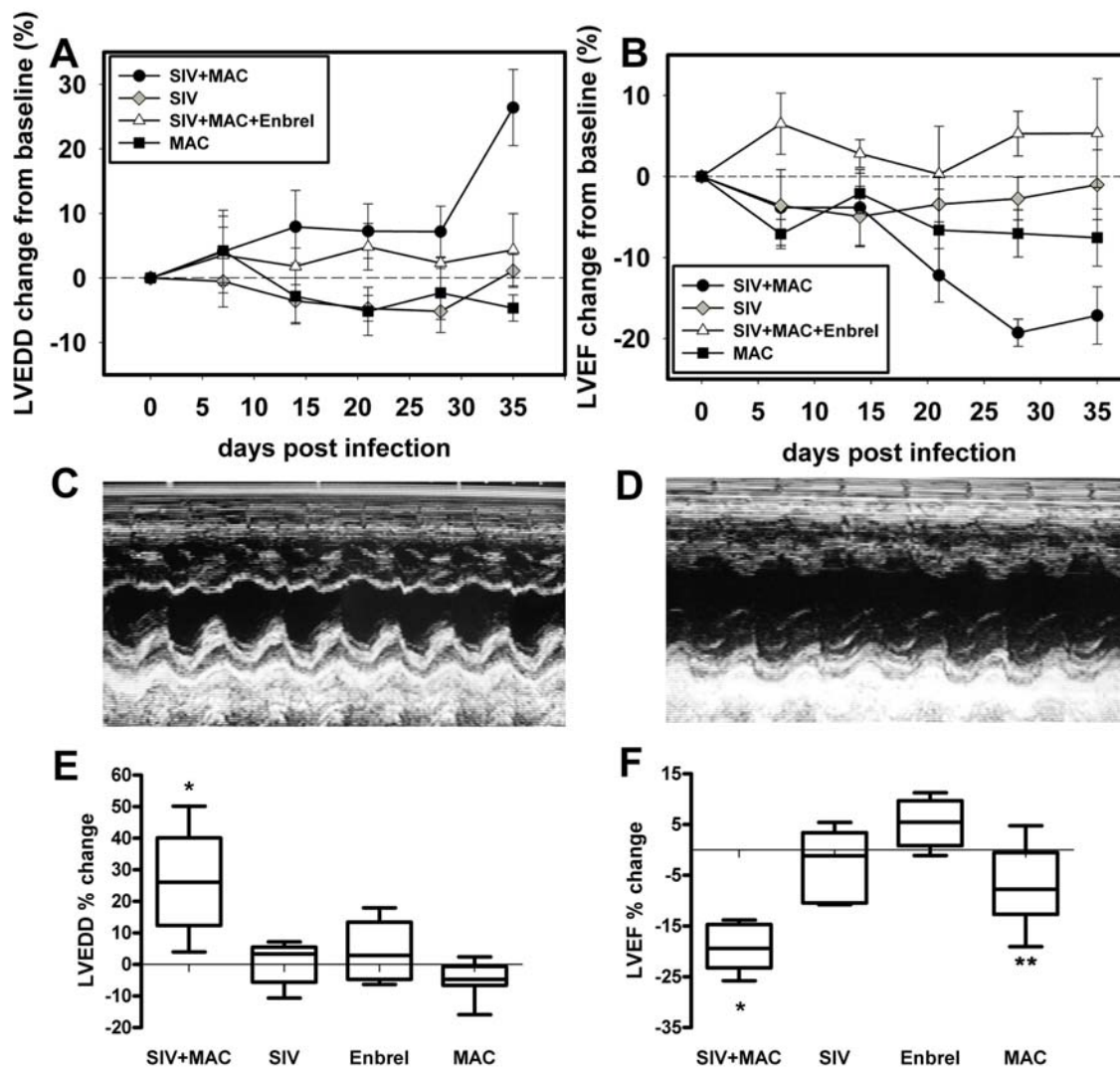
Figure 4.3

Figure 4.4. Myocardial iNOS levels, plasma viral load, myocardial SIV-infected cell burden, and peripheral CD4 T cell count do not correlate significantly with changes in ventricular chamber diameter or systolic function. (A) Myocardial iNOS levels were significantly lower (*) in the MAC control group than in the SIV+MAC group ($P <$ 0.05), but did not significantly differ among SIV-infected groups and did not correlate with any evaluated echocardiographic parameter. (B) Plasma viral loads in the SIV-infected, MAC-treated, etanercept-treated group, which experienced no significant echocardiographic changes, were significantly higher than in the SIV+MAC group, in which prominent structural and functional changes developed ($P < 0.05$). (C) SIV-infected cells within myocardial tissue were rare and their presence and number did not correlate with any evaluated echocardiographic parameter (SIV nef immunohistochemistry with Mayer's hematoxylin. Micron bar = 50 μm). (D) Animals in SIV-infected groups developed significant decreases in CD4 T cell counts relative to the uninfected MAC control group ($P < 0.01$); however, CD4 counts did not correlate significantly with any measure of systolic function or ventricular chamber size. SIV+MAC: SIV-infected, *M. avium* complex (MAC)-treated group; SIV: SIV-infected animals not subjected to MAC treatments; SIV+MAC+Enbrel and Enbrel: SIV-infected, MAC-treated, etanercept-treated animals; MAC: uninfected, MAC-treated controls.
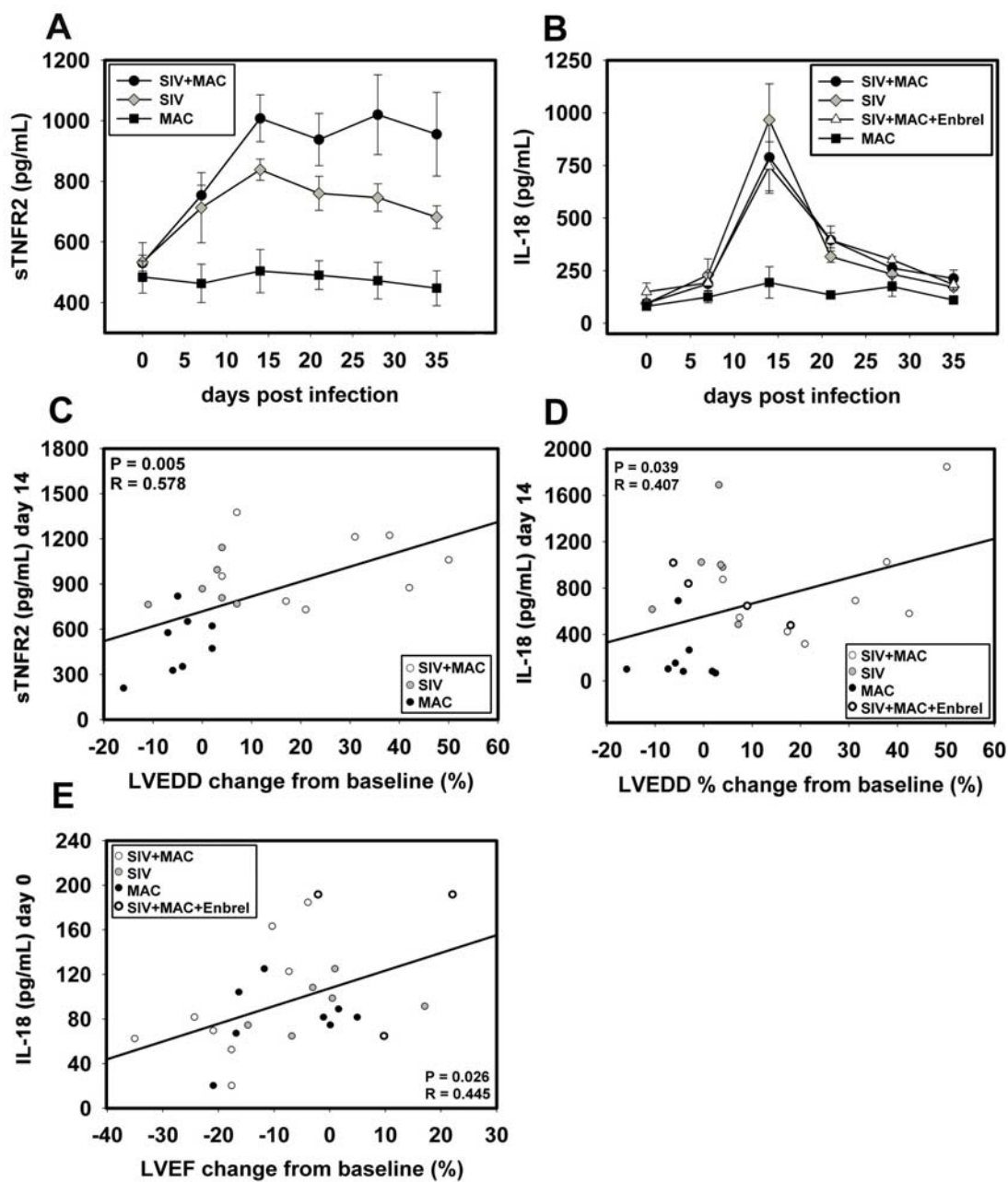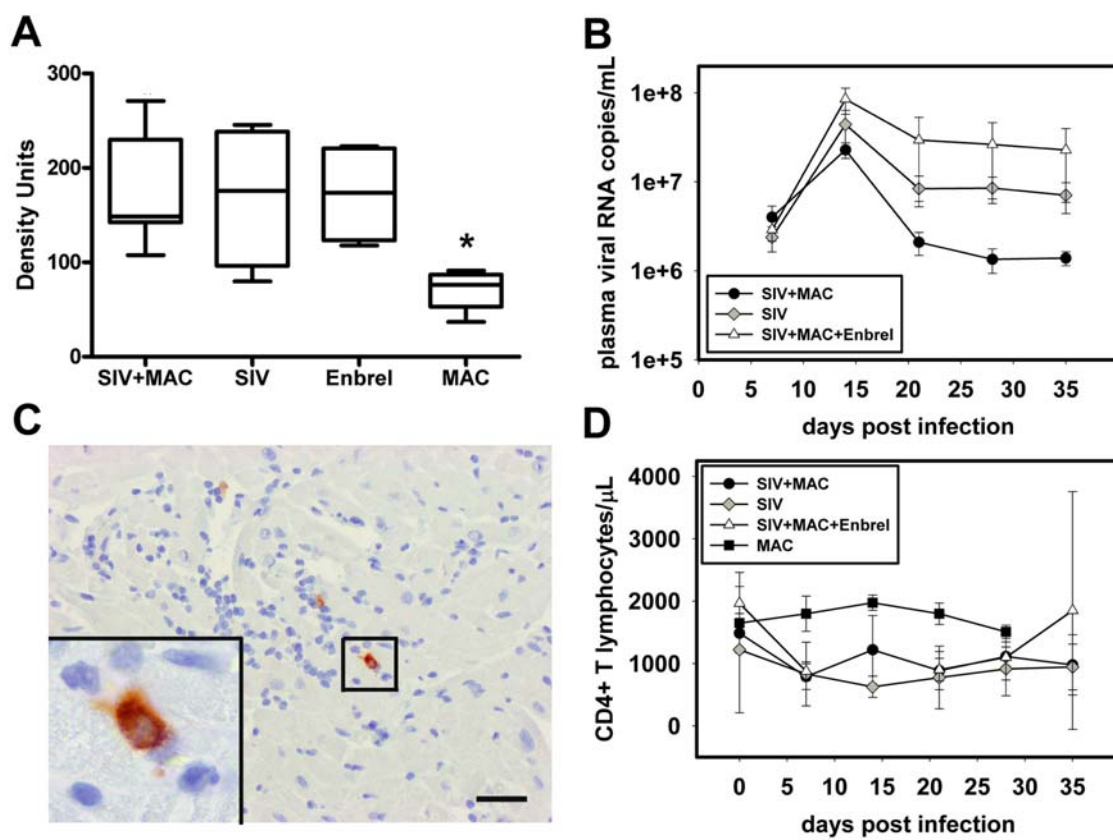
Figure 4.4

CHAPTER V

DISCUSSION

5.1 Introduction

Understanding mechanisms and root causes of disease is necessary to guide intelligent design of therapies and preventative strategies. HIV-associated myocardial disease has been recognized since the early years of the pandemic, but has remained a poorly understood phenomenon with many possible contributors. Better defining features specific to etiology of the condition is important to optimization of efforts at prevention and treatment. Furthermore, HIV infection provides a defined venue for exploring fundamental roles for chronic immune activation and host inflammatory response in the development and progression of myocardial injury, features which have substantial relevance beyond the context of HIV-associated disease alone.

5.2 Summary of Central Findings

Cardiomyopathy and lymphocytic myocarditis have been frequently documented among chronically SIV-infected rhesus monkeys, providing an excellent model system for study of HIV-associated cardiac disease [178]. Initial studies reported here [158, 159] focus on identifying correlates of lymphocytic inflammation, assessing possible causes of the inflammation, and the likelihood of inflammation as an underlying causative factor for development of SIV-associated cardiomyopathy [68-70]. While inflammatory lesions are indeed common, careful review finds them to be typically quite mild. This finding is in agreement with descriptions from the HIV literature, where the mildness of lesions is commonly attributed to the profound immunodeficiencies which occur in late stage infection. Given this mild character, however, it is difficult to attribute significant

functional or structural consequences to the inflammation itself, particularly in the absence of any demonstrable association between extent of inflammation and extent of cardiomyocyte necrosis, cardiomyocyte apoptosis, myocardial fibrosis, contractile dysfunction or ventricular remodeling. This lack of association supports the hypothesis that factors other than direct cardiomyocyte damage resulting from infiltrating lymphocyte populations may be responsible for the development of cardiac dysfunction in HIV/SIV infection. Intramyocardial SIV-infected cells also do not appear likely to play any direct role in cardiac disease pathogenesis given their rarity and lack of significant correlations with evaluated histomorphologic or functional pathologies. In contrast, two subsets of macrophages present in very high numbers throughout the myocardial interstitium and perivascular tissues showed significant correlations variously with extent of T cell infiltration, numbers of SIV-infected cells, and endothelial MHC class II expression, as well as having numbers which differed dramatically between SIV-infected groups as a function of the presence or absence of lymphocytic inflammation. The wide distribution of macrophage populations throughout the myocardium uniquely situates them to assert global effects on myocardial function via actions of secreted soluble mediators. Macrophages characterized by expression of the antigens DC-SIGN and CD163 were found in high numbers in hearts from SIV-infected animals without inflammation, were excluded from or occurred only in very low numbers within inflammatory clusters, and were positively correlated with numbers of SIV-infected cells. Both DC-SIGN and CD163 have been reported to be upregulated in environments rich in T_H2-type cytokines and down-regulated in the presence of LPS or $TNF\alpha$, consistent with

markers of non-classical activation [192, 208, 213, 224, 225]. Specifically, IL-4 and IL-13 have been demonstrated to upregulate DC-SIGN [192, 225, 226], while IL-10 and IL-6 upregulate CD163 [208, 213, 224]. A single report has also found upregulation of DC-SIGN *in vitro* on stimulation with IL-10, and *in vivo* in tissue having a high IL-10/IL-12 ratio, suggesting the possibility of a single microenvironment in which both antigens might be found in abundance [227]. Given that MHC class II expression has been reported to be down-regulated in IL-10-rich contexts [228-230], high levels of myocardial IL-10 could potentially explain the correlation identified between numbers of DC-SIGN+ cells and loss of endothelial MHC class II [158]. In addition, IL-10-mediated inhibition of chemokine production [231] could account for the correlation between numbers of DC-SIGN+ cells and extent of T cell infiltration. There is conflicting evidence as to whether IL-10 enhances or inhibits HIV replication (reviewed in [231]), but HIV replication has been documented to be significantly enhanced in macrophages which have engaged in phagocytosis of apoptotic debris, an activity which incurs upon them a prominently anti-inflammatory phenotype [232-234]. CD163+ macrophages have been associated with an anti-inflammatory phenotype, including IL-10 secretion on ligand-binding, inhibition of lymphocyte proliferation, and decreased expression of lymphocyte activation markers [175, 202, 208-210]. Cross-linking of DC-SIGN, a C-type lectin which serves as a broad-spectrum pathogen receptor (reviewed in [235]), has also been associated with high IL-10 production in the context of concurrent TLR2, TLR4, or TNFα stimulation *in vitro*, significantly modulating the cellular response to otherwise inflammatory stimuli [236].

The findings presented in the first two reports provide initial evidence that myocardial antigen presenting cell populations might be significantly associated with induction or suppression of local myocardial inflammatory responses, expression of antigens by local, non-leukocyte populations, and quite possibly functional effects on cardiomyocytes, through properties of secreted cytokines. More extensive evaluation of the cytokine milieu of the myocardial microenvironment will provide an important starting point for future work.

Given the paucity of literature examining tissue macrophage subsets in the context of HIV/SIV infection, the extent to which the patterns identified in myocardium in current work may also characterize other tissues in HIV/SIV-infection is unknown. In health, certain tissues are known to contain native macrophage populations with non-classical properties. The lamina propria of the intestine for instance, contains a large population of macrophages which do not produce inflammatory cytokines, do not present antigen, and lack many innate immune receptors, but which engage in high efficiency phagocytosis and microbial killing [237]. Similarly, pulmonary alveolar macrophages in the steady state constitutively express DC-SIGN, constitutively secrete IL-10 and constitutively express the IL-10 receptor, though they are capable of responding with vigorous inflammatory responses when appropriately stimulated [238].

In the context of SIV infection, one group has found expansion of the CD163+/CD16+ monocyte population in peripheral blood, with degree of expansion correlating significantly with viral load [239]. Another group has found perivascular

macrophages in both normal and encephalitic brains from HIV- and SIV-infected

individuals to be uniformly CD163 positive, with increased numbers of CD163+ cells

associated with encephalitic lesions [216]. Interestingly however, in case selection for

this study, brains that had significant lymphocytic infiltration were omitted from

consideration (S. Westmoreland, pc) such that any potential distinction in CNS

macrophage phenotype associated with the presence or absence of lymphocytic

inflammation will not have been identified. To the author's knowledge, no work aside

from that presented here has been published which specifically examines differences in

macrophage subsets in tissues in the context of HIV/SIV infection and the possible

consequences of those differences.

In the final report [240], an acute SIV infection model employing recurrent

antigenic stimulation with whole, heat-killed *Mycobacterium avium* complex (MAC)

bacteria assesses the effects of experimentally augmented immune activation on

myocardial structure and function, in order to directly examine the possibility of a role

for inflammatory cytokines in development of HIV/SIV-associated cardiac disease.

In this model, SIV-infected animals developed marked myocardial dysfunction

and structural change in response to antigenic stimulation that was not found in controls,

and which was preventable by concurrent administration of a TNFα antagonist. This

fundamentally different myocardial response to systemic antigenic stimulation in SIV-

infected animals, with the appearance of delayed and progressive structural and

functional pathology after cessation of the stimulus, was associated with myocardium-

specific elevations in TNFα that were significantly higher in antigenically stimulated

SIV-infected animals than in unstimulated SIV-infected animals. Ventricular structural change correlated with markers of systemic immune activation as indicated by significant relationships between circulating plasma levels of sTNFR2 and IL-18 at the time of peak viremia and extent of left ventricular dilatation at the terminal time point. In contrast, decreases in systolic function showed a significant association not with increased immune activation at peak viremia, but with baseline levels of IL-18, a finding which is intriguing given recent studies identifying significant relationships between baseline IL-18 levels and risk of future coronary events [241], myocardial infarction [242], and cardiovascular mortality [243-245], even among large cohorts of healthy men [241].

5.3 Increased Risk of Disease Development in the Context of Microbial Co-infections

Findings reported here imply that significant exposure to antigens from non-HIV/SIV microbial agents, such as occurs in later stages of HIV/SIV infection as immune competence fails, is likely to substantially enhance the probability of cardiac disease development and progression. This finding is consistent with the often noted observation that HIVCM is strongly associated with depressed CD4 T cell counts and advanced infection [30, 38, 39]. Based on experimental findings in our model, this association may in part be a product of TNFα-mediated myocardial hyperresponsivity to antigenic stimulation.

Mycobacterium avium complex bacteria are environmentally ubiquitous and disseminated *M. avium* infection is one of the most frequent opportunistic infections in

both human and simian AIDS [218-220, 246]. Furthermore, primary macrophages from

HIV-infected people have been demonstrated to produce significantly higher levels of

both TNFα and IL-1β on stimulation with *M. avium* than macrophages from uninfected

control individuals [142]. Exaggerated inflammatory cytokine production by

macrophages from HIV-infected people on exposure to common opportunists such as *M.*

avium, particularly in the face of the very high bacterial loads that develop in HIV-

infected individuals with disseminated disease, may provide one explanation for the

common occurrence of HIV-associated cardiac disease in later stages of disease

progression, particularly given our current evidence for myocardial TNFα autoinduction,

as this suggests that increased systemic levels of TNFα may undergo local amplification

within the myocardium.

Co-infection with pathogens other than HIV and stimulation with non-HIV

microbial antigens has been implicated in many reports to contribute to adverse outcomes

in the context of HIV infection, through increased susceptibility to initial infection [247,

248], increased rate of disease progression [83, 247, 248], increasing levels of viral

replication [142, 249-252], and overall enhanced development of further opportunistic

infections and shortened survival [253]. Furthermore, recent investigations in a murine

model of AIDS-associated cardiomyopathy have demonstrated that subseptic

lipopolysaccharide (LPS) exposure resulted in cardiac dysfunction, ventricular

hypertrophy, and ventricular chamber dilatation in infected mice, similar to our findings

with administration of inactivated whole mycobacteria, and found these changes to be

significantly associated with increased levels of non-focal myocardial macrophage

infiltration as well as increased levels of TLR4 expression, implicating a role for macrophage involvement and toll-like receptor signaling in development of the observed pathology [171].

5.4 Anti-TNFα Biologics as Therapeutic Agents: Heart Failure and HIV Infection

While usage of the TNFα antagonist etanercept clearly demonstrated the TNFα dependence of the myocardial changes observed in antigenically stimulated SIV-infected animals by preventing development of systolic dysfunction and left ventricular dilatation, etanercept use was also associated with significantly increased plasma viral loads, suggesting that interference with the TNFα response at these early time points, while protective to the myocardium, resulted in reduced control of viral proliferation. Use of anti-TNFα therapies such as etanercept has been associated with increased risk of a wide variety of infections [254-256], and because of this and the risk of potentially worsening disease progression in HIV-infected individuals, usage of anti-TNFα therapies in HIV-infected people has been infrequently reported. Nevertheless, the majority of reports describing use of anti-TNFα biologics in HIV-infected people describe no significant changes in viral load, no clinical deterioration, and no occurrence of significant opportunistic infections even over periods of therapy lasting greater than 4 years [257-264]. However, as substantial evidence suggests that devastating immunologic damage takes place very early post-infection [265], it is possible that etanercept treatment during

the early acute infection period, as in our experimental model, might be associated with more deleterious outcomes as a result of diminished early viral containment than perhaps would be seen in similarly treated individuals with established, stable infections. Given the small number of cases reported in the literature to this point, however, the safety of anti-TNFα therapies in HIV-infected individuals overall requires further evaluation.

Numerous clinical trials evaluating the utility of anti-TNFα therapies in heart failure treatment have been conducted in recent years based on the considerable evidence in support of a role for inflammatory cytokine involvement in progression of heart failure. However, while small, short-term early trials yielded promising improvements in outcome [266, 267], large multicenter randomized double-blind trials have uniformly yielded disappointing results [268, 269] (reviewed in [270]). While the reasons for this failure are matters of ongoing debate, current evidence suggests that anti-TNFα treatment for existing heart failure is of no benefit and in some cases may actually worsen outcomes [269, 271]. Whether there are circumstances under which anti-TNFα regimens could be employed therapeutically to prevent development of heart failure, as is suggested by our experimental results, is as yet an open question.

5.5 Conclusions

The current studies report work examining potential roles for myocardial macrophages and inflammatory cytokines in susceptibility to HIV/SIV-associated myocardial pathology. Previous work examining roles for inflammatory cytokines in the development and progression of HIV-associated cardiac disease has been very limited,

and the possibility of a role for antigenic stimulation in generation of these tissue-specific cytokine-dependent myocardial responses has not previously been explored. Many possible environmental, viral, and host factors have previously been identified as possible contributors to development of HIV-associated cardiac disease, including direct myocardial infection by cardiotropic and opportunistic pathogens, anti-cardiac autoimmunity, drug-induced cardiotoxicity, cardiodepressant viral proteins, and micronutrient deficiencies, all of which may in some circumstances play contributory roles. Given the complexity of the many interacting features in late-stage HIV infection, it is unlikely that a single etiology will suffice to encompass all cases of cardiomyopathy that arise in affected populations. However, findings from the current studies suggest that characteristics of local myocardial macrophage populations and the local myocardial cytokine milieu may play more important roles than lymphocytic infiltration, direct cardiomyocyte damage, or viral proteins in the pathogenesis of HIVCM, and that the exaggerated levels of antigenic stimulation that occur through multipathogen exposures in later stages of infection may be sufficient in the HIV-infection context to yield progressive myocardial disease.

REFERENCES

1.   Joint United Nations Programme on HIV/AIDS. *AIDS epidemic update*. Geneva: UNAIDS; 2007.

2.   Fink L, Reichek N, Sutton MG. Cardiac abnormalities in acquired immune deficiency syndrome. *Am J Cardiol* 1984;**54**:1161-1163.

3.   Cohen IS, Anderson DW, Virmani R, Reen BM, Macher AM, Sennesh J, DiLorenzo P, Redfield RR. Congestive cardiomyopathy in association with the acquired immunodeficiency syndrome. *N Engl J Med* 1986;**315**:628-630.

4.   Calabrese LH, Proffitt MR, Yen-Lieberman B, Hobbs RE, Ratliff NB. Congestive cardiomyopathy and illness related to the acquired immunodeficiency syndrome (AIDS) associated with isolation of retrovirus from myocardium. *Ann Intern Med* 1987;**107**:691-692.

5.   Levy WS, Varghese PJ, Anderson DW, Leiboff RH, Orenstein JM, Virmani R, Bloom S. Myocarditis diagnosed by endomyocardial biopsy in human immunodeficiency virus infection with cardiac dysfunction. *Am J Cardiol* 1988;**62**:658-659.

6.   Reilly JM, Cunnion RE, Anderson DW, O'Leary TJ, Simmons JT, Lane HC, Fauci AS, Roberts WC, Virmani R, Parrillo JE. Frequency of myocarditis, left ventricular dysfunction and ventricular tachycardia in the acquired immune deficiency syndrome. *Am J Cardiol* 1988;**62**:789-793.

7.   Corallo S, Mutinelli MR, Moroni M, Lazzarin A, Celano V, Repossini A, Baroldi G. Echocardiography detects myocardial damage in AIDS: prospective study in 102 patients. *Eur Heart J* 1988;**9**:887-892.

8.   Anderson DW, Virmani R, Reilly JM, O'Leary T, Cunnion RE, Robinowitz M, Macher AM, Punja U, Villaflor ST, Parrillo JE, et al. Prevalent myocarditis at necropsy in the acquired immunodeficiency syndrome. *J Am Coll Cardiol* 1988;**11**:792-799.

9.   Wilkins CE, Sexton DJ, McAllister HA. HIV-associated myocarditis treated with zidovudine (AZT). *Tex Heart Inst J* 1989;**16**:44-45.

10.   Lipshultz SE, Chanock S, Sanders SP, Colan SD, Perez-Atayde A, McIntosh K. Cardiovascular manifestations of human immunodeficiency virus infection in infants and children. *Am J Cardiol* 1989;**63**:1489-1497.

11. Baroldi G, Corallo S, Moroni M, Repossini A, Mutinelli MR, Lazzarin A, Antonacci CM, Cristina S, Negri C. Focal lymphocytic myocarditis in acquired immunodeficiency syndrome (AIDS): a correlative morphologic and clinical study in 26 consecutive fatal cases. *J Am Coll Cardiol* 1988;**12**:463-469.

12. Beschorner WE, Baughman K, Turnicky RP, Hutchins GM, Rowe SA, Kavanaugh-McHugh AL, Suresch DL, Herskowitz A. HIV-associated myocarditis. Pathology and immunopathology. *Am J Pathol* 1990;**137**:1365-1371.

13. Parravicini C, Baroldi G, Gaiera G, Lazzarin A. Phenotype of intramyocardial leukocytic infiltrates in acquired immunodeficiency syndrome (AIDS): a postmortem immunohistochemical study in 34 consecutive cases. *Mod Pathol* 1991;**4**:559-565.

14. Hansen BF. Pathology of the heart in AIDS. A study of 60 consecutive autopsies. *Apmis* 1992;**100**:273-279.

15. DeCastro S, Migliau G, Silvestri A, D'Amati G, Giannantoni P, Cartoni D, Kol A, Vullo V, Cirelli A. Heart involvement in AIDS: a prospective study during various stages of the disease. *Eur Heart J* 1992;**13**:1452-1459.

16. Luginbuhl LM, Orav EJ, McIntosh K, Lipshultz SE. Cardiac morbidity and related mortality in children with HIV infection. *JAMA* 1993;**269**:2869-2875.

17. Herskowitz A, Vlahov D, Willoughby S, Chaisson RE, Schulman SP, Neumann DA, Baughman KL. Prevalence and incidence of left ventricular dysfunction in patients with human immunodeficiency virus infection. *Am J Cardiol* 1993;**71**:955-958.

18. Herskowitz A, Wu TC, Willoughby SB, Vlahov D, Ansari AA, Beschorner WE, Baughman KL. Myocarditis and cardiotropic viral infection associated with severe left ventricular dysfunction in late-stage infection with human immunodeficiency virus. *J Am Coll Cardiol* 1994;**24**:1025-1032.

19. Currie PF, Jacob AJ, Foreman AR, Elton RA, Brettle RP, Boon NA. Heart muscle disease related to HIV infection: prognostic implications. *British Medical Journal* 1994;**309**:1605-1607.

20. De Castro S, d'Amati G, Gallo P, Cartoni D, Santopadre P, Vullo V, Cirelli A, Migliau G. Frequency of development of acute global left ventricular dysfunction in human immunodeficiency virus infection. *J Am Coll Cardiol* 1994;**24**:1018-1024.

21. Lipshultz SE, Orav EJ, Sanders SP, Colan SD. Immunoglobulins and left ventricular structure and function in pediatric HIV infection. *Circulation* 1995;**92**:2220-2225.

22. Herskowitz A, Willoughby SB, Vlahov D, Baughman KL, Ansari AA. Dilated heart muscle disease associated with HIV infection. *Eur Heart J* 1995;**16 Suppl O**:50-55.

23. Hakim JG, Matenga JA, Siziya S. Myocardial dysfunction in human immunodeficiency virus infection: an echocardiographic study of 157 patients in hospital in Zimbabwe. *Heart* 1996;**76**:161-165.

24. Lipshultz SE. Dilated cardiomyopathy in HIV-infected patients. *N Engl J Med* 1998;**339**:1153-1155.

25. Cooper ER, Hanson C, Diaz C, Mendez H, Abboud R, Nugent R, Pitt J, Rich K, Rodriguez EM, Smeriglio V. Encephalopathy and progression of human immunodeficiency virus disease in a cohort of children with perinatally acquired human immunodeficiency virus infection. Women and Infants Transmission Study Group. *J Pediatr* 1998;**132**:808-812.

26. Longo-Mbenza B, Seghers KV, Phuati M, Bikangi FN, Mubagwa K. Heart involvement and HIV infection in African patients: determinants of survival. *Int J Cardiol* 1998;**64**:63-73.

27. Barbaro G, Di Lorenzo G, Grisorio B, Barbarini G. Cardiac involvement in the acquired immunodeficiency syndrome: a multicenter clinical-pathological study. Gruppo Italiano per lo Studio Cardiologico dei pazienti affetti da AIDS Investigators. *AIDS Res Hum Retroviruses* 1998;**14**:1071-1077.

28. Sani MU, Okeahialam BN, Aliyu SH, Enoch DA. Human immunodeficiency virus (HIV) related heart disease: a review. *Wien Klin Wochenschr* 2005;**117**:73-81.

29. Zareba KM, Miller TL, Lipshultz SE. Cardiovascular disease and toxicities related to HIV infection and its therapies. *Expert Opin Drug Saf* 2005;**4**:1017-1025.

30. Magula NP, Mayosi BM. Cardiac involvement in HIV-infected people living in Africa: a review. *Cardiovasc J S Afr* 2003;**14**:231-237.

31. Sadigh M, Puttagunta S. Cardiac manifestations of HIV. *Front Biosci* 2003;**8**:s305-313.

32. Velasquez EM, Glancy DL. Cardiovascular disease in patients infected with the human immunodeficiency virus. *J La State Med Soc* 2003;**155**:314-324.

33. Cotter BR. Epidemiology of HIV cardiac disease. *Prog Cardiovasc Dis* 2003;**45**:319-326.

34. Zareba KM, Lipshultz SE. Cardiovascular Complications in Patients with HIV Infection. *Curr Infect Dis Rep* 2003;**5**:513-520.

35. Barbaro G. Cardiovascular manifestations of HIV infection. *Circulation* 2002;**106**:1420-1425.

36. Harmon WG, Dadlani GH, Fisher SD, Lipshultz SE. Myocardial and Pericardial Disease in HIV. *Curr Treat Options Cardiovasc Med* 2002;**4**:497-509.

37. Keesler MJ, Fisher SD, Lipshultz SE. Cardiac manifestations of HIV infection in infants and children. *Ann N Y Acad Sci* 2001;**946**:169-178.

38. Fisher SD, Lipshultz SE. Epidemiology of cardiovascular involvement in HIV disease and AIDS. *Ann N Y Acad Sci* 2001;**946**:13-22.

39. Rerkpattanapipat P, Wongpraparut N, Jacobs LE, Kotler MN. Cardiac manifestations of acquired immunodeficiency syndrome. *Arch Intern Med* 2000;**160**:602-608.

40. Panther LA. How HIV infection and its treatment affects the cardiovascular system: what is known, what is needed. *Am J Physiol Heart Circ Physiol* 2002;**283**:H1-4.

41. Klatt EC. Cardiovascular pathology in AIDS. In: *HIV Infection and the Cardiovascular System*. Barbaro G (editor). Basel: Karger; 2003:23-48.

42. Barbarini G, Barbaro G. Incidence of the involvement of the cardiovascular system in HIV infection. *AIDS* 2003;**17 Suppl 1**:S46-50.

43. Twagirumukiza M, Nkeramihigo E, Seminega B, Gasakure E, Boccara F, Barbaro G. Prevalence of dilated cardiomyopathy in HIV-infected African patients not receiving HAART: a multicenter, observational, prospective, cohort study in Rwanda. *Curr HIV Res* 2007;**5**:129-137.

44. Codd MB, Sugrue DD, Gersh BJ, Melton LJ, 3rd. Epidemiology of idiopathic dilated and hypertrophic cardiomyopathy. A population-based study in Olmsted County, Minnesota, 1975-1984. *Circulation* 1989;**80**:564-572.

45. Mosterd A, Hoes AW, de Bruyne MC, Deckers JW, Linker DT, Hofman A, Grobbee DE. Prevalence of heart failure and left ventricular dysfunction in the general population; The Rotterdam Study. *Eur Heart J* 1999;**20**:447-455.

46. Towbin JA, Lowe AM, Colan SD, Sleeper LA, Orav EJ, Clunie S, Messere J, Cox GF, Lurie PR, Hsu D, Canter C, Wilkinson JD, Lipshultz SE. Incidence, causes, and outcomes of dilated cardiomyopathy in children. *JAMA* 2006;**296**:1867-1876.

47. Damasceno A, Cotter G, Dzudie A, Sliwa K, Mayosi BM. Heart failure in sub-saharan Africa: time for action. *J Am Coll Cardiol* 2007;**50**:1688-1693.

48. Lubega S, Zirembuzi GW, Lwabi P. Heart disease among children with HIV/AIDS attending the paediatric infectious disease clinic at Mulago Hospital. *Afr Health Sci* 2005;**5**:219-226.

49. Nzuobontane D, Blackett KN, Kuaban C. Cardiac involvement in HIV infected people in Yaounde, Cameroon. *Postgrad Med J* 2002;**78**:678-681.

50. Fisher SD, Easley KA, Orav EJ, Colan SD, Kaplan S, Starc TJ, Bricker JT, Lai WW, Moodie DS, Sopko G, Lipshultz SE. Mild dilated cardiomyopathy and increased left ventricular mass predict mortality: the prospective P2C2 HIV Multicenter Study. *Am Heart J* 2005;**150**:439-447.

51. Diogenes MS, Succi RC, Machado DM, Moises VA, Novo NF, Carvalho AC. [Cardiac longitudinal study of children perinatally exposed to human immunodeficiency virus type 1]. *Arq Bras Cardiol* 2005;**85**:233-240.

52. Al-Attar I, Orav EJ, Exil V, Vlach SA, Lipshultz SE. Predictors of cardiac morbidity and related mortality in children with acquired immunodeficiency syndrome. *J Am Coll Cardiol* 2003;**41**:1598-1605.

53. Starc TJ, Lipshultz SE, Easley KA, Kaplan S, Bricker JT, Colan SD, Lai WW, Gersony WM, Sopko G, Moodie DS, Schluchter MD. Incidence of cardiac abnormalities in children with human immunodeficiency virus infection: The prospective P2C2 HIV study. *J Pediatr* 2002;**141**:327-334.

54. Langston C, Cooper ER, Goldfarb J, Easley KA, Husak S, Sunkle S, Starc TJ, Colin AA. Human immunodeficiency virus-related mortality in infants and children: data from the pediatric pulmonary and cardiovascular complications of vertically transmitted HIV (P(2)C(2)) Study. *Pediatrics* 2001;**107**:328-338.

55. Lipshultz SE, Easley KA, Orav EJ, Kaplan S, Starc TJ, Bricker JT, Wyman WL, Moodie DS, Sopko G, Schluchter MD, Colan SD. Cardiovascular status of infants

and children of women infected with HIV-1 (P^{2}C^2 HIV): a cohort study. *The Lancet* 2002;**360**:368-373.

56. Lipshultz SE, Easley KA, Orav EJ, Kaplan S, Starc TJ, Bricker JT, Lai WW, Moodie DS, McIntosh K, Schluchter MD, Colan SD. Left ventricular structure and function in children infected with human immunodeficiency virus: the prospective P2C2 HIV Multicenter Study. Pediatric Pulmonary and Cardiac Complications of Vertically Transmitted HIV Infection (P2C2 HIV) Study Group. *Circulation* 1998;**97**:1246-1256.

57. Johann-Liang R, Cervia JS, Noel GJ. Characteristics of human immunodeficiency virus-infected children at the time of death: an experience in the 1990s. *Pediatr Infect Dis J* 1997;**16**:1145-1150.

58. Barbaro G, Di Lorenzo G, Soldini M, Giancaspro G, Grisorio B, Pellicelli A, Barbarini G. Intensity of myocardial expression of inducible nitric oxide synthase influences the clinical course of human immunodeficiency virus-associated cardiomyopathy. *Circulation* 1999;**100**:933-939.

59. Pugliese A, Isnardi D, Saini A, Scarabelli T, Raddino R, Torre D. Impact of highly active antiretroviral therapy in HIV-positive patients with cardiac involvement. *J Infect* 2000;**40**:282-284.

60. Joint United Nations Programme on HIV/AIDS. *Report on the global AIDS epidemic: executive summary*. Geneva: UNAIDS; 2006.

61. El-Sadr WM, Lundgren JD, Neaton JD, Gordin F, Abrams D, Arduino RC, Babiker A, Burman W, Clumeck N, Cohen CJ, Cohn D, Cooper D, Darbyshire J, Emery S, Fatkenheuer G, Gazzard B, Grund B, Hoy J, Klingman K, Losso M, Markowitz N, Neuhaus J, Phillips A, Rappoport C. CD4+ count-guided interruption of antiretroviral treatment. *N Engl J Med* 2006;**355**:2283-2296.

62. Barbaro G. HIV-associated cardiomyopathy etiopathogenesis and clinical aspects. *Herz* 2005;**30**:486-492.

63. Currie PF, Boon NA. Immunopathogenesis of HIV-related heart muscle disease: current perspectives. *AIDS* 2003;**17(Suppl 1)**:S21-28.

64. Barbaro G. Pathogenesis of HIV-associated heart disease. *AIDS* 2003;**17 Suppl 1**:S12-20.

65. Barbaro G, Fisher SD, Lipshultz SE. Pathogenesis of HIV-associated cardiovascular complications. *The Lancet Infectious Diseases* 2001;**1**:115-124.

66. Barbaro G, Lipshultz SE. Pathogenesis of HIV-associated cardiomyopathy. *Ann N Y Acad Sci* 2001;**946**:57-81.

67. Barbaro G. HIV-associated myocarditis. *Heart Fail Clin* 2005;**1**:439-448.

68. Feldman AM, McNamara D. Myocarditis. *N Engl J Med* 2000;**343**:1388-1398.

69. Mason JW. Myocarditis and dilated cardiomyopathy: an inflammatory link. *Cardiovasc Res* 2003;**60**:5-10.

70. Kawai C. From myocarditis to cardiomyopathy: mechanisms of inflammation and cell death: learning from the past for the future. *Circulation* 1999;**99**:1091-1100.

71. Liu QN, Reddy S, Sayre JW, Pop V, Graves MC, Fiala M. Essential role of HIV type 1-infected and cyclooxygenase 2-activated macrophages and T cells in HIV type 1 myocarditis. *AIDS Res Hum Retroviruses* 2001;**17**:1423-1433.

72. Bowles NE, Kearney DL, Ni J, Perez-Atayde AR, Kline MW, Bricker JT, Ayres NA, Lipshultz SE, Shearer WT, Towbin JA. The detection of viral genomes by polymerase chain reaction in the myocardium of pediatric patients with advanced HIV disease. *J Am Coll Cardiol* 1999;**34**:857-865.

73. d'Amati G, di Gioia CR, Gallo P. Pathological findings of HIV-associated cardiovascular disease. *Ann N Y Acad Sci* 2001;**946**:23-45.

74. Wu TC, Pizzorno MC, Hayward GS, Willoughby S, Neumann DA, Rose NR, Ansari AA, Beschorner WE, Baughman KL, Herskowitz A. In situ detection of human cytomegalovirus immediate-early gene transcripts within cardiac myocytes of patients with HIV-associated cardiomyopathy. *AIDS* 1992;**6**:777-785.

75. Monsuez JJ, Escaut L, Teicher E, Charniot JC, Vittecoq D. Cytokines in HIV-associated cardiomyopathy. *Int J Cardiol* 2007;**120**:150-157.

76. Fisher SD, Bowles NE, Towbin JA, Lipshultz SE. Mediators in HIV-associated cardiovascular disease: a focus on cytokines and genes. *AIDS* 2003;**17(Suppl 1)**:S29-35.

77. Prabhu SD. Cytokine-induced modulation of cardiac function. *Circ Res* 2004;**95**:1140-1153.

78. Mann DL. Inflammatory mediators and the failing heart: past, present, and the foreseeable future. *Circulation Research* 2002;**91**:988-998.

79. Connolly NC, Riddler SA, Rinaldo CR. Proinflammatory cytokines in HIV disease-a review and rationale for new therapeutic approaches. *AIDS Rev* 2005;**7**:168-180.

80. Kedzierska K, Crowe SM. Cytokines and HIV-1: interactions and clinical implications. *Antivir Chem Chemother* 2001;**12**:133-150.

81. Fauci AS. Host factors and the pathogenesis of HIV-induced disease. *Nature* 1996;**384**:529-534.

82. Decrion AZ, Dichamp I, Varin A, Herbein G. HIV and inflammation. *Curr HIV Res* 2005;**3**:243-259.

83. Brenchley JM, Price DA, Schacker TW, Asher TE, Silvestri G, Rao S, Kazzaz Z, Bornstein E, Lambotte O, Altmann D, Blazar BR, Rodriguez B, Teixeira-Johnson L, Landay A, Martin JN, Hecht FM, Picker LJ, Lederman MM, Deeks SG, Douek DC. Microbial translocation is a cause of systemic immune activation in chronic HIV infection. *Nat Med* 2006;**12**:1365-1371.

84. Grody WW, Cheng L, Lewis W. Infection of the heart by the human immunodeficiency virus. *Am J Cardiol* 1990;**66**:203-206.

85. Lipshultz SE, Fox CH, Perez-Atayde AR, Sanders SP, Colan SD, McIntosh K, Winter HS. Identification of human immunodeficiency virus-1 RNA and DNA in the heart of a child with cardiovascular abnormalities and congenital acquired immune deficiency syndrome. *Am J Cardiol* 1990;**66**:246-250.

86. Rodriguez ER, Nasim S, Hsia J, Sandin RL, Ferreira A, Hilliard BA, Ross AM, Garrett CT. Cardiac myocytes and dendritic cells harbor human immunodeficiency virus in infected patients with and without cardiac dysfunction: detection by multiplex, nested, polymerase chain reaction in individually microdissected cells from right ventricular endomyocardial biopsy tissue. *Am J Cardiol* 1991;**68**:1511-1520.

87. Fiala M, Popik W, Qiao JH, Lossinsky AS, Alce T, Tran K, Yang W, Roos KP, Arthos J. HIV-1 induces cardiomyopathy by cardiomyocyte invasion and gp120, Tat, and cytokine apoptotic signaling. *Cardiovasc Toxicol* 2004;**4**:97-107.

88. Rebolledo MA, Krogstad P, Chen F, Shannon KM, Klitzner TS. Infection of human fetal cardiac myocytes by a human immunodeficiency virus-1-derived vector. *Circ Res* 1998;**83**:738-742.

89. Chen F, Shannon K, Ding S, Silva ME, Wetzel GT, Klitzner TS, Krogstad P. HIV type 1 glycoprotein 120 inhibits cardiac myocyte contraction. *AIDS Res Hum Retroviruses* 2002;**18**:777-784.

90. Kan H, Xie Z, Finkel MS. HIV gp120 enhances NO production by cardiac myocytes through p38 MAP kinase-mediated NF-kappaB activation. *Am J Physiol Heart Circ Physiol* 2000;**279**:H3138-3143.

91. Kay DG, Yue P, Hanna Z, Jothy S, Tremblay E, Jolicoeur P. Cardiac disease in transgenic mice expressing human immunodeficiency virus-1 nef in cells of the immune system. *Am J Pathol* 2002;**161**:321-335.

92. Raidel SM, Haase C, Jansen NR, Russ RB, Sutliff RL, Velsor LW, Day BJ, Hoit BD, Samarel AM, Lewis W. Targeted myocardial transgenic expression of HIV Tat causes cardiomyopathy and mitochondrial damage. *Am J Physiol Heart Circ Physiol* 2002;**282**:H1672-1678.

93. Lewis W, Miller YK, Haase CP, Ludaway T, McNaught J, Russ R, Steltzer J, Folpe A, Long R, Oshinski J. HIV viral protein R causes atrial cardiomyocyte mitosis, mesenchymal tumor, dysrhythmia, and heart failure. *Lab Invest* 2005;**85**:182-192.

94. Twu C, Liu NQ, Popik W, Bukrinsky M, Sayre J, Roberts J, Rania S, Bramhandam V, Roos KP, MacLellan WR, Fiala M. Cardiomyocytes undergo apoptosis in human immunodeficiency virus cardiomyopathy through mitochondrion- and death receptor-controlled pathways. *Proc Natl Acad Sci U S A* 2002;**99**:14386-14391.

95. Currie PF, Goldman JH, Caforio AL, Jacob AJ, Baig MK, Brettle RP, Haven AJ, Boon NA, McKenna WJ. Cardiac autoimmunity in HIV related heart muscle disease. *Heart* 1998;**79**:599-604.

96. Nanavati KA, Fisher SD, Miller TL, Lipshultz SE. HIV-related cardiovascular disease and drug interactions. *Am J Cardiovasc Drugs* 2004;**4**:315-324.

97. Vigano A, Giacomet V. Nucleoside analogues toxicities related to mitochondrial dysfunction: focus on HIV-infected children. *Antivir Ther* 2005;**10 Suppl 2**:M53-64.

98. Breuckmann F, Neumann T, Kondratieva J, Wieneke H, Ross B, Nassenstein K, Barkhausen J, Kreuter A, Brockmeyer N, Erbel R. Dilated cardiomyopathy in two adult human immunodeficiency positive (HIV+) patients possibly related to highly active antiretroviral therapy (HAART). *Eur J Med Res* 2005;**10**:395-399.

99. Frerichs FC, Dingemans KP, Brinkman K. Cardiomyopathy with mitochondrial damage associated with nucleoside reverse-transcriptase inhibitors. *N Engl J Med* 2002;**347**:1895-1896.

100. Herskowitz A, Willoughby SB, Baughman KL, Schulman SP, Bartlett JD. Cardiomyopathy associated with antiretroviral therapy in patients with HIV infection: a report of six cases. *Ann Intern Med* 1992;**116**:311-313.

101. Brownley KA, Milanovich JR, Motivala SJ, Schneiderman N, Fillion L, Graves JA, Klimas NG, Fletcher MA, Hurwitz BE. Autonomic and cardiovascular function in HIV spectrum disease: early indications of cardiac pathophysiology. *Clin Auton Res* 2001;**11**:319-326.

102. Plein D, Van Camp G, Cosyns B, Alimenti A, Levy J, Vandenbossche J-L. Cardiac and autonomic evaluation in a pediatric population with human immunodeficiency virus. *Clin Cardiol* 1999;**22**:33-36.

103. Gluck T, Degenhardt E, Scholmerich J, Lang B, Grossman J, Straub RH. Autonomic Neuropathy in patients with HIV: course, impact of disease stage, and medication. *Clin Auton Res* 2000;**10**:17-22.

104. Mittal CM, Wig N, Mishra S, Deepak KK. Heart rate variability in human immunodeficiency virus-positive individuals. *Int J Cardiol* 2004;**94**:1-6.

105. Rogstad KE, Shah R, Tesfaladet G, Abdullah M, Ahmed-Jushuf I. Cardiovascular autonomic neuropathy in HIV infected patients. *Sex Transm Infect* 1999;**75**:264-267.

106. Becker K, Gorlach I, Frieling T, Haussinger D. Characterization and natural course of cardiac autonomic nervous dysfunction in HIV-infected patients. *AIDS* 1997;**11**:751-757.

107. Natanson C, Eichenholz PW, Danner RL, Eichacker PQ, Hoffman WD, Kuo GC, Banks SM, MacVittie TJ, Parrillo JE. Endotoxin and tumor necrosis factor challenges in dogs simulate the cardiovascular profile of human septic shock. *J Exp Med* 1989;**169**:823-832.

108. Mehra VC, Ramgolam VS, Bender JR. Cytokines and cardiovascular disease. *J Leukoc Biol* 2005;**78**:805-818.

109. Kelly RA, Smith TW. Cytokines and cardiac contractile function. *Circulation* 1997;**95**:778-781.

110. Yndestad A, Holm AM, Muller F, Simonsen S, Froland SS, Gullestad L, Aukrust P. Enhanced expression of inflammatory cytokines and activation markers in T-cells from patients with chronic heart failure. *Cardiovasc Res* 2003;**60**:141-146.

111. Anker SD, von Haehling S. Inflammatory mediators in chronic heart failure: an overview. *Heart* 2004;**90**:464-470.

112. Eichenholz PW, Eichacker PQ, Hoffman WD, Banks SM, Parrillo JE, Danner RL, Natanson C. Tumor necrosis factor challenges in canines: patterns of cardiovascular dysfunction. *Am J Physiol* 1992;**263**:H668-675.

113. Woldbaek PR, B. SJ, Stromme TA, Lunde PK, Djurovic S, Lyberg T, Christensen G, Tonnessen T. Daily administration of interleukin-18 causes myocardial dysfunction in healthy mice. *Am J Physiol* 2005;**289**:H708-H714.

114. Woldbaek PR, Tonnessen T, Henriksen UL, Florholmen G, Lunde PK, Lyberg T, Christensen G. Increased cardiac IL-18 mRNA, prol-IL-18 and plasma IL-18 after myocardial infarction in the mouse; a potential role in cardiac dysfunction. *Cardiovasc Res* 2003;**59**:122-131.

115. Raeburn CD, Dinarello CA, Zimmerman MA, Calkins CM, Pomerantz BJ, McIntyre RC, Jr., Harken AH, Meng X. Neutralization of IL-18 attenuates lipopolysaccharide-induced myocardial dysfunction. *Am J Physiol Heart Circ Physiol* 2002;**283**:H650-657.

116. Pomerantz BJ, Reznikov LL, Harken AH, Dinarello CA. Inhibition of caspase 1 reduces human myocardial ischemic dysfunction via inhibition of IL-18 and IL-1β. *Proc Natl Acad Sci* 2001;**98**:2871-2876.

117. Naito Y, Tsujino T, Fujioka Y, Ohyanagi M, Okamura H, Iwasaki T. Increased circulating interleukin-18 in patients with congestive heart failure. *Heart* 2002;**88**:296-297.

118. Torre-Amione G, Kapadia S, Benedict C, Oral H, Young JB, Mann DL. Proinflammatory cytokine levels in patients with depressed left ventricular ejection fraction: a report from the studies of left ventricular dysfunction (SOLVD). *J Am Coll Cardiol* 1996;**27**:1201-1206.

119. Levine B, Kalman J, Mayer L, Fillit HM, Packer M. Elevated circulating levels of tumor necrosis factor in severe chronic heart failure. *N Engl J Med* 1990;**323**:236-241.

120. Testa M, Yeh M, Lee P, Fanelli R, Loperfido F, Berman JW, LeJemtel TH. Circulating levels of cytokines and their endogenous modulators in patients with

mild to severe congestive heart failure due to coronary artery disease or hypertension. *J Am Coll Cardiol* 1996;**28**:964-971.

121. Francis SE, Holden H, Holt CM, Duff GW. Interleukin-1 in myocardium and coronary arteries of patients with dilated cardiomyopathy. *J Mol Cell Cardiol* 1998;**30**:215-223.

122. Mallat Z, Heymes C, Corbaz A, Logeart D, Alouani S, Cohen-Solal A, Seidler T, Hasenfuss G, Chvatchko Y, Shah AM, Tedgui A. Evidence for altered interleukin 18 (IL)-18 pathway in human heart failure. *FASEB J* 2004;**18**:1752-1754.

123. Hosenpud JD, Campbell SM, Mendelson DJ. Interleukin-1-induced myocardial depression in an isolated beating heart preparation. *J Heart Transplant* 1989;**8**:460-464.

124. Cain BS, Meldrum DR, Dinarello CA, Meng X, Joo KS, Banerjee A, Harken AH. Tumor necrosis factor-alpha and interleukin-1beta synergistically depress human myocardial function. *Crit Care Med* 1999;**27**:1309-1318.

125. Chandrasekar B, Mummidi S, Claycomb WC, Mestril R, Nemer M. Interleukin-18 is a pro-hypertrophic cytokine that acts through a phosphatidylinositol 3-kinase-phosphoinositide-dependent kinase-1-Akt-GATA4 signaling pathway in cardiomyocytes. *J Biol Chem* 2005;**280**:4553-4567.

126. Meldrum DR. Tumor necrosis factor in the heart. *Am J Physiol* 1998;**274**:R577-595.

127. Kumar A, Paladugu B, Mensing J, Kumar A, Parrillo JE. Nitric oxide-dependent and -independent mechanisms are involved in TNF-alpha -induced depression of cardiac myocyte contractility. *Am J Physiol Regul Integr Comp Physiol* 2007;**292**:R1900-1906.

128. Wang M, Meldrum DR. Biology and Mechanisms of Action of Interleukin 18 in the Heart. *Shock* 2007.

129. Sivasubramanian N, Coker ML, Kurrelmeyer KM, MacLellan WR, DeMayo FJ, Spinale FG, Mann DL. Left ventricular remodeling in transgenic mice with cardiac restricted overexpression of tumor necrosis factor. *Circulation* 2001;**104**:826-831.

130. Bozkurt B, Kribbs SB, Clubb FJ, Michael LH, Didenko VV, Hornsby PJ, Seta Y, Oral H, Spinale F, Mann DL. Pathophysiologically relevant concentrations of tumor necrosis factor-a promote progressive left ventricular dysfunction and remodeling in rats. *Circulation* 1998;**97**:1382-1391.

131. Colston JT, Boylston WH, Feldman MD, Jenkinson CP, de la Rosa SD, Barton A, Trevino RJ, Freeman GL, Chandrasekar B. Interleukin-18 knockout mice display maladaptive cardiac hypertrophy in response to pressure overload. *Biochem Biophys Res Commun* 2007;**354**:552-558.

132. Haudek SB, Taffet GE, Schneider MD, Mann DL. TNF provokes cardiomyocyte apoptosis and cardiac remodeling through activation of multiple cell death pathways. *J Clin Invest* 2007;**117**:2692-2701.

133. Torre-Amione G, Wallace CK, Young JB, Koerner MM, Thohan V, McRee S, Bogaev RC. The effect of etanercept on cardiac transplant recipients: a study of TNFalpha antagonism and cardiac allograft hypertrophy. *Transplantation* 2007;**84**:480-483.

134. Bryant D, Becker L, Richardson J, Shelton J, Franco F, Peshock R, Thompson M, Giroir B. Cardiac failure in transgenic mice with myocardial expression of tumor necrosis factor-α. *Circulation* 1998;**97**:1375-1381.

135. Yndestad A, Damas JK, Oie E, Ueland T, Gullestad L, Aukrust P. Role of inflammation in the progression of heart failure. *Curr Cardiol Rep* 2007;**9**:236-241.

136. Matsumori A, Yamada T, Suzuki H, Matoba Y, Sasayama S. Increased circulating cytokines in patients with myocarditis and cardiomyopathy. *Br Heart J* 1994;**72**:561-566.

137. Sanchez-Lazaro IJ, Almenar L, Reganon E, Vila V, Martinez-Dolz L, Martinez-Sales V, Moro J, Aguero J, Ortiz-Martinez V, Salvador A. Inflammatory markers in stable heart failure and their relationship with functional class. *Int J Cardiol* 2007.

138. Mallat Z, Henry P, Fressonnet R, Alouani S, Scoazec A, Beaufils P, Chvatchko Y, Tedgui A. Increased plasma concentrations of interleukin-18 in acute coronary syndromes. *Heart* 2002;**88**:467-469.

139. Brenchley JM, Price DA, Douek DC. HIV disease: fallout from a mucosal catastrophe? *Nat Immunol* 2006;**7**:235-239.

140. Aukrust P, Liabakk N-B, Muller F, Lien E, Espevik T, Froland SS. Serum levels of tumor necrosis factor-α (TNFα) and soluble TNF receptors in human immunodeficiency virus type 1 infection--correlations to clinical, immunologic, and virologic parameters. *J Infect Dis* 1994;**169**:420-424.

141. Molina JM, Scadden DT, Byrn R, Dinarello CA, Groopman JE. Production of tumor necrosis factor alpha and interleukin 1 beta by monocytic cells infected with human immunodeficiency virus. *J Clin Invest* 1989;**84**:733-737.

142. Denis M, Ghadirian E. Interaction between Mycobacterium avium and human immunodeficiency virus type 1 (HIV-1) in bronchoalveolar macrophages of normal and HIV-1-infected subjects. *Am J Respir Cell Mol Biol* 1994;**11**:487-495.

143. Stylianou E, Bjerkeli V, Yndestad A, Heggelund L, Waehre T, Damas JK, Aukrust P, Froland SS. Raised serum levels of interleukin-18 is associated with disease progression and may contribute to virological treatment failure in HIV-1-infected patients. *Clin Exp Immunol* 2003;**132**:462-466.

144. Belec L, Meillet D, Hernvann A, Gresenguet G, Gherardi R. Differential elevation of circulating interleukin-1 beta, tumor necrosis factor alpha, and interleukin-6 in AIDS-associated cachectic states. *Clin Diagn Lab Immunol* 1994;**1**:117-120.

145. Lathey JL, Kanangat S, Rouse BT, Agosti JM, Spector SA. Dysregulation of cytokine expression in monocytes from HIV-positive individuals. *J Leukoc Biol* 1994;**56**:347-352.

146. Torre D, Speranza F, Martegani R, Pugliese A, Castelli F, Basilico C, Biondi G. Circulating levels of IL-18 in adult and paediatric patients with HIV-1 infection. *AIDS* 2000;**14**:2211-2212.

147. Ahmad R, Sindhu ST, Toma E, Morisset R, Ahmad A. Elevated levels of circulating interleukin-18 in human immunodeficiency virus-infected individuals: role of peripheral blood mononuclear cells and implications for AIDS pathogenesis. *J Virol* 2002;**76**:12448-12456.

148. Gordon MA, Gordon SB, Musaya L, Zijlstra EE, Molyneux ME, Read RC. Primary macrophages from HIV-infected adults show dysregulated cytokine responses to Salmonella, but normal internalization and killing. *AIDS* 2007;**21**:2399-2408.

149. Ledru E, Christeff N, Patey O, de Truchis P, Melchior J-C, Gougeon M-L. Alteration of tumor necrosis factor-α T-cell homeostasis following potent antiretroviral therapy: contribution to the development of human immunodeficiency virus-associated lipodystrophy syndrome. *Blood* 2000;**95**:3191-3198.

150. Aukrust P, Muller F, Lien E, Nordoy I, Liabakk N-B, Kvale D, Espevik T, Froland SS. Tumor necrosis factor (TNF) system levels in human immunodeficiency virus-infected patients during highly active antiretroviral

therapy: persistent TNF activation is associated with virologic and immunologic treatment failure. *J Infect Dis* 1999;**179**:74-82.

151.   Yue P, Massie BM, Simpson PC, Long CS. Cytokine expression increases in nonmyocytes from rats with postinfarction heart failure. *Am J Physiol* 1998;**275**:H250-258.

152.   Kapadia S, Lee J, Torre-Amione G, Birdsall HH, Ma TS, Mann DL. Tumor necrosis factor-α gene and protein expression in adult feline myocardium after endotoxin administration. *J Clin Invest* 1995;**96**:1042-1052.

153.   Mann DL. Recent Insights into the Role of Tumor Necrosis Factor in the Failing Heart. In: *The Role of Inflammatory Mediators in the Failing Heart*. Mann DL (editor). Boston: Kluwer Academic Publishers; 2001.

154.   Giroir BP, Johnson JH, Brown T, Allen GL, Beutler B. The tissue distribution of tumor necrosis factor biosynthesis during endotoxemia. *J Clin Invest* 1992;**90**:693-698.

155.   Long CS. The Role of Interleukin-1 in the Failing Heart. In: *The Role of Inflammatory Mediators in the Failing Heart*. Mann DL (editor). Boston: Kluwer Academic Publishers; 2001:13-25.

156.   Spencer SC, Fabre JW. Characterization of the tissue macrophage and the interstitial dendritic cell as distinct leukocytes normally resident in the connective tissue of rat heart. *J Exp Med* 1990;**171**:1841-1851.

157.   Yokoyama H, Kuwao S, Kohno K, Suzuki K, Kameya T, Izumi T. Cardiac dendritic cells and acute myocarditis in the human heart. *Jpn Circ J* 2000;**64**:57-64.

158.   Yearley JH, Pearson C, Carville A, Shannon RP, Mansfield KG. SIV-associated myocarditis: viral and cellular correlates of inflammation severity. *AIDS Res Hum Retroviruses* 2006;**22**:529-540.

159.   Yearley JH, Pearson C, Shannon RP, Mansfield KG. Phenotypic variation in myocardial macrophage populations suggests a role for macrophage activation in SIV-associated cardiac disease. *AIDS Res Hum Retroviruses* 2007;**23**:515-524.

160.   Cassol E, Alfano M, Biswas P, Poli G. Monocyte-derived macrophages and myeloid cell lines as targets of HIV-1 replication and persistence. *J Leukoc Biol* 2006;**80**:1018-1030.

161. Donaghy H, Wilkinson J, Cunningham AL. HIV interactions with dendritic cells: has our focus been too narrow? *J Leukoc Biol* 2006;**80**:1001-1012.

162. Simard MC, Chrobak P, Kay DG, Hanna Z, Jothy S, Jolicoeur P. Expression of simian immunodeficiency virus nef in immune cells of transgenic mice leads to a severe AIDS-like disease. *J Virol* 2002;**76**:3981-3995.

163. Hart DN, Fabre JW. Demonstration and characterization of Ia-positive dendritic cells in the interstitial connective tissues of rat heart and other tissues, but not brain. *J Exp Med* 1981;**154**:347-361.

164. Austyn JM, Hankins DF, Larsen CP, Morris PJ, Rao AS, Roake JA. Isolation and characterization of dendritic cells from mouse heart and kidney. *J Immunol* 1994;**152**:2401-2410.

165. Zhang J, Yu ZX, Fujita S, Yamaguchi ML, Ferrans VJ. Interstitial dendritic cells of the rat heart. Quantitative and ultrastructural changes in experimental myocardial infarction. *Circulation* 1993;**87**:909-920.

166. Larsen CP, Morris PJ, Austyn JM. Migration of dendritic leukocytes from cardiac allografts into host spleens. A novel pathway for initiation of rejection. *J Exp Med* 1990;**171**:307-314.

167. Gordon S. Alternative activation of macrophages. *Nat Rev Immunol* 2003;**3**:23-35.

168. Almeida M, Cordero M, Almeida J, Orfao A. Persistent abnormalities in peripheral blood dendritic cells and monocytes from HIV-1-positive patients after 1 year of antiretroviral therapy. *J Acquir Immune Defic Syndr* 2006;**41**:405-415.

169. Eriksson U, Ricci R, Hunziker L, Kurrer MO, Oudit GY, Watts TH, Sonderegger I, Bachmaier K, Kopf M, Penninger JM. Dendritic cell-induced autoimmune heart failure requires cooperation between adaptive and innate immunity. *Nat Med* 2003;**9**:1484-1490.

170. Matsumoto Y, Tsukada Y, Miyakoshi A, Sakuma H, Kohyama K. C protein-induced myocarditis and subsequent dilated cardiomyopathy: rescue from death and prevention of dilated cardiomyopathy by chemokine receptor DNA therapy. *J Immunol* 2004;**173**:3535-3541.

171. Chaves AA, Baliga RS, Mihm MJ, Schanbacher BL, Basuray A, Liu C, Cook AC, Ayers LW, Bauer JA. Bacterial lipopolysaccharide enhances cardiac dysfunction but not retroviral replication in murine AIDS: roles of macrophage infiltration and toll-like receptor 4 expression. *Am J Pathol* 2006;**168**:727-735.

172. Steinman RM, Hawiger D, Liu K, Bonifaz L, Bonnyay D, Mahnke K, Iyoda T, Ravetch J, Dhodapkar M, Inaba K, Nussenzweig M. Dendritic cell function in vivo during the steady state: a role in peripheral tolerance. *Ann N Y Acad Sci* 2003;**987**:15-25.

173. Mosser DM. The many faces of macrophage activation. *J Leukoc Biol* 2003;**73**:209-212.

174. Goerdt S, Orfanos CE. Other functions, other genes: alternative activation of antigen-presenting cells. *Immunity* 1999;**10**:137-142.

175. Verreck FA, de Boer T, Langenberg DM, van der Zanden L, Ottenhoff TH. Phenotypic and functional profiling of human proinflammatory type-1 and anti-inflammatory type-2 macrophages in response to microbial antigens and IFN-gamma- and CD40L-mediated costimulation. *J Leukoc Biol* 2006;**79**:285-293.

176. Gao F, Bailes E, Robertson DL, Chen Y, Rodenburg CM, Michael SF, Cummins LB, Arthur LO, Peeters M, Shaw GM, Sharp PM, Hahn BH. Origin of HIV-1 in the chimpanzee Pan troglodytes troglodytes. *Nature* 1999;**397**:436-441.

177. Hahn BH, Shaw GM, De Cock KM, Sharp PM. AIDS as a zoonosis: scientific and public health implications. *Science* 2000;**287**:607-614.

178. Shannon RP, Simon MA, Mathier MA, Geng YJ, Mankad S, Lackner AA. Dilated cardiomyopathy associated with simian AIDS in nonhuman primates. *Circulation* 2000;**101**:185-193.

179. Shannon RP. SIV cardiomyopathy in non-human primates. *Trends Cardiovasc Med* 2001;**11**:242-246.

180. Han X, Stolarski C, Hentosz T, Carville A, Simon M, Shannon RP. Up-regulation of NOS3 and induction of NOS2 and TNFα in myocardium from simian immunodeficiency virus-infected non-human primates. *Circulation Suppl II* 2001;**104**:163.

181. Desrosiers RC. The simian immunodeficiency viruses. *Annu Rev Immunol* 1990;**8**:557-578.

182. Letvin NL, King NW. Immunologic and pathologic manifestations of the infection of rhesus monkeys with simian immunodeficiency virus of macaques. *J Acquir Immune Defic Syndr* 1990;**3**:1023-1040.

183. Simon MA, Chalifoux LV, Ringler DJ. Pathologic features of SIV-induced disease and the association of macrophage infection with disease evolution. *AIDS Res Hum Retroviruses* 1992;**8**:327-337.

184. King NW, Chalifoux LV, Ringler DJ, Wyand MS, Sehgal PK, Daniel MD, Letvin NL, Desrosiers RC, Blake BJ, Hunt RD. Comparative biology of natural and experimental SIVmac infection in macaque monkeys: a review. *J Med Primatol* 1990;**19**:109-118.

185. Baskin GB, Murphey-Corb M, Watson EA, Martin LN. Necropsy findings in rhesus monkeys experimentally infected with cultured simian immunodeficiency virus (SIV)/delta. *Vet Pathol* 1988;**25**:456-467.

186. McClure HM, Anderson DC, Fultz PN, Ansari AA, Lockwood E, Brodie A. Spectrum of disease in macaque monkeys chronically infected with SIV/SMM. *Vet Immunol Immunopathol* 1989;**21**:13-24.

187. Horvath CJ, Hunt RD, Simon MA, Sehgal PK, Ringler DJ. An immunohistologic study of granulomatous inflammation in SIV-infected rhesus monkeys. *J Leukoc Biol* 1993;**53**:532-540.

188. Aretz HT, Billingham ME, Edwards WD, Factor SM, Fallon JT, Fenoglio JJ, Jr., Olsen EG, Schoen FJ. Myocarditis. A histopathologic definition and classification. *Am J Cardiovasc Pathol* 1987;**1**:3-14.

189. Novembre FJ, De Rosayro J, O'Neil SP, Anderson DC, Klumpp SA, McClure HM. Isolation and characterization of a neuropathogenic simian immunodeficiency virus derived from a sooty mangabey. *J Virol* 1998;**72**:8841-8851.

190. Geijtenbeek TB, Torensma R, van Vliet SJ, van Duijnhoven GC, Adema GJ, van Kooyk Y, Figdor CG. Identification of DC-SIGN, a novel dendritic cell-specific ICAM-3 receptor that supports primary immune responses. *Cell* 2000;**100**:575-585.

191. Yu Kimata MT, Cella M, Biggins JE, Rorex C, White R, Hicks S, Wilson JM, Patel PG, Allan JS, Colonna M, Kimata JT. Capture and transfer of simian immunodeficiency virus by macaque dendritic cells is enhanced by DC-SIGN. *J Virol* 2002;**76**:11827-11836.

192. Chehimi J, Luo Q, Azzoni L, Shawver L, Ngoubilly N, June R, Jerandi G, Farabaugh M, Montaner LJ. HIV-1 transmission and cytokine-induced expression of DC-SIGN in human monocyte-derived macrophages. *J Leukoc Biol* 2003;**74**:757-763.

193. Schwartz AJ, Alvarez X, Lackner AA. Distribution and immunophenotype of DC-SIGN-expressing cells in SIV-infected and uninfected macaques. *AIDS Res Hum Retroviruses* 2002;**18**:1021-1029.

194. Lawson CM, O'Donoghue HL, Reed WD. Mouse cytomegalovirus infection induces antibodies which cross-react with virus and cardiac myosin: a model for the study of molecular mimicry in the pathogenesis of viral myocarditis. *Immunology* 1992;**75**:513-519.

195. O'Donoghue HL, Lawson CM, Reed WD. Autoantibodies to cardiac myosin in mouse cytomegalovirus myocarditis. *Immunology* 1990;**71**:20-28.

196. Fairweather D, Lawson CM, Chapman AJ, Brown CM, Booth TW, Papadimitriou JM, Shellam GR. Wild isolates of murine cytomegalovirus induce myocarditis and antibodies that cross-react with virus and cardiac myosin. *Immunology* 1998;**94**:263-270.

197. Hendricks EE, Lin KC, Boisvert K, Pauley D, Mansfield KG. Alterations in expression of monocyte chemotactic protein-1 in the simian immunodeficiency virus model of disseminated Mycobacterium avium complex. *J Infect Dis* 2004;**189**:1714-1720.

198. Chesebro B, Wehrly K, Nishio J, Perryman S. Macrophage-tropic human immunodeficiency virus isolates from different patients exhibit unusual V3 envelope sequence homogeneity in comparison with T-cell-tropic isolates: definition of critical amino acids involved in cell tropism. *J Virol* 1992;**66**:6547-6554.

199. Toohey K, Wehrly K, Nishio J, Perryman S, Chesebro B. Human immunodeficiency virus envelope V1 and V2 regions influence replication efficiency in macrophages by affecting virus spread. *Virology* 1995;**213**:70-79.

200. Williams KC, Corey S, Westmoreland SV, Pauley D, Knight H, deBakker C, Alvarez X, Lackner AA. Perivascular macrophages are the primary cell type productively infected by simian immunodeficiency virus in the brains of macaques: implications for the neuropathogenesis of AIDS. *J Exp Med* 2001;**193**:905-915.

201. Kristiansen M, Graversen JH, Jacobsen C, Sonne O, Hoffman HJ, Law SK, Moestrup SK. Identification of the haemoglobin scavenger receptor. *Nature* 2001;**409**:198-201.

202. Moestrup SK, Moller HJ. CD163: a regulated hemoglobin scavenger receptor with a role in the anti-inflammatory response. *Ann Med* 2004;**36**:347-354.

203. Gown AM, Tsukada T, Ross R. Human atherosclerosis. II. Immunocytochemical analysis of the cellular composition of human atherosclerotic lesions. *Am J Pathol* 1986;**125**:191-207.

204. Adams CW, Poston RN. Macrophage histology in paraffin-embedded multiple sclerosis plaques is demonstrated by the monoclonal pan-macrophage marker HAM-56: correlation with chronicity of the lesion. *Acta Neuropathol (Berl)* 1990;**80**:208-211.

205. Scholler N, Hayden-Ledbetter M, Dahlin A, Hellstrom I, Hellstrom KE, Ledbetter JA. Cutting edge: CD83 regulates the development of cellular immunity. *J Immunol* 2002;**168**:2599-2602.

206. Zhou LJ, Tedder TF. CD14+ blood monocytes can differentiate into functionally mature CD83+ dendritic cells. *Proc Natl Acad Sci U S A* 1996;**93**:2588-2592.

207. Banchereau J, Briere F, Caux C, Davoust J, Lebecque S, Liu YJ, Pulendran B, Palucka K. Immunobiology of dendritic cells. *Annu Rev Immunol* 2000;**18**:767-811.

208. Porcheray F, Viaud S, Rimaniol AC, Leone C, Samah B, Dereuddre-Bosquet N, Dormont D, Gras G. Macrophage activation switching: an asset for the resolution of inflammation. *Clin Exp Immunol* 2005;**142**:481-489.

209. Philippidis P, Mason JC, Evans BJ, Nadra I, Taylor KM, Haskard DO, Landis RC. Hemoglobin scavenger receptor CD163 mediates interleukin-10 release and heme oxygenase-1 synthesis: antiinflammatory monocyte-macrophage responses in vitro, in resolving skin blisters in vivo, and after cardiopulmonary bypass surgery. *Circ Res* 2004;**94**:119-126.

210. Baeten D, Moller HJ, Delanghe J, Veys EM, Moestrup SK, De Keyser F. Association of CD163+ macrophages and local production of soluble CD163 with decreased lymphocyte activation in spondylarthropathy synovitis. *Arthritis Rheum* 2004;**50**:1611-1623.

211. Frings W, Dreier J, Sorg C. Only the soluble form of the scavenger receptor CD163 acts inhibitory on phorbol ester-activated T-lymphocytes, whereas membrane-bound protein has no effect. *FEBS Lett* 2002;**526**:93-96.

212. Hogger P, Sorg C. Soluble CD163 inhibits phorbol ester-induced lymphocyte proliferation. *Biochem Biophys Res Commun* 2001;**288**:841-843.

213. Buechler C, Ritter M, Orso E, Langmann T, Klucken J, Schmitz G. Regulation of scavenger receptor CD163 expression in human monocytes and macrophages by pro- and antiinflammatory stimuli. *J Leukoc Biol* 2000;**67**:97-103.

214. Schebesch C, Kodelja V, Muller C, Hakij N, Bisson S, Orfanos CE, Goerdt S. Alternatively activated macrophages actively inhibit proliferation of peripheral blood lymphocytes and CD4+ T cells in vitro. *Immunology* 1997;**92**:478-486.

215. Porcheray F, Samah B, Leone C, Dereuddre-Bosquet N, Gras G. Macrophage activation and human immunodeficiency virus infection: HIV replication directs macrophages towards a pro-inflammatory phenotype while previous activation modulates macrophage susceptibility to infection and viral production. *Virology* 2006;**349**:112-120.

216. Kim WK, Alvarez X, Fisher J, Bronfin B, Westmoreland S, McLaurin J, Williams K. CD163 identifies perivascular macrophages in normal and viral encephalitic brains and potential precursors to perivascular macrophages in blood. *Am J Pathol* 2006;**168**:822-834.

217. Choi YK, Whelton KM, Mlechick B, Murphey-Corb MA, Reinhart TA. Productive infection of dendritic cells by simian immunodeficiency virus in macaque intestinal tissues. *J Pathol* 2003;**201**:616-628.

218. von Reyn CF, Maslow JN, Barber TW, Falkinham JO, Arbeit RD. Persistent colonisation of potable water as a source of *Mycobacterium avium* infection in AIDS. *Lancet* 1994;**343**:1137-1141.

219. Yajko DM, Chin DP, Gonzalez PC, Nassos PS, Hopewell PC, Reingold AL, Horsburgh CR, Yakrus MA, Ostroff SM, Hadley WK. Mycobacterium avium complex in water, food, and soil samples collected from the environment of HIV-infected individuals. *J Acquir Immune Defic Syndr Hum Retrovirol* 1995;**9**:176-182.

220. Horsburgh CR, Jr. Mycobacterium avium complex infection in the acquired immunodeficiency syndrome. *N Engl J Med* 1991;**324**:1332-1338.

221. Mansfield KG, Veazey RS, Hancock A, Carville A, Elliott M, Lin KC, Lackner AA. Induction of disseminated Mycobacterium avium in simian AIDS is dependent upon simian immunodeficiency virus strain and defective granuloma formation. *Am J Pathol* 2001;**159**:693-702.

222. Suryanarayana K, Wiltrout TA, Vasquez GM, Hirsch VM, Lifson JD. Plasma SIV RNA viral load determination by real-time quantification of product generation in

reverse transcriptase-polymerase chain reaction. *AIDS Res Hum Retroviruses* 1998;**14**:183-189.

223.   Mori K, Yoshida K, Komatsu A, Tani J, Nakagawa Y, Hoshikawa S, Ito S. Autoinduction of tumor necrosis factor-alpha in FRTL-5 rat thyroid cells. *J Endocrinol* 2005;**187**:17-24.

224.   Sulahian TH, Hogger P, Wahner AE, Wardwell K, Goulding NJ, Sorg C, Droste A, Stehling M, Wallace PK, Morganelli PM, Guyre PM. Human monocytes express CD163, which is upregulated by IL-10 and identical to p155. *Cytokine* 2000;**12**:1312-1321.

225.   Puig-Kroger A, Serrano-Gomez D, Caparros E, Dominguez-Soto A, Relloso M, Colmenares M, Martinez-Munoz L, Longo N, Sanchez-Sanchez N, Rincon M, Rivas L, Sanchez-Mateos P, Fernandez-Ruiz E, Corbi AL. Regulated expression of the pathogen receptor dendritic cell-specific intercellular adhesion molecule 3 (ICAM-3)-grabbing nonintegrin in THP-1 human leukemic cells, monocytes, and macrophages. *J Biol Chem* 2004;**279**:25680-25688.

226.   Relloso M, Puig-Kroger A, Pello OM, Rodriguez-Fernandez JL, de la Rosa G, Longo N, Navarro J, Munoz-Fernandez MA, Sanchez-Mateos P, Corbi AL. DC-SIGN (CD209) expression is IL-4 dependent and is negatively regulated by IFN, TGF-beta, and anti-inflammatory agents. *J Immunol* 2002;**168**:2634-2643.

227.   Gurney KB, Elliott J, Nassanian H, Song C, Soilleux E, McGowan I, Anton PA, Lee B. Binding and transfer of human immunodeficiency virus by DC-SIGN+ cells in human rectal mucosa. *J Virol* 2005;**79**:5762-5773.

228.   Lee KS, Baek DW, Kim KH, Shin BS, Lee DH, Kim JW, Hong YS, Bae YS, Kwak JY. IL-10-dependent down-regulation of MHC class II expression level on monocytes by peritoneal fluid from endometriosis patients. *Int Immunopharmacol* 2005;**5**:1699-1712.

229.   de Waal Malefyt R, Haanen J, Spits H, Roncarolo MG, te Velde A, Figdor C, Johnson K, Kastelein R, Yssel H, de Vries JE. Interleukin 10 (IL-10) and viral IL-10 strongly reduce antigen-specific human T cell proliferation by diminishing the antigen-presenting capacity of monocytes via downregulation of class II major histocompatibility complex expression. *J Exp Med* 1991;**174**:915-924.

230.   Redpath S, Angulo A, Gascoigne NR, Ghazal P. Murine cytomegalovirus infection down-regulates MHC class II expression on macrophages by induction of IL-10. *J Immunol* 1999;**162**:6701-6707.

231. Moore KW, de Waal Malefyt R, Coffman RL, O'Garra A. Interleukin-10 and the interleukin-10 receptor. *Annu Rev Immunol* 2001;**19**:683-765.

232. Lima RG, Van Weyenbergh J, Saraiva EM, Barral-Netto M, Galvao-Castro B, Bou-Habib DC. The replication of human immunodeficiency virus type 1 in macrophages is enhanced after phagocytosis of apoptotic cells. *J Infect Dis* 2002;**185**:1561-1566.

233. Voll RE, Herrmann M, Roth EA, Stach C, Kalden JR, Girkontaite I. Immunosuppressive effects of apoptotic cells. *Nature* 1997;**390**:350-351.

234. Fadok VA, Bratton DL, Konowal A, Freed PW, Westcott JY, Henson PM. Macrophages that have ingested apoptotic cells in vitro inhibit proinflammatory cytokine production through autocrine/paracrine mechanisms involving TGF-beta, PGE2, and PAF. *J Clin Invest* 1998;**101**:890-898.

235. Geijtenbeek TB, van Vliet SJ, Engering A, t Hart BA, van Kooyk Y. Self- and nonself-recognition by C-type lectins on dendritic cells. *Annu Rev Immunol* 2004;**22**:33-54.

236. Caparros E, Munoz P, Sierra-Filardi E, Serrano-Gomez D, Puig-Kroger A, Rodriguez-Fernandez JL, Mellado M, Sancho J, Zubiaur M, Corbi AL. DC-SIGN ligation on dendritic cells results in ERK and PI3K activation and modulates cytokine production. *Blood* 2006;**107**:3950-3958.

237. Smith PD, Meng G, Salazar-Gonzalez JF, Shaw GM. Macrophage HIV-1 infection and the gastrointestinal tract reservoir. *J Leukoc Biol* 2003;**74**:642-649.

238. Lim S, Caramori G, Tomita K, Jazrawi E, Oates T, Chung KF, Barnes PJ, Adcock IM. Differential expression of IL-10 receptor by epithelial cells and alveolar macrophages. *Allergy* 2004;**59**:505-514.

239. Fischer-Smith T, Croul S, Bell C, Lewis M, Rappaport J. Alterations in CD163+/CD16+ monocytes/macrophages in CNS and blood in HIV-1 and SIV associated CNS disease. *FASEB J* 2007;**21**:lb312.

240. Yearley JH, Mansfield KG, Carville AAL, Sokos GG, Xia D, Pearson CB, Shannon RP. Antigenic stimulation in the simian model of HIV infection yields dilated cardiomyopathy through effects of TNFalpha. *AIDS* 2008;**22**:in press.

241. Blankenberg S, Luc G, Ducimetiere P, Arveiler D, Ferrieres J, Amouyel P, Evans A, Cambien F, Tiret L. Interleukin-18 and the risk of coronary heart disease in European men: the Prospective Epidemiological Study of Myocardial Infarction (PRIME). *Circulation* 2003;**108**:2453-2459.

242. Thompson SR, Novick D, Stock CJ, Sanders J, Brull D, Cooper J, Woo P, Miller G, Rubinstein M, Humphries SE. Free Interleukin (IL)-18 Levels, and the Impact of IL18 and IL18BP Genetic Variation, in CHD Patients and Healthy Men. *Arterioscler Thromb Vasc Biol* 2007.

243. Tiret L, Godefroy T, Lubos E, Nicaud V, Tregouet DA, Barbaux S, Schnabel R, Bickel C, Espinola-Klein C, Poirier O, Perret C, Munzel T, Rupprecht HJ, Lackner K, Cambien F, Blankenberg S. Genetic analysis of the interleukin-18 system highlights the role of the interleukin-18 gene in cardiovascular disease. *Circulation* 2005;**112**:643-650.

244. Espinola-Klein C, Rupprecht HJ, Bickel C, Lackner K, Schnabel R, Munzel T, Blankenberg S. Inflammation, atherosclerotic burden and cardiovascular prognosis. *Atherosclerosis* 2007;**195**:e126-134.

245. Blankenberg S, Tiret L, Bickel C, Peetz D, Cambien F, Meyer J, Rupprecht HJ. Interleukin-18 is a strong predictor of cardiovascular death in stable and unstable angina. *Circulation* 2002;**106**:24-30.

246. Maslow JN, Brar I, Smith G, Newman GW, Mehta R, Thornton C, Didier P. Latent infection as a source of disseminated disease caused by organisms of the Mycobacterium avium complex in simian immunodeficiency virus-infected rhesus macaques. *J Infect Dis* 2003;**187**:1748-1755.

247. Quinn TC, Piot P, McCormick JB, Feinsod FM, Taelman H, Kapita B, Stevens W, Fauci AS. Serologic and immunologic studies in patients with AIDS in North America and Africa. The potential role of infectious agents as cofactors in human immunodeficiency virus infection. *Jama* 1987;**257**:2617-2621.

248. Rizzardini G, Trabattoni D, Saresella M, Piconi S, Lukwiya M, Declich S, Fabiani M, Ferrante P, Clerici M. Immune activation in HIV-infected African individuals. Italian-Ugandan AIDS cooperation program. *AIDS* 1998;**12**:2387-2396.

249. Blanchard A, Montagnier L, Gougeon ML. Influence of microbial infections on the progression of HIV disease. *Trends Microbiol* 1997;**5**:326-331.

250. Moriuchi H, Moriuchi M, Mizell SB, Ehler LA, Fauci AS. In vitro reactivation of human immunodeficiency virus 1 from latently infected, resting CD4+ T cells after bacterial stimulation. *J Infect Dis* 2000;**181**:2041-2044.

251. Moriuchi M, Moriuchi H, Turner W, Fauci AS. Exposure to bacterial products renders macrophages highly susceptible to T-tropic HIV-1. *J Clin Invest* 1998;**102**:1540-1550.

252. Bafica A, Scanga CA, Schito M, Chaussabel D, Sher A. Influence of coinfecting pathogens on HIV expression: evidence for a role of Toll-like receptors. *J Immunol* 2004;**172**:7229-7234.

253. Whalen C, Horsburgh CR, Hom D, Lahart C, Simberkoff M, Ellner J. Accelerated course of human immunodeficiency virus infection after tuberculosis. *Am J Respir Crit Care Med* 1995;**151**:129-135.

254. Ellerin T, Rubin RH, Weinblatt ME. Infections and anti-tumor necrosis factor alpha therapy. *Arthritis Rheum* 2003;**48**:3013-3022.

255. Kroesen S, Widmer AF, Tyndall A, Hasler P. Serious bacterial infections in patients with rheumatoid arthritis under anti-TNF-alpha therapy. *Rheumatology (Oxford)* 2003;**42**:617-621.

256. Aboulafia DM, Bundow D, Wilske K, Ochs UI. Etanercept for the treatment of human immunodeficiency virus-associated psoriatic arthritis. *Mayo Clin Proc* 2000;**75**:1093-1098.

257. Cepeda EJ, Williams FM, Ishimori ML, Weisman MH, Reveille JD. The use of anti-Tumor Necrosis Factor therapy in HIV positive individuals with rheumatic disease. *Ann Rheum Dis* 2007.

258. Ting PT, Koo JY. Use of etanercept in human immunodeficiency virus (HIV) and acquired immunodeficiency syndrome (AIDS) patients. *Int J Dermatol* 2006;**45**:689-692.

259. Romero-Mate A, Garcia-Donoso C, Cordoba-Guijarro S. Efficacy and safety of etanercept in psoriasis/psoriatic arthritis: an updated review. *Am J Clin Dermatol* 2007;**8**:143-155.

260. Kaur PP, Chan VC, Berney SN. Successful etanercept use in an HIV-positive patient with rheumatoid arthritis. *J Clin Rheumatol* 2007;**13**:79-80.

261. Sellam J, Bouvard B, Masson C, Rousiere M, Villoutreix C, Lacombe K, Khanine V, Chennebault JM, Leclech C, Audran M, Berenbaum F. Use of infliximab to treat psoriatic arthritis in HIV-positive patients. *Joint Bone Spine* 2007;**74**:197-200.

262. Gaylis N. Infliximab in the treatment of an HIV positive patient with Reiter's syndrome. *J Rheumatol* 2003;**30**:407-411.

263. Linardaki G, Katsarou O, Ioannidou P, Karafoulidou A, Boki K. Effective etanercept treatment for psoriatic arthritis complicating concomitant human immunodeficiency virus and hepatitis C virus infection. *J Rheumatol* 2007;**34**:1353-1355.

264. Wallis RS, Kyambadde P, Johnson JL, Horter L, Kittle R, Pohle M, Ducar C, Millard M, Mayanja-Kizza H, Whalen C, Okwera A. A study of the safety, immunology, virology, and microbiology of adjunctive etanercept in HIV-1-associated tuberculosis. *AIDS* 2004;**18**:257-264.

265. Mattapallil JJ, Douek DC, Hill B, Nishimura Y, Martin M, Roederer M. Massive infection and loss of memory CD4+ T cells in multiple tissues during acute SIV infection. *Nature* 2005;**434**:1093-1097.

266. Deswal A, Bozkurt B, Seta Y, Parilti-Eiswirth S, Hayes FA, Blosch C, Mann DL. Safety and efficacy of a soluble P75 tumor necrosis factor receptor (Enbrel, etanercept) in patients with advanced heart failure. *Circulation* 1999;**99**:3224-3226.

267. Bozkurt B, Torre-Amione G, Warren MS, Whitmore J, Soran OZ, Feldman AM, Mann DL. Results of targeted anti-tumor necrosis factor therapy with etanercept (ENBREL) in patients with advanced heart failure. *Circulation* 2001;**103**:1044-1047.

268. Mann DL, McMurray JJ, Packer M, Swedberg K, Borer JS, Colucci WS, Djian J, Drexler H, Feldman A, Kober L, Krum H, Liu P, Nieminen M, Tavazzi L, van Veldhuisen DJ, Waldenstrom A, Warren M, Westheim A, Zannad F, Fleming T. Targeted anticytokine therapy in patients with chronic heart failure: results of the Randomized Etanercept Worldwide Evaluation (RENEWAL). *Circulation* 2004;**109**:1594-1602.

269. Chung ES, Packer M, Lo KH, Fasanmade AA, Willerson JT. Randomized, double-blind, placebo-controlled, pilot trial of infliximab, a chimeric monoclonal antibody to tumor necrosis factor-alpha, in patients with moderate-to-severe heart failure: results of the anti-TNF Therapy Against Congestive Heart Failure (ATTACH) trial. *Circulation* 2003;**107**:3133-3140.

270. Gupta S, Tripathi CD. Current status of TNF blocking therapy in heart failure. *Indian J Med Sci* 2005;**59**:363-366.

271. Anker SD, Coats AJ. How to RECOVER from RENAISSANCE? The significance of the results of RECOVER, RENAISSANCE, RENEWAL and ATTACH. *Int J Cardiol* 2002;**86**:123-130.